UNIVERSITY OF CRETE

TEMPLE UNIVERSITY

Molecular Basis of Human Disease

Effects of combined PPARα and PPARγ activation in Cardiac Lipotoxicity

"....the impact on Anti-Diabetic Treatment with Dual-PPARα/γ Agonists..."

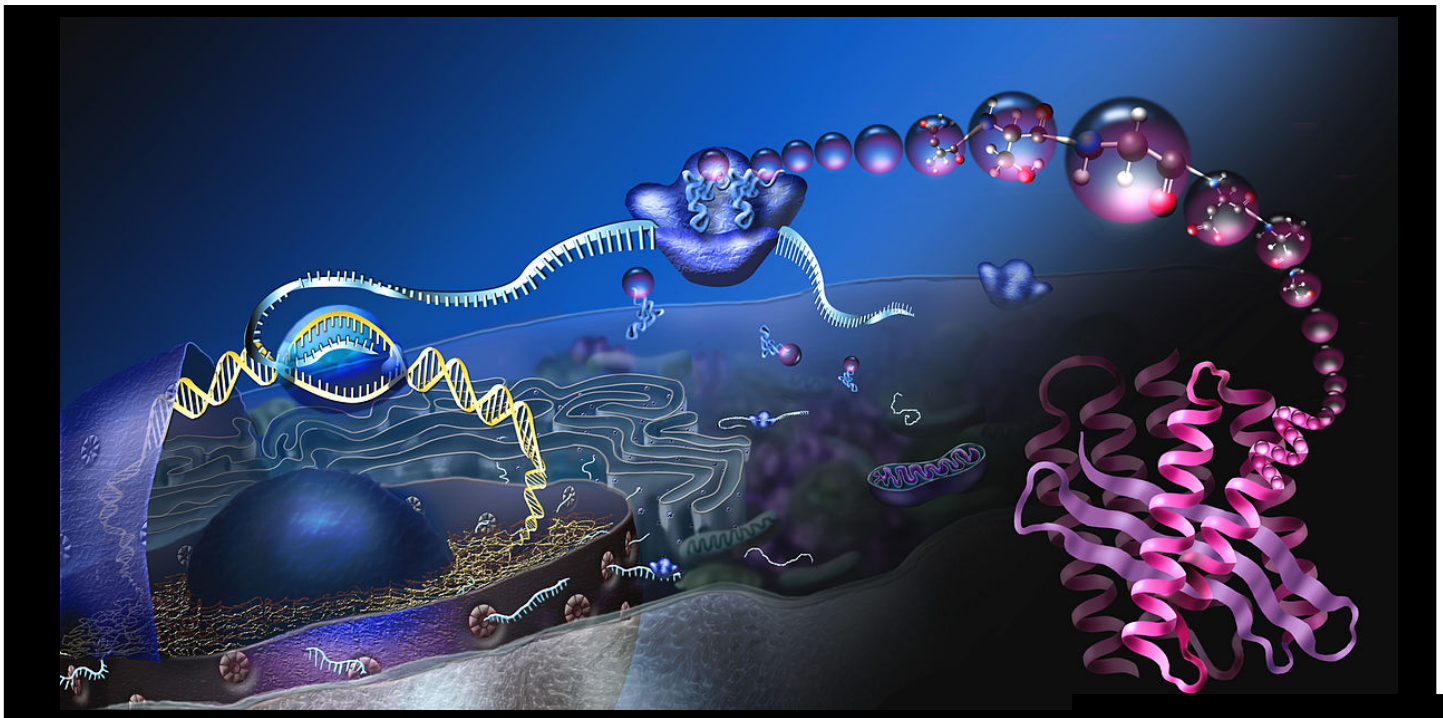

Charikleia Kalliora, MD

University of Crete
Temple University, Philadelphia, PA

2016-1017

Kalliora, MD, Student in Graduate Program “Molecular Basis o

mittee: **Konstantinos Drosatos, MSc, PhD**

Dimitris Kardassis, PhD

Christos Tsatsanis, PhD

Supervisor-Mentor: **Konstantinos Drosatos, MSc, PhD**

Affiliations: **University of Crete, School of Medicine**

Temple University, Lewis Katz School of Medicine, Center for Translational Medicine

Cover Page Picture: A look into a eukaryote cell to see how proteins are made. DNA in the nucleus is ‘read’ by RNA polymerase, then ribosomes in the cytoplasm produce an amino acid strand that folds into a functional protein.

Retrived by: http://www.darpa.mil/NewsEvents/Releases/2013/08/05.aspx

Contents

TABLES……

ABSTRACT

Improvements in hyperglycemia and hyperlipidemia constitute the major focus of various therapies for treatment of type 2 Diabetes. Agonists of peroxisome proliferator-activated receptor (PPAR)α and PPARγ are used for the treatment of hyperlipidemia and hyperglycemia, respectively. PPARα activation reduces circulating triglyceride levels and PPARγ improves insulin sensitivity. PPARs belong to the nuclear receptors super-family and regulate fatty acid (FA) metabolism. PPARα ligands, such as fibrates, lower plasma triglyceride levels and increase HDL-cholesterol levels . Thiazolidinediones (TZDs) are PPARγ ligands. PPARγ agonists increased salt and water retention and were associated with heart failure. The dual-PPARα/γ agonists (glitazars) have been developed to combine the beneficial effects of PPARα and PPARγ agonism. Although these dual-agonists improve metabolic parameters, they have been paradoxically found to aggravate congestive heart failure in patients with type 2 diabetes via mechanisms that remain unknowv. PPARs are important for cardiac FA metabolism . Different PPAR isoforms can regulate the same FA metabolism-related genes. Dominance of one PPAR isoform over the other in controlling FA metabolism in a tissue depends on the abundance of the respective isoform, as well as on the availability of endogenous ligands. Cardiac PPARα regulates the expression of genes that modulate FA oxidation (FAO). PPARγ can also promote cardiac FA, especially when PPARα expression is reduced or ablated. FAO accounts for the production of 70% of the ATP that is produced in the heart. Thus, it is surprising that combined activation of two positive regulators of cardiac FAO, PPARα and PPARγ, causes cardiac dysfunction.

PGC1α, the common transcriptional coactivator of PPARα and PPARγ, is involved in cardiac FAO and regulates mitochondrial biogenesis and respiration. PGC1α activation is

controlled through reversible lysine side chain hyperacetylation that is regulated by the enzymatic activity of the deacetylase Sirtuin1 (SIRT1) .

Our study focused on the mechanistic basis that underlies the cardiac dysfunction caused by combined activation of PPARα/γ, which constitutes the basis for an antidiabetic treatment. Our data from experiments in mice presented that dual-PPARα/γ agonist, Tesaglitazar, caused cardiac dysfunction associated with reduced PGC1α expression and activation. These effects are driven by competition between PPARα and PPARγ for regulation of *Pgc1α* gene expression, as well as by decreased cardiac SIRT1 expression. Activation of SIRT1 with Resveratrol, attenuated Tesaglitazar-mediated cardiac dysfunction in WT and diabetic (*db/db*) mice but not in mice with cardiomyocyte-specific ablation of SIRT1. In conclusion, our study elucidated the mechanism that underlies dual PPARα/γ agonist cardiotoxicity and we present a new pharmacologic approach that blunted the cardiotoxic effect of the anti-diabetic dual-PPARα/γ therapy, while it maintained its beneficial anti-hyperlipidemic and anti-hyperglycemic effects.

CHAPTER ONE

1. Significance of Controlling and Treating Diabetes

1.1 Diabetes - *A global emergency*

1.1.1 Etymology and Definition

The word *diabetes* has a latin background (*diabetes)*, which actually comes from the ancient Greek word διαβήτης (*diabētēs*), which means "a passer through" (Roberts, (2015).). Aretaeus, a Greek physician of Cappadocia *(1st century CE)* was the first who used the word diabetes that he defined as "excessive emptying of urine bladder" (Dictionary, 2011; Knowler et al., 2002). The word "diabetes" was first reported in English with the term *diabete* around 1425, .

Diabetes melitus is one of the most prevalent chronic metabolic diseases with high complexity and socioeconomic impact (American Diabetes, 2010). It is characterized by hyperglycemia resulting from defective insulin production, function or combination of both. Chronic hyperglycemia is linked to progressive dysfunction and finally failure of different organs, such as the pancreas, eyes, renal system, peripheral nervous system and cardiovascular system. Diabetes is classified into two basic forms, type 1 and 2. The most common type is type 2 diabetes (T2D) that is primarily characterized by insulin resistance.

1.1.2 Etiologic Classification

Diabetes is classified in several types according to the etiology of onset (1998; American Diabetes, 2010) (**Table 1**) represents the international classification of diabetes but the most common types are four and they are described below.

Type 1 DM: Type 1 diabetes (T1D) is classified as immune-mediated and idiopathic T1D. The first form is characterized by insufficient insulin secretion by the pancreas. This phenomenon is mainly driven by autoimmune damage of the pancreatic β-cells that normally produce the hormone (American Diabetes, 2010). T1D was previously encompassed by the terms "insulin-dependent diabetes mellitus" (IDDM) or "juvenile diabetes". It commonly affects childhood and adolescence, but the last years it has been shown that it appears at any age. The idiopathic form has been described in patients with permanent insulinopenia but with no significant evidence of autoimmunity (Cooke and Plotnick, 2008).

Type 2 DM: Type 2 DM is associated with obesity and insulin resistance combined with insufficient compensatory insulin secretion. Insulin resistance is a condition in which cells are not able to respond to insulin appropriately (World Health Organization, , WHO, 2012). During the progression of the disease, a consequent insulin deficiency develops due to exhaustion of the pancreas for insulin production (DeFronzo et al., 1992) or accumulation of lipids in the pancreas too (lipotoxicity). The risk of developing this form of diabetes is highly related to the lifestyle as it increases with age, obesity, and absence of physical activity. Type 2 diabetes was previously noted as "non-insulin-dependent diabetes mellitus" (NIDDM) or "adult-onset diabetes"(American Diabetes, 2010).

Gestational diabetes: THis form of diabetes describes any grade of glucose intolerance in pregnant women without a previous history of diabetes (Matthews et al., 1998). Obesity increases the risk for T2D in women of childbearing age. As obesity is a major global epidemic the number of pregnant women with undiagnosed type 2 diabetes has increased significantly.

Maturity onset diabetes of the young (MODY):. This type of diabetes is characterized by defects in insulin production, which is caused by one of several single-gene mutations and they lead to onset of hyperglycemia at an early age (usually before the age of 25 years) (Kahn et al., 1993). It is significantly less common than the other types and varies in age of first appearance, as well as in severity. In fact, there are at least 13 subtypes of MODY. MODY is often under control without insulin administration.

Classification of Diabetes

I. **Type 1 diabetes** (β-cell destruction, usually leading to absolute insulin deficiency)
   A. Immune mediated
   B. Idiopathic

II. **Type 2 diabetes** (may range from predominantly insulin resistance with relative insulin deficiency to a predominantly secretory defect with insulin resistance)

III. Other specific types

A. Genetic defects of β-cell function
1. Chromosome 12, HNF-1α (MODY3)
2. Chromosome 7, glucokinase (MODY2)
3. Chromosome 20, HNF-4α (MODY1)
4. Chromosome 13, insulin promoter factor-1 (IPF-1; MODY4)
5. Chromosome 17, HNF-1β (MODY5)
6. Chromosome 2, *NeuroD1* (MODY6)
7. Mitochondrial DNA
8. Others

B. Genetic defects in insulin action
1. Type A insulin resistance
2. Leprechaunism
3. Rabson-Mendenhall syndrome
4. Lipoatrophic diabetes
5. Others

C. Diseases of the exocrine pancreas
1. Pancreatitis
2. Trauma/pancreatectomy
3. Neoplasia
4. Cystic fibrosis
5. Hemochromatosis
6. Fibrocalculous pancreatopathy
7. Others

D. Endocrinopathies
1. Acromegaly
2. Cushing's syndrome

3. Glucagonoma 4. Pheochromocytoma 5. Hyperthyroidism 6. Somatostatinoma 7. Aldosteronoma 8. Others **E. Drug or chemical induced** 1. Vacor 2. Pentamidine 3. Nicotinic acid 4. Glucocorticoids 5. Thyroid hormone 6. Diazoxide 7. β-adrenergic agonists 8. Thiazides 9. Dilantin 10. γ-Interferon 11. thers **F. Infections** 1. Congenital rubella 2. Cytomegalovirus 3. Others **G. Uncommon forms of immune-mediated diabetes** 1. “Stiff-man” syndrome 2. Anti-insulin receptor antibodies 3. Others **H. Other genetic syndromes sometimes associated with diabetes** 1. Down syndrome 2. Klinefelter syndrome 3. Turner syndrome 4. Wolfram syndrome 5. Friedreich ataxia 6. Huntington chorea 7. Laurence-Moon-Biedl syndrome 8. Myotonic dystrophy 9. Porphyria 10. Prader-Willi syndrome 11. Others	
IV. Gestational diabetes	

Table 1. Classification of Diabetes according to the etiology of onset. *Modified by* (American Diabetes, 2010)

1.1.4 1.1.3 Epidemiology

Diabetes is a complex and insidious disease that affects 8.8% of the world population (**Figure 1 and Table 2).**The Western Pacific region, including China has the majority of diabetic patients, i.e. 153.2 million individuals. Approximately 30 million Americans (9.4% of the population) have diabetes (**Figure 1 and Table 2).** Unless the disease is tackled, the International Diabetes Federation (IDF)has predicted that the number of diabetic adults worldwide will be approximately 9 billion by 2040. (Olefsky et al., 1973) (International Diabetes Federation, IDF, 2013; www.cdc.gov/diabetes).

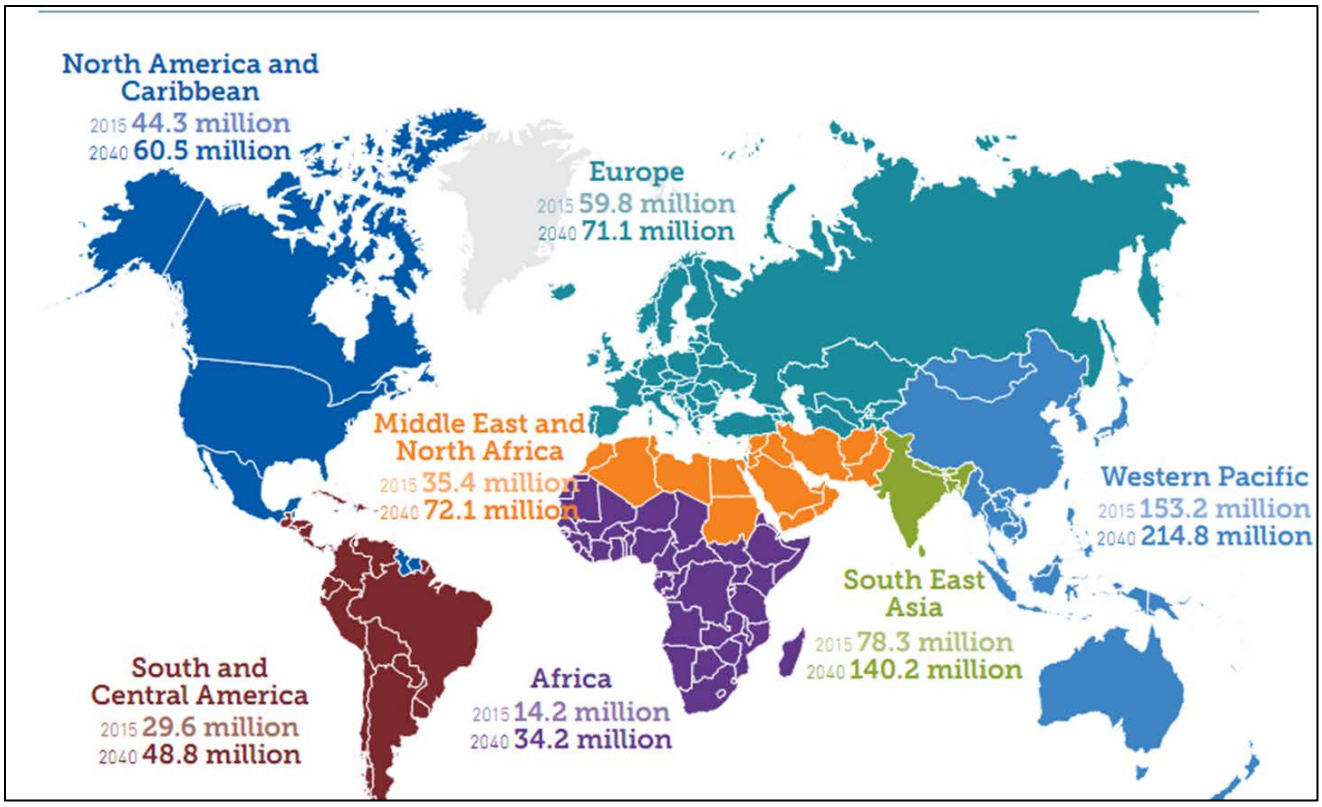

Figure 1. Estimated number of people (20-79 years old) with diabetes worldwide and per region in 2015 and 2040. Modified by www.idf.org/

Parameter	2015	2040
Total world population	7.3 billion	9.0 billion
Adult population	4.72 billion	6.16 billion
Child population	1.92 billion	-
Diabetes (20-79 years old)		
Global prevalence	8.8% (7.2-11.4%)	10.4% (8.5-13.5%)
Number of people with diabetes	415 million (340-536 million)	642 million (521-829 million)
Munber of deaths due to diabetes	5.0 million	-
Health expenditure due to diabetes (20-79 years old)		
Total health expenditure, R=2* 2015 USD	673 billion	802 billion
Hyperglycemia in pregnancy (20-49 years old)		
Proportion of live births affected	16,2%	-
Number of live births affected	20.9 million	-
Impaired glucose tolerance (20-79 years old)		
Global prevalence	6.7% (4.5-12.1%)	7.8% (5.2-13.9%)
Number of people with impaired glucose tolerance	318 million (212.2-571.6)	481 million (317.1-855.7)
Type 1 diabetes (0-14 years)		
Number of children with type 1 diabetes	542000	**-**
Number of newly diagnosed cases each year	86000	**-**

Table 2. *Estimated percentages related to diabetes disease in 2015 and 2040*

1.2. Type 2 Diabetes

T2D is the most prevalent form of diabetes accounting for 90% to 95% of cases (Knowler et al., 2002). It can be inherited as the offspring of diabetic parents have a greater risk to develop the disease. It mostly affects African-Americans, Latinos, Asian Americans, Native Americans, and Pacific Islanders. Also, pregnant women who develop gestational diabetes have a higher risk of getting T2D within 5 to 10 years.

1.2.1 Signs and Symptoms

Type 2 diabetes is characterized by chronic hyperglycemia which causes symptoms including polyuria (increased urination), polydipsia (increased thirst), polyphagia (increased hunger) and blurred vision. Prolonged high blood glucose can cause retinopathy , nephropathy, peripheral neuropathy, autonomic neuropathy and susceptibility to certain infections *(www.uptodate.com*). Acute, life-threatening effects of untreated diabetes are hyperglycemia with ketoacidosis or the non-ketotic hyperosmolar syndrome (Kitabchi et al., 2009). Diabetic patients have an increased incidence of atherosclerotic cardiovascular, peripheral arterial, and cerebrovascular consequences.

1.2.2. Pathophysiology

Pancreas

- The impairment of insulin signaling starts in the early stages of T2D (Turner et al., 1999). Insulin resistance can be observed in individuals with even normal glucose tolerance who are prone to develop T2D, 10–20 years before the disease is diagnosed (Matthews et al., 1998). Further, during the period of transition from impaired glucose tolerance to T2DM, the individuals may have already lost up to 80% of their β-cell function (Diabetes Study (UKPDS), Lancet, 1998). *Genetics*

  The genetic susceptibility to beta cell dysfunction of T2DM in families has long been recognized and is still under investigation (Mills et al., 2004). There is a specific number of genes which have been linked with insulin and β-cell dysfunction and they have been identified in patients with T2DM, including genetic variants associated with pancreatic growth and insulin release and function (Grant et al., 2009). Furthermore, GWAS studies identified genetic

polymorphisms in patients predisposed to T2DM that result in failure of the β-cells to respond to increased demand for insulin (Grant et al., 2009; Kahn, 2001).

- *Age and Lifestyle*

  Several studies support that the prevalence of T2DM increases progressively with aging and this is consistent to the age-related decline in β-cell function and insulin secretion.

  Regarding to the impact of lifestyle on diabetes pathophysiology, unhealthy dietary habits resulting to obesity and physical inactivity have a crucial role in the increased prevalence of T2DM worldwide (Hu, 2011) and contribute to the development of insulin resistance (Defronzo, 2009). Preference for foods with high lipid concentrations increases deposition of fat in liver and muscle that contributes to insulin resistance.(Defronzo, 2009)

- *Glucotoxicity and Lipotoxicity*

  Undoubtedly chronic hyperglycemia and hyperlipidemia can exert toxic effects on β-cell secretory function which is respectively noted as glucotoxicity and lipotoxicity.

  Chronic hyperglycemia impairs the normal function of pancreatic b-cells and the glucose-induced insulin secretion by causing distinct phenomena including glucose desensitization, β-cell exhaustion and finally glucotoxicity. On the other hand, glucotoxicity refers to slow and irreversible consequences of chronic hyperglycemia on β-cell function upon long-term exposure to high plasma glucose levels (Koonen et al., 2005). Consequences include decrease of β-cell mass as a result to apoptosis (Gollamudi et al., 2008; Poulsen et al., 2012).Interestingly, the molecular mechanisms of glucotoxicity have been

proposed to stimulate oxidative stress (16–19). Tanaka et al showed that treatment of Zucker diabetic fatty (ZDF) rats with antioxidants such as with amino-guanidine or NAC restores insulin mRNA levels, insulin secretion and eventually plasma glucose levels (Hill and Schulze, 2014).

Hyperglycemia in T2D is accompanied by hyperlipidemia, which drives pancreatic β-cell lipotoxicity. **Lipotoxicity** is generally defined as the process where the lipids are extremely accumulated and the lipid signaling pathways are over-activated triggering cellular dysfunction and distress, which may be performed as insulin resistance, dysfunctional or damaged mitochondria, energy deficiency, endoplasmic reticulum stress or cell apoptosis death (lipo-apoptosis) (Christ et al., 1997; Unger and Zhou, 2001). Although fatty acids are normally essential β-cell fuels, prolonged exposure of β-cells to lipids leads to inhibition of glucose-induced insulin gene expression and secretion (Luiken et al., 2004).

Adipose tissue

In T2DM, adipocytes show insulin resistance, which promotes lipolysis, resulting in increased FFAs in the circulation. Chronic elevation of the circulatory FFAs impairs further insulin secretion, promotes hepatic and muscle insulin resistance and stimulates gluconeogenesis .(Reibel et al., 1981; Unger and Zhou, 2001). The contribution of hyperlipidemia in insulin resistance is also characterized by excessive inflammatory and atherogenic cytokines release that are produced by the “dysfunctional” adipose tissue.(Reibel et al., 1981).

Liver

Liver is the organ with the most crucial role in glucose metabolism. It is responsible for glucose production (Lopaschuk et al., 2010) and release into circulation. Hepatic glucose is formed both from gluconeogenesis and glycogenolysis (How et al., 2005; Lopaschuk et al., 2010). Patients with T2D have increased glucose production (Defronzo, 2009). In parallel, increased levels of glucagon in circulation because of the pancreatic α cells incapability to suppress the postprandial glucagon secretion (How et al., 2005) increases the sensitivity of liver to glucagon and enhances even more hepatic glucose production and release (Defronzo, 2009).

Muscle

Glucose is the main fuel that is used by skeletal muscles for energy production. Plasma glucose is transferred via an insulin-stimulated transport into skeletal myocytes (How et al., 2006). The glucose transportation or "glucose uptake" is settled by the glucose transporter 4 (GLUT4) (How et al., 2006), which is also expressed in cardiac myocytes and adipocytes and is responsible for insulin-stimulated glucose uptake intracellularly (Sharma et al., 2004). Insulin stimulates translocation of GLUT4 to the membrane of muscle cells, resulting in increased glucose uptake (How et al., 2006; Sharma et al., 2004). In T2DM, the defective insulin signaling impairs GLUT4 translocation and glucose uptake, which leads to hyperglycemis (Young et al., 2002).

The pathophysiological events and the respective impaired signaling pathways are summarized in **(Figure 2).**

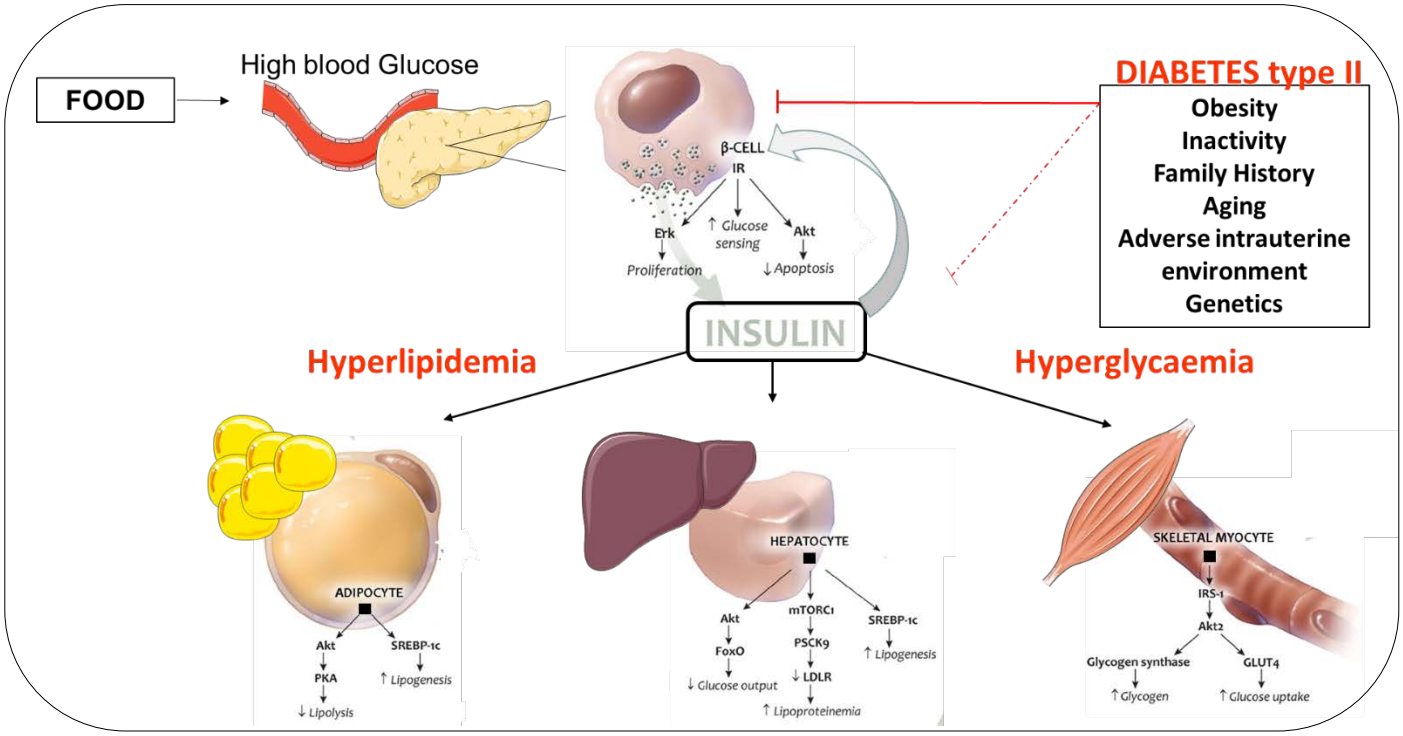

Figure 2. Effects of Type 2 diabetes in pancreas, adipose tissue, liver and skeletal muscle. Type 2 diabetes is characterized by reduced insulin sensitivity of the adipose tissue , the liver and the skeletal muscle. Also its pathophysiology includes the progressive decline of pancreatic β cells that are responsible for insulin production by leading to impaired insulin signaling and eventually to hyperglycemia, Adipose tissue: there is increased lipid release by adipose tissue and decreased levels of lipolysis which is normally increased by insulin. These conditions contribute to high triglyceride levels in circulation (hyperlipidemia). Skeletal muscle: Skeletal muscle which mostly uses glucose as fuel for energy production cannot effectively uptake it as normally happens via Glucose transporter 4 (GLUT 4) which translocation to cell membrane is regulated by insulin. This lack of glucose uptake increases the demand for fuel and the glycogen synthesis is stimulated. Liver: The increased levels of circulating glucose levels promote lipogenesis in liver and the high demanding for fuel promotes hepatic glucose output that eventually increases even more plasma glucose levels

1.2.3. Drugs and Therapy

The first recommended treatment of diabetes emphasizes on changes in the patients' lifestyle, such as healthy nutrition combined with physical activity, weight loss and self-monitoring of blood glucose levels (Nathan et al., 2009). An early intervention with intensive lifestyle modifications could prevent or slow down the development of T2DM in people with high susceptibility (Knowler et al., 2002). However, for some

patients the changes in lifestyle may not be adequate to control the complications of the disease pharmacotherapy is required to achieve and preserve glycemic control (Nathan et al., 2009).

Patients with T2DM usually require multiple drugs. Currently no single agent can treat all pathophysiological mechanisms involved in T2DM pathogenesis (Nathan et al., 2009). The most common classes of drugs, mechanisms of action, and major precautions, contraindications and adverse effects are presented in **Table 3.**

Drugs available for type 2 diabetes mellitus			
Class	**Mechanism of action**	**Glucose target**	**Major precautions, contraindications, adverse effects**
Oral agents			
Biguanide (metformin)	Decreases hepatic glucose production; hepatic insulin sensitizer; decreases intestinal glucose absorption	Fasting	Gastrointestinal symptoms, lactic acidosis, contraindicated in renal insufficiency
Sulfonylurea (glyburide, glipizide, glimepiride)	Increases insulin secretion	Fasting and postprandial	Weight gain, hypoglycemia
α-glucosidase inhibitor (acarbose, miglitol)	Delays carbohydrate absorption	Postprandial	Gastrointestinal symptoms
Thiazolidinedione (pioglitazone, rosiglitazone) **Dual PPARα/γ agonists (glitazars)**	Insulin sensitizer Insulin sensitizer Anti-hyperlipidemic action	Fasting and postprandial	Edema, weight gain, bone fractures, may cause or exacerbate heart failure, contraindicated in **heart failure.** Rosiglitazone has been withdrawn from the EU owing to potential increased risk of CV

			events. Pioglitazone may be associated with an increased risk of bladder cancer.
Meglitinide (nateglinide, repaglinide)	Increases insulin secretion	Postprandial	Weight gain, hypoglycemia
DPP-4 inhibitors (sitagliptin, saxagliptin, linagliptin, alogliptin)	Increases GLP-1 and GIP levels	Postprandial	Urticaria/angioedema
Dopamine agonist (bromocriptine)	Modulates central neurotransmitters, resulting in improved glycemic control and glucose tolerance	Postprandial	Orthostatic hypotension, syncope, nausea
Bile acid sequestrant (colesevelam)	Lowers plasma glucose and LDL cholesterol	Postprandial	Constipation
SGLT2 inhibitors (canagliflozin, dapagliflozin, empagliflozin)	Increase renal glucose excretion	Fasting and postprandial	Genital and urinary tract infections. Contraindicated in moderate to severe renal impairment
Injectable agents			
GLP-1 receptor agonist (exenatide, exenatide long-acting release, liraglutide)	Increases glucose-dependent insulin secretion, decreases glucagon secretion, slows gastric emptying	Postprandial, some fasting	Gastrointestinal symptoms
Amylin analog (pramlintide)	Delays gastric emptying, decreases glucagon secretion	Postprandial, some fasting	Hypoglycemia, gastrointestinal symptoms
Insulin (various analogs)	Stimulate glucose uptake	Basal, fasting bolus, postprandial	Weight gain, hypoglycemia
GLP-1 receptor agonist (exenatide, exenatide long-acting release,	Increases glucose-dependent insulin secretion, decreases	Postprandial, some fasting	Gastrointestinal symptoms

liraglutide)	glucagon secretion, slows gastric emptying		
Amylin analog (pramlintide)	Delays gastric emptying, decreases glucagon secretion	Postprandial, some fasting	Hypoglycemia, gastrointestinal symptoms
Insulin (various analogs)	Stimulate glucose uptake	Basal, fasting bolus, postprandial	Weight gain, hypoglycemia

Table 3. Drugs available for type 2 diabetes mellitus

1.2.4. Research on antidiabetic treatments

The International Diabetes Federation (IDF) has estimated total annual diabetes-related expenditures to at least 100-250 million dollars for most of the countries worldwide and more than 500 million dollars for 17 economically developed countries. Estimation for global health care costs to treat and control diabetes were approximately 673 million dollars in 2015 and may exceed 802 million dollars by 2040 **(Figure 3).**

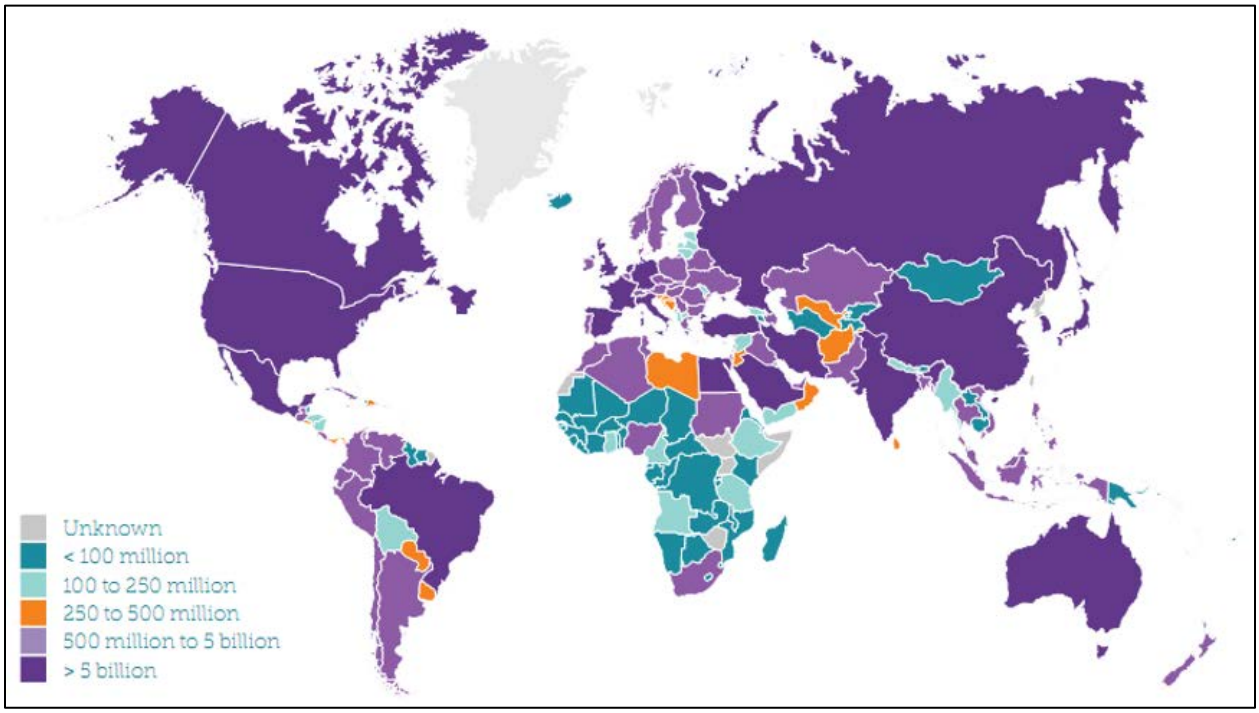

Figure 3. Total annual diabetes related healthcare expenditures (20-79 years) (International Dollars), R=2*, 2015 Modified by www.idf.org/

There are two types of antidiabetic drugs therapeutics: the short term, such as insulin injections and the long-term that are used to maintain normoglycemic balance in plasma. Metformin and sulfonylureas which increase insulin levels and reduce high blood glucose levels, have been used to treat type 2 diabetes for many years ((ADA); (www.cdc.gov/diabetes); Medicine). However, Thiazolinediones, which are PPARγ agonists, are effective drugs against diabetes as they increase insulin sensitivity. However, they are indicated only for patients, who are not at high risk of heart failure, due to cardiovascular adverse effects. Glitazars (dual PPARα/γ agonists) were developed to combine the anti-hyperglycemic beneficial effects of PPARγ agonists, with the anti-hyperlipidemic effects of PPARα agonists (i.e. Fibrates). However, they also had heart-related side effects as they were associated with heart failure. Therefore, additional studies are needed to address the association of effective antidiabetic drugs with cardiac dysfunction.

CHAPTER TWO
2. PPAR agonists; an effective anti-diabetic treatment

2.1 Introduction to PPARs

2.1.1. Nomeclature and classification of PPAR receptors

Peroxisomes are cellular organelles which were identified in the late 1960s in rat liver (de Duve, 1969). Peroxisomes are involved in several cellular processes that pertain to fatty acid metabolism and alleviation of reactive oxygen species (ROS) (Gabaldon, 2010). There is a big variety of molecules (ex. Clofibrate) that promote "proliferation" of peroxisomes The first receptor of peroxisome proliferators was discovered in 1990 (Issemann and Green, 1990) and it was named with the generic term PPAR, in 1992, It has been shown that these receptors could transcriptionally activate the acyl coenzyme A oxidase gene, which encodes the key enzyme (ACOX) of peroxisomal fatty acid β-oxidation (Dreyer et al., 1992)

Peroxisome proliferator-activated receptors (PPARs) belong to the superfamily nuclear receptors (Nuclear Receptors Nomeclature Commitee 1999) There are two types of nuclear receptors:

- Type I NR, such as steroid hormones receptors, that are located in the cytoplasm where they are binded to chaperone proteins (e.g., HSP90) (Echeverria and Picard, 2010). Upon ligand binding, the receptors de-attach from the chaperone, initiating homodimerization, exposure of the nuclear localization sequence, and transfer from cytoplasm to nucleus. In the nucleus,

the ligand–receptor complex interacts with transcriptional coactivators that mediates binding to and transcription of target genes (Bulynko and O'Malley, 2011; Carroll et al., 2006; Glass and Rosenfeld, 2000).

- Type II NR (NRNR2B1/2/3) that form heterodimers with the retinoid-X-receptors (RXR-α/β/γ). PPARs are ligand-activated transcription factors. Upon ligand binding, they undergo alteration of their 3-D configuration and recognize specific hormone-response elements (HRE), which are described as PPAR response elements (PPRE) on the promoters of genes, resulting in their activation or repression. Their activation is performed as transcription of their target genes (**Figure 4).** There are three PPAR isoforms: PPAR-α (*NR1C1*), PPAR-γ (*NR1C3*) and PPAR-ß/δ (*NR1C2*) (Poulsen et al., 2012).

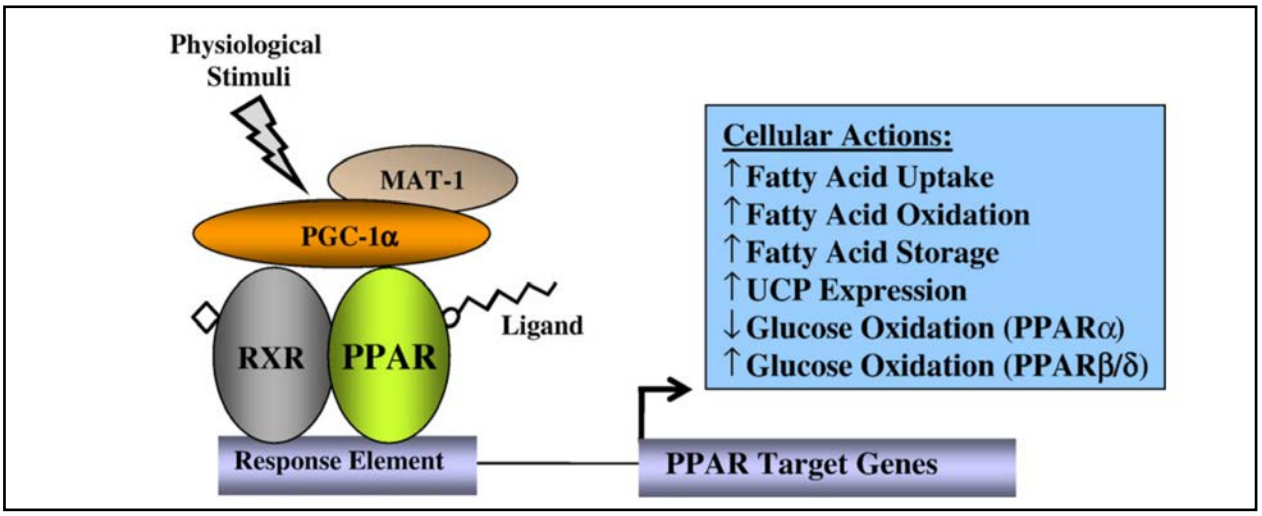

Figure 4. PPARs belong to nuclear receptors that act as transcriptional factors by forming heterodimers with RXRs. PPAR transcriptional activity is dependent on endogenous ligands and protein coactivators such as PGC-1 and its regulator MAT-1. Some of the major actions of PPARs in the heart are presented in the blue box. Modified by (Madrazo and Kelly, 2008)

- **PPARα** is predominately expressed in the heart, liver, macrophages, muscle and kidneys. It is expressed in tissues with high capacity for FAO (Tyagi et al., 2011)

and regulates the expression of genes that are involved in this process (Finck et al., 2002). (**Figure 5 and Table 4)**

- **PPARβ/δ** is mostly observed mostly in skeletal muscle as well as in brain, in adipose tissue and in skin. It regulates the expression of genes that drive FAO in skeletal muscles and in adipose tissue. (Berger and Moller, 2002; Tyagi et al., 2011) (**Figure 5 and Table 4)**
- **PPARγ** is expressed mainly in the adipose tissue, especially in brown adipose tissue. It has a pivotal role in adipogenesis, thermogenesis and the fatty acid FA and triglyceride TG storage. There are three subtypes of the PPAR-γ superfamily which are transcribed from the same gene and undergo alternative splicing (***γ1***: expressed in heart, spleen, kidneys, muscles, pancreas and colon / ***γ2***: expressed mostly in adipose tissue and ***γ3***: expressed in adipose tissue too but also in macrophages and in large intestine) (Berger and Moller, 2002; Son et al., 2007; Tyagi et al., 2011) **Figure 5 and Table 4).**

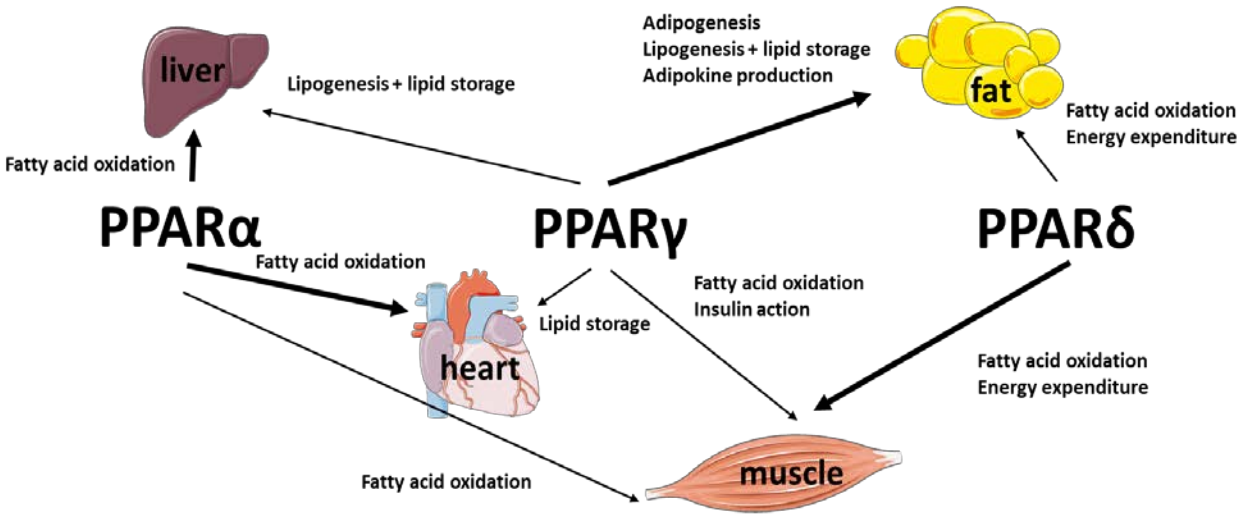

Figure 5. PPARs regulate metabolic pathways in heart, liver, skeletal muscle and adipose tissue. PPARα is the major regulator of fatty acid oxidation in heart as well as in liver and skeletal muscle. PPARγ regulates adipogenesis, lipogenesis and lipid storage in adipose tissue

and controls insulin sensitivity in skeletal muscle. PPARδ also regulates fatty acid oxidation in skeletal muscle and in adipose tissue. Modified by (Pol et al., 2015)

	PPARα	PPARγ	PPARδ
Location	Liver, endothelial cells	Adipocytes, vascular cells	Skeletal muscle
Main actions in target tissues	↑ FA uptake ↑ FA oxidation ↑ Apo AI, Apo AII	↑ FA uptake ↓ FA release ↓ Pro inflammatory cytokines ↓ Insulin action	↑ FA oxidation ↑ Mitochondrial genesis
Consequential effects	↓ Circulating TG ↑ HDL-C ↓ Atherosclerosis ↓ Liver fat	↓ Insulin resistance ↑ Body weight gain ↑ Vasoprotection	↓ Body fat ↓ Circulating TG ↑ HDL-C ↑ Insulin action

Table 4. Primary location of PPAR subtypes and metabolic effects. FA fatty acid, TG triglycerides, HDL-C HDL-cholesterol.

2.2 Transcriptional co-factors: *PPARγ Coactivator 1 (PGC-1)*

PPARs either activate or inhibit transcription of target genes depending on their association with co-activators or co-repressor proteins including the CBP/p300, the p160/SRC family (SRC-2/GRIP1/TIF2, SRC-3/Pcip/rac3/ACTR/AIB1/TRAM-1) or the PGC-1 family (PGC-1α, PGC-1β) (Gollamudi et al., 2008).

PGC-1 was first discovered by Spiegelman et al. 50 in a yeast 2-hybrid screen during the efforts to distinguish the biology of brown adipose tissue from white adipose tissue. PGC-1α was the first among three isoforms that was identified and found to interact with PPARγ in the mitochondria-rich brown adipose tissue (Puigserver et al., 1998). Two other related coactivators, PGC-1β (PERC) and PGC-1–related coactivator (PRC), have been discovered (Kressler et al., 2002; Lin et al., 2002). PGC-1α and PGC-1β are predominately expressed in tissues with high oxidative capacity, such as cardiac muscle, skeletal muscle, and BAT, where they play a crucial role in orchestrating cellular energy metabolism (Kamei et al., 2003; Kressler et al., 2002; Puigserver et al., 1998; St-Pierre et al., 2003; Wu et al., 1999).

Studies from the past decade revealed that PGC-1 is the main coactivator for both of PPARα and PPARγ that serves as a scaffold, which recruits regulatory proteins for chromatin remodeling and transcription activation (Puigserver et al., 1999; Puigserver et al., 1998; Wallberg et al., 2003). PGC-1 interacts with histone acetyltransferases (HAT), such as CREB-binding protein/p300 and steroid receptor coactivator-1 (SRC-1) (Puigserver et al., 1999). These proteins mediate remodeling of histones within chromatin. In addition, PGC-1 docks with a protein called ménage-à-trois 1, (an element of the cyclin-dependent kinase 7 complex) that phosphorylates RNA polymerase II and selectively regulates its activity (Sano et al., 2007). Another activating complex, the thyroid hormone receptor–associated protein/vitamin D receptor–interacting protein (TRAP/DRIP), complex docks on PGC-1α (Wallberg et al., 2003) and mediates the link with RNA polymerase II (Wallberg et al., 2003) **(Figure 6).**

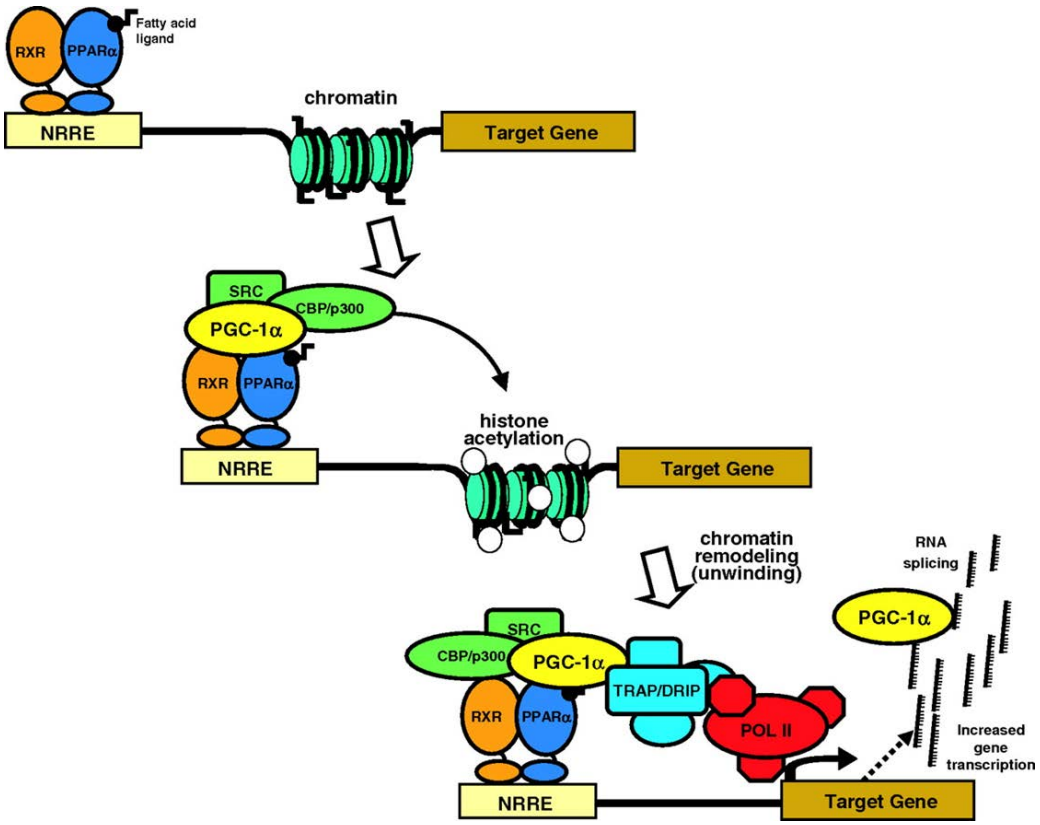

Figure 6. PGC-1 is a transcriptional coactivator for PPARα and PPARγ, as well as for other nuclear receptors. The PPAR-RXR heterodimer binds cognate nuclear receptor response elements (NRRE) within the promoter region of the target gene. PPAR then recruits PGC-1, which facilitates interactions of the DNA-bound complex with other coactivators that modify chromatin by promoting acetylation of histones (eg, SRC-1, p300). PGC-1 also directly interacts with the transcription initiation machinery (TRAP/DRIP), which sets a molecular bridge between the coactivator complex and RNA polymerase II (POL II). PGC-1plays a role in RNA processing via an RNA recognition motif in its C-terminus. Modified by (Finck and Kelly, 2007).

2.2.1. Post-Translational Modifications regulate PGC1a Activiity

The activity of PGC1α is regulated by post-translational mechanisms, such as phosphorylation and acetylation, which are the most common, ubiquitination, methylation, and O-GlcNAcylation. **(Figure 7)**.

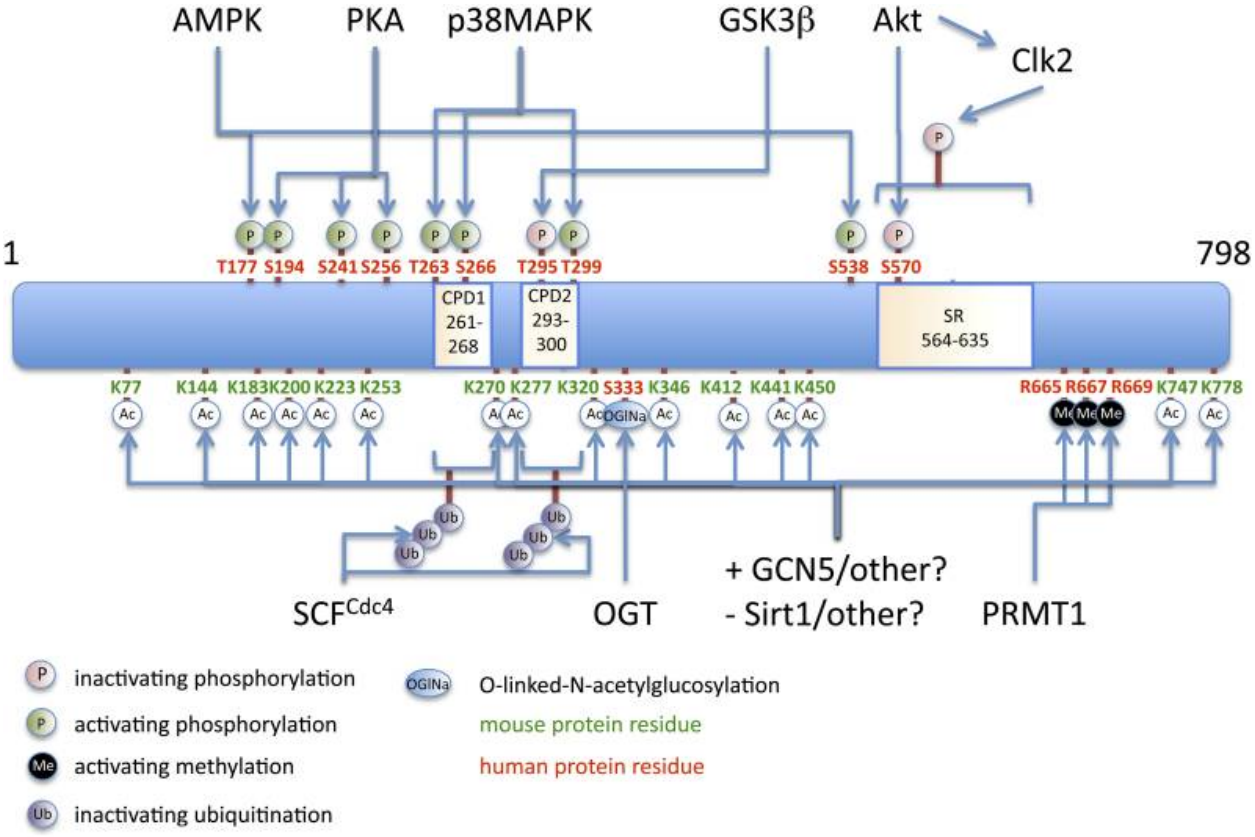

Figure 7. Sites for posttranslational modifications on the peroxisome proliferator-activated receptor γ coactivator 1α (PGC-1α) polypeptide. Modified by (Fernandez-Marcos and Auwerx, 2011)

2.2.1.1 PGC-1α phosphorylation

PGC1a is phosphorylated by the protein kinases AMP-activated protein kinase (AMPK), Akt and p38 MAPK. AMPK-mediated phosphorylation and thus activation of PGC1α at threonine 177 and serine 538 promotes mitochondrial biogenesis (Jager et al., 2007). Similarly, p38 MAPK-mediated phosphorylation of muscle PGC1a at threonine 262, serine 265 and threonine 298 activates it. The targets of that phosphorylation are (Puigserver et al., 2001). On the other hand, insulin-mediated PGC1a phosphorylation at serine 570 inhibits its activity (Li et al., 2007; Southgate et al., 2005).

Recently it has been shown that during oxidative stress glycogen synthase kinase 3β (GSK3β) also inhibits PGC1a via phosphorylation that results to proteasomal degradation . However, the actual function of this inhibitory phosphorylation remain unclear (Anderson et al., 2008).

2.2.1.2 PGC-1α acetylation

Lysine-side chain hyperacetylation also controls the activity of PGC1α. The acetylation status of PGC1α is mainly controlled by the enzymatic activities of the acetyltransferase (general control of amino acid synthesis) GCN5 and the deacetylase SIRT1 **(Figure 8).**

It has been shown that GCN5 acetylates and inhibits PGC1a activity either in vitro or in vivo (Kelly et al., 2009; Lerin et al., 2006). GCN5 activity is enhanced by the acetyl-transferase SRC-3. The expression of both SRC-3 and GCN5 is increased during caloric excess.

SIRT1 belongs to the family of sirtuins, which is the mammalian homolog of yeast silent information regulator 2 (Sir2) (Shore et al., 1984). In mice, SIRT1 activation or overexpression increases the life span and seems to protect against cancer induction (Canto et al., 2009; Gerhart-Hines et al., 2007; Houtkooper et al., 2010). SIRT1 is coenzyme nicotinamide adenine dinucleotide (NAD^+)-dependent deacetylase. It is most active in high energy demand, when NAD^+ or the NAD^+/NADH ratio are at their highest levels (Canto and Auwerx, 2009). Sirt1-mediated deacetylation and activation of PGC-1α increases mitochondrial metabolism when energy demands increase. Interestingly, phosphorylation of PGC1α by AMPK is required for the subsequent Sirt1-mediated

deacetylation (Gerhart-Hines et al., 2007) .On the other hand, SIRT1 has also direct action on PGC1a regulation

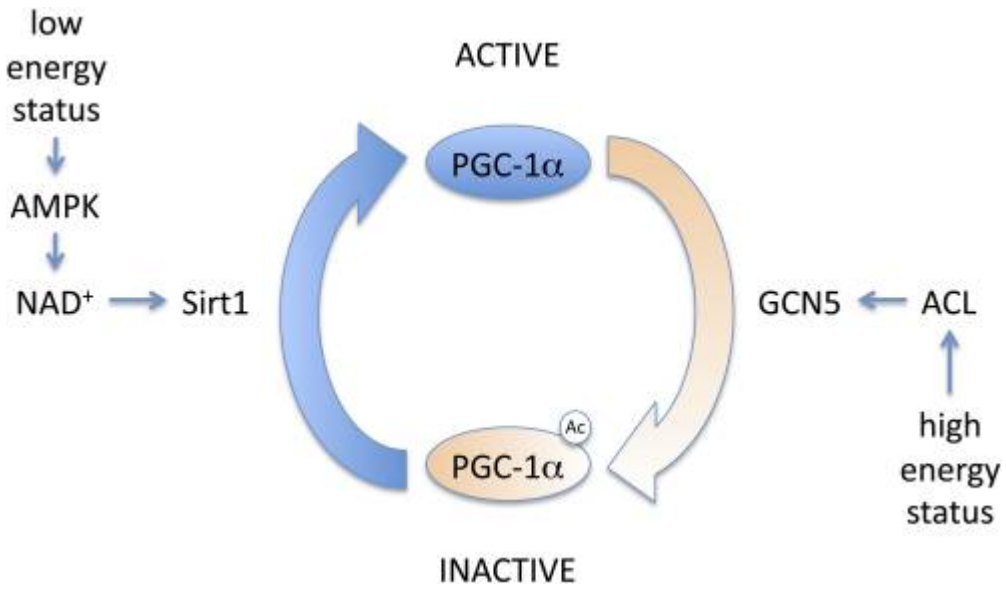

Figure 8. Acetylation of PGC1a suppresses its activity. AMP-activated protein kinase (AMPK) increases NAD^+ levels and activates Sirt1 by mediating its deacetylation. During high energetic levels, GCN5 acetylates and inhibits PGC-1α; ATP-citrate lyase (ACL) provides the acetyl-CoA group (rate-liming factor for GCN5-induced acetylation of PGC-1α). Modified by (Fernandez-Marcos and Auwerx, 2011)

2.3. PPAR ligands and Agonists

PPARs respond to a broad range of endogenous ligands such as steroids, retinoids, long-chain fatty acid and other cholesterol metabolites (Chandra et al., 2008; Mozaffarian et al., 2015). However, it remains unclear whether there is specificity of certain endogenous ligands for activation of any of the three PPAR isoforms (Puigserver et al., 1999).

As PPARs control cellular lipid metabolism, they were uniquely suited as ideal pharmacologic targets in clinical practice. Several pharmacologic agents, such as lipid-

lowering (fibrates) and insulin-sensitizing compounds (thiazolidinediones or TZDs) can stimulate PPARα and PPARγ, respectively (Madrazo and Kelly, 2008).

3.2 *2.3.1 PPARα agonists*

PPAR-α agonists include fibric acid derivatives (fibrates) such as fenofibrate, bezafibrate, ciprofibrate, and clofibrate. Fibrates are widely used in clinical practice as lipid-lowering agents for treating dyslipidemias such as primary hypertriglyceridemia, combined hyperlipidemia, and primary hypercholesterolemia (Staels et al., 1998) (Fruchart, 2009).

Despite their beneficial anti-hyperlipidemic effects, the fibrates are reported to have no effect on reducing the risk of HF in patients with diabetes (ACCORD Study, 2010; Rubins et al., 1999). An older double-blind study (Rubins et al., 1999) in men with coronary heart disease treated with gemfibrozil showed that fibrates (Jun et al., 2010; Rubins et al., 1999) reduce coronary events but they did not show any significant difference in the prevalence of HF .

3.3 *2.3.2. PPARβ/δ agonists*

The effect of PPAR-ß/δ agonists has been tested primarily in experimental animal models. PPAR-ß/δ agonists increase fatty acid uptake in skeletal muscle and adipose tissue (Group et al., 2010)suggesting a potential effect in treating metabolic syndrome. Currently, telmisartan is one drug in the market that targets PPARδ, as well as PPARγ (Amano et al., 2012). Telmisartan is indicated for hypertension, as it is an

angiotensin II receptor blocker (ARB), but it can also partially target PPAR*δ* (Amano et al., 2012)

3.4 2.3.3. *PPARg agonists*

PPAR-γ agonists include TZDs, which increase the capacity for fat storage in adipose tissue. They alleviate the effects of lipolysis on muscle and hepatic insulin resistance. TZDs, such as rosiglitazone, pioglitazone, and troglitazone bind to the PPARγ-RXR heterodimer and enhance transcriptional activity by preventing interactions with corepressor. TZDs are widely used in patients with T2D to reduce HbA1c, increase insulin sensitivity in adipose tissue, skeletal muscle, and liver either by increasing adiponectin levels (Tonelli et al., 2004; Yu et al., 2002) or by increasing glucose uptake (Hauner, 2002). Additionally, PPARγ agonists decrease the levels of circulating inflammatory markers (Giannini et al., 2004).

Despite these beneficial actions, TZDs have elicited adverse cardiovascular-related effects. Pioglitazone was associated with an increased risk of bladder cancer (Lewis et al., 2015) and troglitazone has been discontinued since 2000 due to its hepatotoxic effects (Kaul et al., 2010). The PROactive study and a meta-analysis of randomized trials supported that despite increased heart failure prevalence in T2D patients treated with pioglitazone, the drug decreased subsequent all-cause mortality, MI, or stroke (Erdmann et al., 2007; Lincoff et al., 2007).

A retrospective study that included 17 million patients concluded that TZD was associated with a 60% increased risk for HF due to direct cardiovascular effects or other

indirect effects such as salt and water retention (Guan et al., 2005) (Delea et al., 2003; Graham et al., 2010).

Compared to other TZDs, rosiglitazone was linked with a higher risk of HF and other cardiovascular-related events, like stroke and MI (Graham et al., 2010). A meta-analysis of randomized trials using rosiglitazone treatment revealed strong association between rosiglitazone and increased risk for MI (Nesto et al., 2003). This finding was consistent with another study that correlated TZDs with HF which noted a high risk (43%) of MI in patients who received rosiglitazone (Nissen and Wolski, 2007).

On the other hand, the RECORD trial revealed a link of that rosiglitazone treatment to an increased risk for heart failure, but not for MI, stroke, or cardiovascular mortality (Home et al., 2009; Mahaffey et al., 2013).. A 2010 AHA/ACCF Science Advisory recapitulated TZDs-cardiovascular risks based on more recent clinical trials and meta-analyses and concluded that an association between rosiglitazone and HF could not be clearly verified (Kaul et al., 2010). In 2013 the FDA retracted restrictions on rosiglitazone

3.5 2.3.4 *Dual PPARα/γ agonists*

Given that PPARγ agonists were associated with heart failure, a fourth class of PPAR agonists with the name dual-PPARα/γ agonists or glitazars, was developed to combine the beneficial effects of PPARα and PPARγ agonism and alleviate simultaneously insulin resistance (PPAR-γ action) and atherogenic dyslipidemia (PPAR-α action) **(Figure 9).** Although glitazars improved metabolic parameters (Gross and Staels, 2007), they paradoxically aggravated congestive heart failure in patients with type 2

diabetes (Staels and Fruchart, 2005) . The mechanisms that underlie these side effects still remain unknown. (Pol et al., 2015).

Historically, the first dual agonist was the farglitazar, which was discontinued due to the evidence of edema (Henke et al., 1998). The retraction of farglitazar was followed by discontinuation of ragaglitazar (Lohray et al. 2001), and tesaglitazar (Hegarty et al., 2004) trials, due to carcinogenicity in rodent toxicity models and elevated creatinine levels in serum. Similarly, muraglitazar development was discontinued due to higher rates of all-cause mortality compared to pioglitazone; and also higher incidences of edema, HF, and increased weight gain rates (Kendall et al., 2006) **(Table 5).**

Saroglitazar is a representative dual PPARα/γ agonist with impressive lowering effects on serum lipids and glucose.**(Table 6).** 23 male and 11 female patients with type T2D and dyslipidaemia were treated with the dual PPARα/γ agonist (Saroglitazar), had a significant reduction in total cholesterol, LDL cholesterol and plasma triglycerides (Chatterjee et al., 2015). However, their HDL-cholesterol level remained unaltered. These findings combined with the respective ones from older studies for other dual PPARα/γ agonists such as Aleglitazar, Muraglitazar and Tesaglitazar .presented the high efficiency of dual PPARα/γ agonists against both hyperglycemia and hyperlipidemia (Stirban et al., 2016) (Harrity et al., 2006; Wallenius et al., 2013)

Only, saroglitazar is still in development. It was approved in June 2013 for clinical use in India (Sharma A, 2014). Saroglitazar has a higher affinity for PPAR*α* than PPAR*γ*. It's still early to associate saroglitazar with any cardiovascular consequences, although its product information contains a warning and precautionary statement with its use in type II diabetics with congestive HF(Discovery Z. Lipaglyn—Product Information).

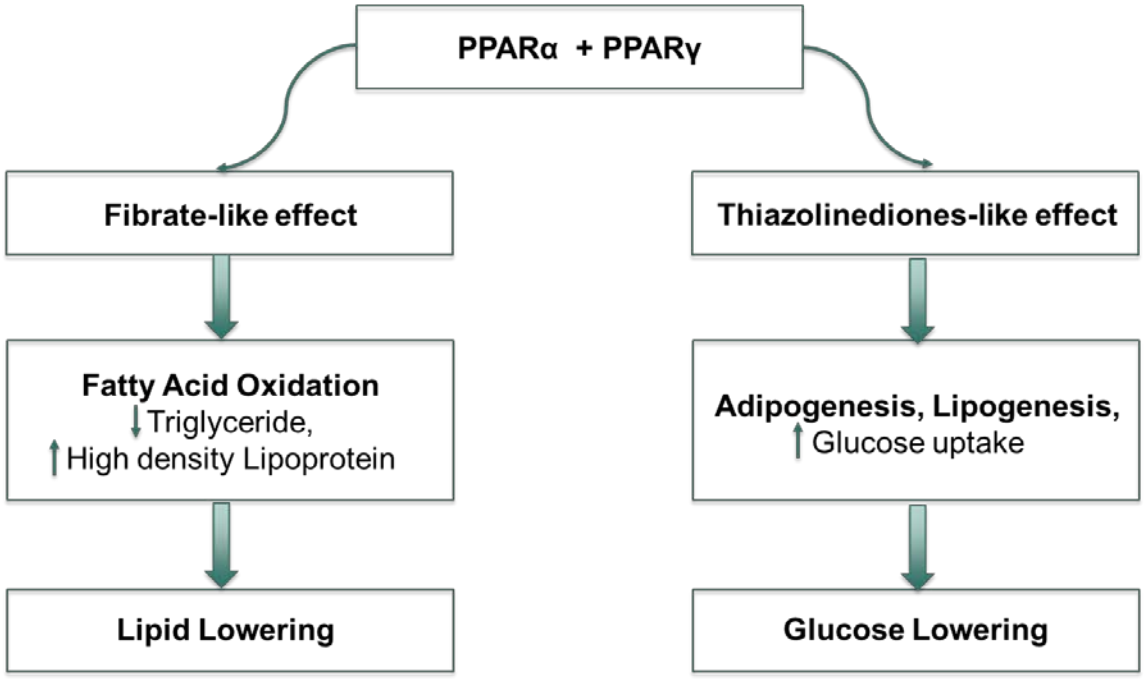

Figure 9. Mechanism of action of Dual PPARα/γ agonists. Modified by

Dual PPAR-α/γ activators that have been in clinical development		
Molecule	**Company**	**Comments**
Muraglitazar [25]	Bristol-Myers Squibb (United States of America)	Approved then withdrawn from market in 2006 due to CV events (heart failure)
Tesoglitazar [26]	AstraZeneca (United Kingdom)	Discontinued following phase III trials due to elevated creatinine levels associate with decreased glomerular filtration
Ragaglitazar [27]	Novo Nordisk (Denmark) (outlicensed by Dr. Reddy's	Discontinued 2002 due to bladder tumors in rodents
Chiglitazar [28]	Shenzhen Chipscreen, (China)	Development suspended in Phase II
Cevoglitazar [29]	Novartis (Switzerland)	Discontinued in 2008 due to the lack of a sufficiently positive benefit/risk
Aleglitazar [30]	Hoffman-La-Roche (Switzerland)	Halted at Phase III in 2013 due to GI bleeding, bone fractures, heart failure
TAK-559 [31]	Takeda (Japan)	Discontinued in 2005 in Phase III following abnormalities in liver enzymes
Naveglitazar [32]	Eli Lilly (USA)	Discontinued in 2006 due to adverse preclinical findings in rodents
AVE-0847	Sanofi-Aventis (France)	Development terminated due to glitazar: reprioritization of product portfolio
Sipoglitazar [33]	Takeda (Japan)	Discontinued in 2006 due to serious safety concerns

Table 5. Dual PPARα/γ agonists that have been in clinical development. Modified by www.ijpcs.net

Lab parameters	Baseline Mean ± SD	Follow up Mean ± SD	Mean change ± SD	P value
Triglycerides (mg/dL)	346.78 ± 246.01	154.00 ± 127.73	−192.78 [±91.06]	0.0001
Non HDLc (mg/dL)	157.34 ± 53.44	108.63 ± 34.47	−48.72 [±17.09]	<0.0001
LDLc (mg/dL)	108.34 ± 46.94	84.31 ± 23.26	−24.04 [±16.14]	0.0048
Total Cholesterol (mg/dL)	195.91 ± 56.97	147.75 ± 36.08	−48.16 [±17.32]	<0.0001
HDLc (mg/dL)	38.88 ± 9.79	39.34 ± 11.37	+0.47 [±3.45]	0.7836
TG/HDL ratio	9.60 ± 7.84	4.30 ± 4.12	−5.30 [±2.82]	0.0006
FPG (mg/dL)	160.53 ± 53.71	123.82 ± 54.91	−36.71 [±20.06]	0.0007
PPG (mg/dL)	243.68 ± 114.59	177.39 ± 60.87	−66.29 [±34.71]	0.0005
HbA1c (%)	8.34 ± 1.58	7.21 ± 1.33	−1.13 [±0.43]	<0.0001

Table 6. Laboratory values of 34 patients, treated with Saroglitazar (dualPPARα/g agonist), in a dose of 4 mg daily, resulted in significant improvement in both glycaemic and lipid parameters. Modified by www.ijpcs.net

CHAPTER THREE
3. Effects of PPAR activation on Cardiac metabolism

3.1 3.1 Physiology of Cardiac Metabolism

In order to perform a vast amount of work that includes continuous contraction, the cardiac muscle has high energetic demands (Lopaschuk et al., 2010; Opie, 1969). Accordingly, it must continuously generate ATP at a high rate. Heart utilizes multiple sources that fuel ATP synthesis, such as FA, carbohydrates, amino acids and ketone bodies (An et al., 2005; Opie, 1969)(An et al., 2005; Opie, 1969). Among these, carbohydrates and FAs are the major fuels from which the heart derives most of its energy. In a basal aerobic setting, 30% of energy in heart is produced by glucose and lactate utilization and the rest 70 % of energy and ATP generation is through FA oxidation (An et al., 2005; Myrmel et al., 1992; Opie, 1969). Given that the heart does not have the ability to synthesize all the amount of FA that it needs to produce energy, it increases its FA pool from exogenous supplies. FAs are released from the adipose tissue and after making complexes with albumin are supplied to heart as free fatty acids (FFAs). Alternatively, FAs are provided from breakdown of either endogenous or lipoprotein-derived cardiac triglycerides (TG) contained in circulating lipoproteins (VLDL and chylomicrons). Lipoprotein lipase (LPL), which is located at the apical side of endothelial cell (EC) surface of the coronary lumen, hydrolyzes circulating TG to release FA that are then taken up by cardiomyocytes via FA transporters. FAs re first stored as TG components and then they are hydrolyzed to enter the β-oxidation process in

mitochondria, to generate acetyl-CoA, which is further oxidized to generate ATP **(**Lopaschuk et al., 2010**;** Neely and Morgan, 1974**;** Opie, 1969**)**

ATP synthesis mainly occurs in mitochondria, where mitochondrial oxidative phosphorylation takes place t. Only 5% of the ATP is derived from glycolysis and GTP formation in the tricarboxylic acid (TCA) cycle. The heart has a low ATP content (5 mol/g wet wt) and high rate of ATP hydrolysis (30 mol/g wet wt1 min1 at rest). Under normal conditions, complete turnover of the myocardial ATP pool occurs every 10 seconds (Neely and Morgan, 1974; Opie, 1969).

3.2. Glucose metabolism in heart

Glucose metabolism including oxidation of pyruvate has minor contribution in cardiac energy production (30%). Glucose enters the cardiac myocyte by diffusion through glucose transporters (GLUT). GLUT1 and GLUT4 are the expressed isoforms in the heart; GLUT1 mediates insulin-independent and GLUT4 mediates insulin-dependent glucose transport. In the cytoplasm, glucose is phosphorylated by hexokinase to glucose-6-phosphate (G-6-P) and it forms pyruvate via glycolysis pathway. Alternatively, pyruvate is formed via lactate oxidation, catalyzed by Lactate dehydrogenase (LDH) (Gertz et al., 1988; Stanley et al., 1997) (Doenst et al., 2013). Pyruvate-dehydrogenase (PDH) that is located in mitochondrial matrix (Patel and Korotchkina, 2006), is regulated allosterically and it is inactive when phosphorylated by the PDH-kinase (PDK4). The expression of PDK4 is rapidly induced by fasting, diabetes, and PPAR activation

The oxidation of pyruvate and the PDH activity in cardiomyocytes are decreased by high FAO-rates of fatty acid -oxidation. Alternatively, pyruvate oxidation is increased by suppression of FAO (Lopaschuk et al., 1994; Schwenk et al., 2008) (**Figure 10**).

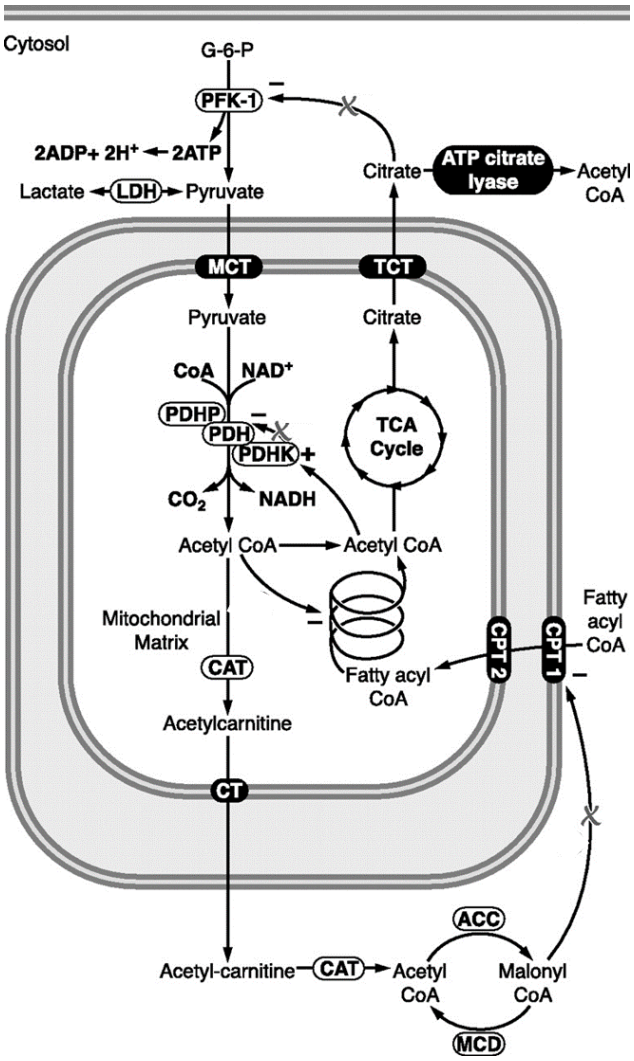

Figure 10. Glycolysis and cardiac glucose oxidation. Glycolysis of G-6-P to pyruvate is mediated by Phosphofructokinase (PFK1). Pyruvate enters mitochondria via monocarboxylate transporter MCT-1 that catalyzes the rapid transport across the plasma membrane of many monocarboxylates such (lactate, pyruvate). Pyruvate is further oxidized and its oxidation is catalyzed by the multienzyme complex pyruvate dehydrogenase (PDH), whose activity is highly regulated by its products (acetyl-CoA, NADH) and by phosphorylation of its E_1subunit. The increased production of acetyl CoA derived from fatty acid β-oxidation reduces glucose (pyruvate) oxidation via the activation of pyruvate dehydrogenase kinase (PDK) which phosphorylates and inhibits pyruvate dehydrogenase (PDH). PDK is also activated by increased mitochondrial NADH/NAD+ ratios in response to increased fatty acid β-oxidation. The increased supply of fatty acid β-oxidation derived acetyl CoA to the TCA cycle can decrease glycolysis because of the inhibitory action of citrate [a TCA cycle intermediate which passes to cytosol via the tricarboylate transporter(TCT)] on phosphor-fructo-kinase-1 (PFK-1) The inhibition of

glucose (pyruvate) oxidation is the major inhibitory effect of fatty acid β-oxidation on the glucose metabolism. The increased generation of acetyl CoA derived from pyruvate oxidation inhibits fatty acid β-oxidation, as the terminal enzyme of fatty acid β-oxidation, 3-keto-acyl CoA thiolase, is inhibited by acetyl CoA. Acetyl CoA derived from pyruvate oxidation due to the activity of carnitine acetyl transferase (CAT) and formation of acetyl-carnitine is also a substrate for carnitine:acetyl-carnitine transferase (CACT). CACT exports acetyl-carnitine to the cytosol, where it is re-converted to acetyl CoA through the activity of cytosolic CAT. The acetyl CoA in cytosol is a substrate for acetyl CoA carboxylase (ACC), which can increase the production of malonyl CoA, an endogenous inhibitor of CPT I, and therefore decrease fatty acid β-oxidation when glucose oxidation is increased. Modified by (Lopaschuk et al., 2010)

3.3 Cardiac FA metabolism

3.3.1 FA uptake and oxidation

FAs that will be utilized for β-oxidation are derived from either plasma free fatty acids bound to albumin or fatty acids released from TG contained in chylomicrons or very-low-density lipoproteins (VLDL) (Hauton et al., 2001) (Goldberg et al., 2009). The transportation of fatty acids inside the cardiomyocytes is facilitated by the CD36/FATP transporters or it will be done via passive diffusion **(Figure 11)** (Schwenk et al., 2008). Once in cytosol of the cardiac myocyte, fatty acids are esterified to fatty acyl CoA by fatty acyl CoA synthase (FACS) (Schwenk et al., 2008; van der Vusse et al., 2000). Fatty acyl-CoAs are then be stored after esterification to complex lipids such as TG, or they will be used for ATP production. The latter takes place in mitochondria. In order to enter mitochondria, the acyl group is exchanged with carnitine that leads to formation of long-chain acylcarnitine is catalyzed by carnitine palmitoyl-transferase (CPT) 1 (McGarry and Brown, 1997). Acylcarnitine is then shuttled into the mitochondria, where it is converted back to fatty acyl CoA by CPT 2 and carnitine returns to the cytosol **(Figure 11)** (Weis et al., 1994).

CPT 1 activity is regulated allosterically by malonyl CoA, which inhibits it.(Zierz and Engel, 1987). Cardiac malonyl CoA concentrations are dependent on the balance between its synthesis from acetyl CoA via acetyl CoA carboxylase (ACC) (Lopaschuk GD, 1994.) and its degradation via malonyl CoA decarboxylase (MCD) (Sakamoto J, 2000.). A key determinant of ACC activity in the heart is the activity of AMPK (Dyck and Lopaschuk, 2006). It has been demonstrated by Lopaschuk et al. that in rat hearts AMPK is able to phosphorylate ACC, resulting in an almost complete loss of ACC activity (Kudo et al., 1996). Moreover, heart ACC seems to interact with the 2 isoform of the catalytic subunit of AMPK (Dyck JR, 1999.), suggesting a tight association between AMPK and ACC in the heart. This outcome supports a close correlation which eventually connects increased AMPK activity with decreased ACC activity, and increased fatty acid β-oxidation in the heart **(Figure 11)** (Baartscheer et al., 2005).

Upon mitochondrial FA uptake and the conversion to fatty acyl CoA, the majority of this fatty acyl CoA then undergoes the fatty acid β-oxidation cycle that involves the sequential metabolism of acyl CoAs by acyl CoA dehydrogenase, enoyl CoA hydratase, L-3-hydroxyacyl CoA dehydrogenase, and 3-ketoacyl CoA thiolase (3- KAT) Each cycle of fatty acid β-oxidation leads in the shortening of the fatty acyl moiety by two carbons, as well as the production of acetyl CoA that is further oxidized in the TCA cycle and generates high energy-molecules such as flavin adenine dinucleotide (FADH2), and nicotinamide adenine dinucleotide (NADH) (Schultz H, 2007). These molecules are the major source of electrons for the Electron Transport Chain (ETC) resulting in a protein gradient across the inner mitochondrial membrane which finally drives ATP synthesis from ATP synthase **(Figure 11).**

Mitochondrial thioesterase (MTE) can cleave long-chain acyl CoA to fatty acid anions (FA^-), which may leave the mitochondrial matrix via uncoupling proteins. Uncoupling proteins (UCP1–UCP5) are a family of mitochondrial transport proteins that provide an alternate means for the reentry of protons from the inter-membrane space to the mitochondrial matrix that is not coupled to the synthesis of ATP. These inner mitochondrial membrane-bound proteins have been shown to uncouple ATP synthesis from oxidative metabolism, subsequently dissipating energy as heat (Rousset et al., 2004).

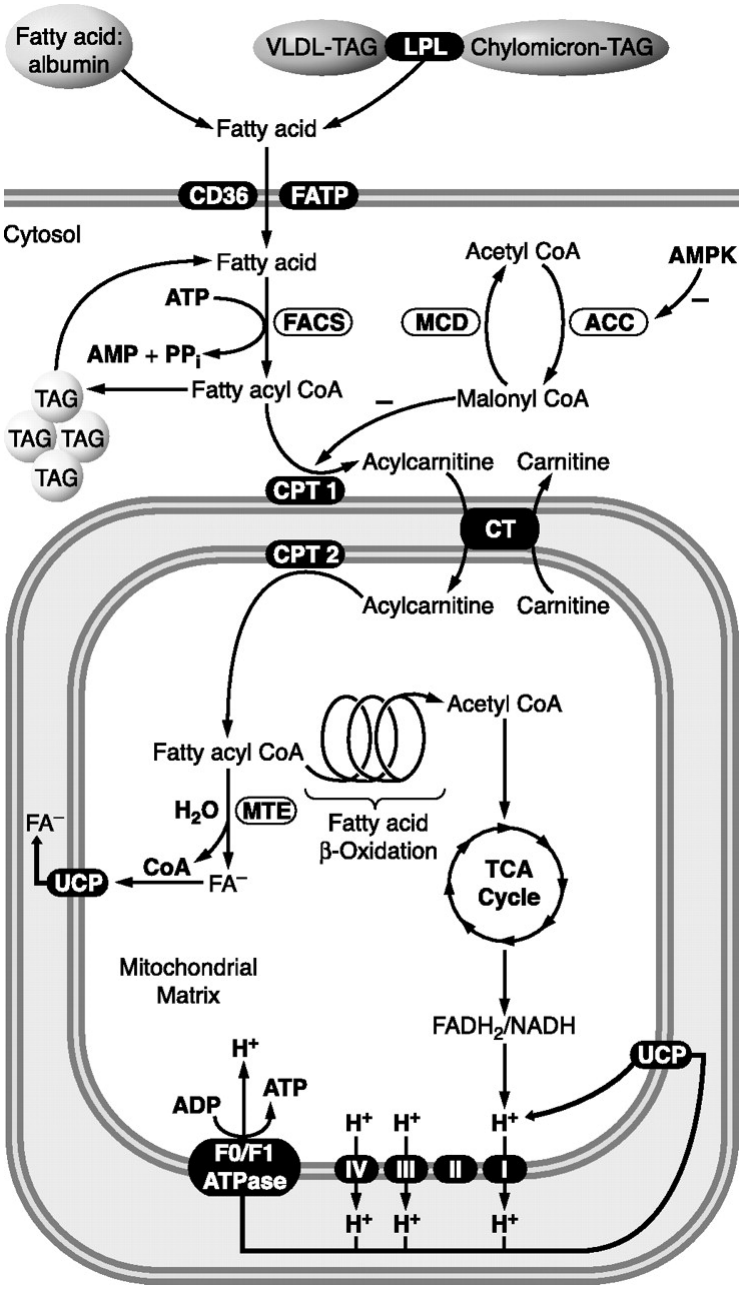

Figure 11. Cardiac fatty acid uptake and oxidation. Fatty acids source of heart is either plasma fatty acids bound to albumin or fatty acids contained within chylomicron or very-low-density lipoproteins (VLDL) triacylglycerol (TAG). Fatty acids are taken up by the heart via diffusion or via CD36/FATP transporters. In the cytosol fatty acids are esterified to fatty acyl CoA by fatty acyl coA synthase (FACS). Fatty acyl-CoAs can then be esterified to complex lipids such as TAG, or the acyl group is transferred to carnitine via carnitine palmitoyltransferase (CPT) 1. The acylcarnitine is then shuttled into the mitochondria, where it is re-converted to fatty acyl CoA by CPT 2. The fatty acyl CoA undergoes the fatty acid β-oxidation cycle, producing acetyl CoA, NADH, and FADH2. Mitochondrial thioseterase (MTE) is an enzyme that cleaves long-chain acyl CoA to fatty acid anions (FA−), which may leave the mitochondrial matrix via uncoupling protein. Modified by (Lopaschuk et al., 2010)

3.3.2 Transcriptional Control of Cardiac Fatty Acid -Oxidation

PPARs and PGC1α regulate transcription of most of the enzymes of fatty acid β-oxidation (Desvergne et al., 2006; Finck and Kelly, 2002, 2007; Huss and Kelly, 2004; Madrazo and Kelly, 2008).

3.3.2.1 PPARα in cardiac FAO

PPARα is abundantly expressed in heart muscle and its target genes include those encoding proteins involved in fatty acid uptake (FAT/CD36, FATP1), cytosolic fatty acid binding and esterification (FABP, FACS, glycerol-3-phosphate acyltransferase, diacylglycerol acyltransferase), malonyl CoA metabolism (MCD), mitochondrial fatty acid uptake (CPT1), fatty acid -oxidation [very-long-chain acyl CoA dehydrogenase, long-chain acyl CoA dehydrogenase, medium-chain acyl CoA dehydrogenase (MCAD), 3-KAT], mitochondrial uncoupling [including mitochondrial thioesterase (MTE-1) and uncoupling proteins (UCP2, UCP3)], and glucose oxidation [PDH kinase (PDK) 4]

Numerous studies have shown the regulatory role of PPARα on fatty acid metabolism either with a “loss of function” or a “gain of function” approaches. Finck et al. showed that constitutive overexpression of PPARα in mouse heart leads in a remarkable increase in cardiac fatty acid uptake, fatty acid β-oxidation and lipid overload because of the increased expression of the enzymes involved in these pathways (Finck et al., 2002). On the other hand, deletion of PPARa (PPARa-/-) leads to reduced expression of FAO-related genes and FAO process (Watanabe et al., 2000), which is accompanied by a a parallel increase in glucose oxidation (Campbell et al., 2002).

3.3.2.2 PPARγ in cardiac FAO

PPARγ has low expression levels in the heart. PPARγ activation can dramatically decrease circulating fatty acid levels (Yang and Li, 2007) (379, 703). PPARγ agonists, such as the Thiezolinediones, are widely used as insulin-sensitizing agents, which may in part be due to lowering circulating fatty acid levels. However, direct PPAR overexpression in the heart has recently been shown to produce a phenotype similar to PPAR overexpression (i.e., increased expression of fatty acid -oxidation genes, but an increased expression of glucose transporters) (Son et al., 2007).

3.3.2.3 PGC-1 in cardiac FAO

PGC-1s are transcriptional co-activators for several nuclear receptors including PPARα and PPARγ.

The most common PGC-1 isoforms, PGC1α and PGC1β are mostly expressed in tissues enriched in mitochondrial systems with high oxidative capacity as well as in heart, slow-twitch skeletal muscle fibers, BAT and kidney (Lin et al., 2002; Puigserver et al., 1998). PGC-1 is expressed in response to physiological conditions demanding mitochondrial ATP synthesis, such as stress, cold exposure, short-term exercise, and fasting (Lin et al., 2002). Cardiac PGC-1α expression is induced after birth, when cardiac muscle starts showing preference to mitochondrial fatty acid oxidation as the main source of energy production (Lehman et al., 2000). PGC-1α functions as the master regulator of mitochondrial biogenesis by regulating the expression of the mitochondrial transcription factor α which in turn controls the transcription and replication of the mitochondrial genome.(Gleyzer et al., 2005; Kelly and Scarpulla, 2004; Scarpulla, 2002)**.** Furthermore, it has been shown that PGC1α coordinates activation of nuclear and mitochondrial genes driving OXPHOS (Lehman et al., 2000) (**Figure 12).**

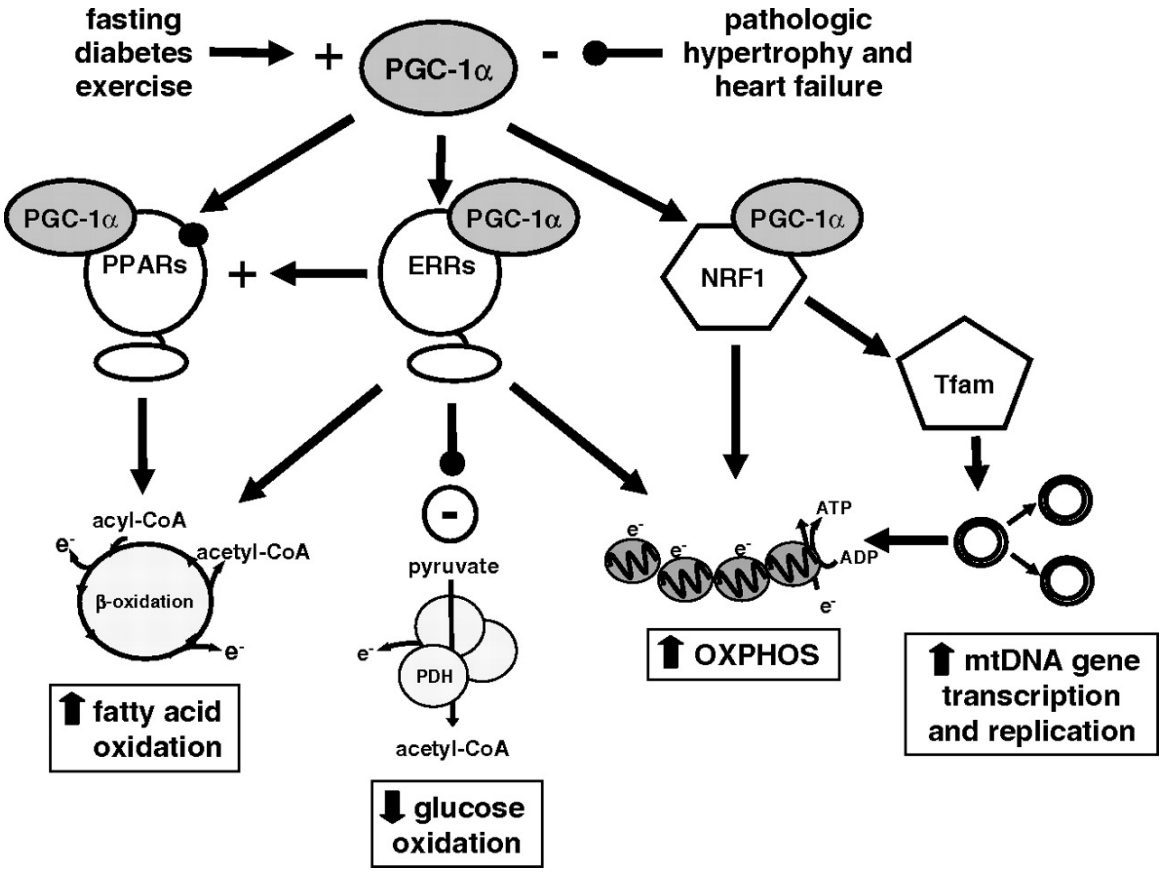

Figure 12. The PGC-1 gene regulatory cascade. PGC-1α coactivates PPARs to promote the expression of target genes involved in fatty acid β-oxidation. PGC-1α coactivates also other nuclear receptors such as ERRs to enhance expression of fatty acid oxidation and OXPHOS proteins and inhibit glucose oxidation and NRF-1 to increase expression of nuclear- and mitochondrial-encoded enzymes involved in OXPHOS. Specifically, PGC-1α induces mitochondrial transcription factor (Tfam) that subsequently promotes replication of mitochondrial DNA (mtDNA).Modified by (Finck and Kelly, 2006)

3.3.2.4 The Critical Role of PGC-1α in Cardiac Metabolism

Genetic gain-of-function and loss-of-function studies in transgenic mice have demonstrated the critical role of PGC-1α in heart in vivo. Inducible, **cardiac-specific overexpression** of PGC-1α revealed its' role in the activation of cardiomyocyte mitochondrial biogenesis (Lehman et al., 2000).

Gain-of-function: Overexpression of PGC-1α in **neonatal heart** caused dramatic mitochondrial growth within the cardiomyocytes. Moreover, acute overexpression of

cardiac PGC-1α in **adult** mice graded a modest mitochondrial response and, after several weeks, resulted to cardiomyopathy associated with structural mitochondrial abnormality. The pathological mechanism involves dysregulated mitochondrial metabolism but it still remains unknown (Finck and Kelly, 2006).

Loss-of-function: Loss of function studies further support the critical role of PGC-1α in regulating mitochondria. Mouse models with targeted gene deletion (knockout, KO) exhibit moderate, age-related base-line cardiac dysfunction as determined by 2D-echocardiography (Arany et al., 2005). Heart-tissue isolated from these mice also exhibit deficiency to maintain ATP and phosphocreatine homeostasis in response to β-adrenergic activation by dobutamine as determined by NMR spectroscopy. These metabolic defects are associated with decreased expression of genes implicated in mitochondrial FAO-pathway, the TCA cycle, and OXPHOS.

On the other hand, another line of PGC-1α–deficient mice do not display dysfunction under normal conditions as it was shown by echocardiography. However, they exhibit impaired heart rate response to exercise and β-adrenergic stimuli. (Leone et al., 2005). The discrepancy in the phenotypes of the two αMHC-PGC1α-/- mouse-lines of mice remain unknown.

Heart failure: Cardiac hypertrophy that progressively leads to heart failure, is characterized by decreased expression of PGC1α and derangements in mitochondrial metabolism (Arany et al., 2006a; Garnier et al., 2003; Lehman et al., 2000; Sano et al., 2007; Sano M et al., 2004; van den Bosch et al., 2005). This gene regulatory response has been shown to be a primary event in these pathological conditions as it occurs at the early stages. Consistently, three studies showed that the expression of ERRα,

PPARα and PGC1α is decreased in cultured cardiomyocytes treated with hypertrophic agonists (Arany et al., 2006a; Barger et al., 2000; Sano M et al., 2004)**.** In contrast, PGC-1α expression is increased in physiological forms of hypertrophy that occurs either in postnatal growth51 or after physical activity (A. Wende and D. Kelly, unpublished data, 2005) **(Figure 13)**

Heart failure in humans: A big number of studies support that metabolism is impaired in the failing heart, given that during the cardiac remodeling, the heart changes its preference from fatty acid to glucose utilization–(Heusch et al., 2014) This switch is associated with decreased levels of high energy phosphate reserves (Doenst et al., 2013), suggesting that the failing heart is a fuel-deficient organ (Hill and Schulze, 2014). It has been shown that, heart failure in humans suppresses the transcription of a broad range of metabolic enzymes and does not have selective inhibitory function on expression of fatty acid-oxidation enzymes, nor upregulating function. However, DNA microarray data from patients with heart failure showed downregulation of PGC-1 target genes that participate in fatty acid metabolism. Moreover, a number of genes controlled by the estrogen-related receptor (ERR) that interacts with PGC-1, were also downregulated in heart failure. The changes in these target genes which transcription is promoted by ERR and PGC-1 were positively correlated with LV ejection fraction, proposing that both PGC-1 and ERR may drive the decrease in the mRNA for genes encoding enzymes in the fatty acid metabolism pathway of human heart during heart failure (Sihag et al., 2009).

In conclusion, these data suggest that PGC-1 plays a crucial role in the regulation of a high-oxidative-capacity mitochondrial system.

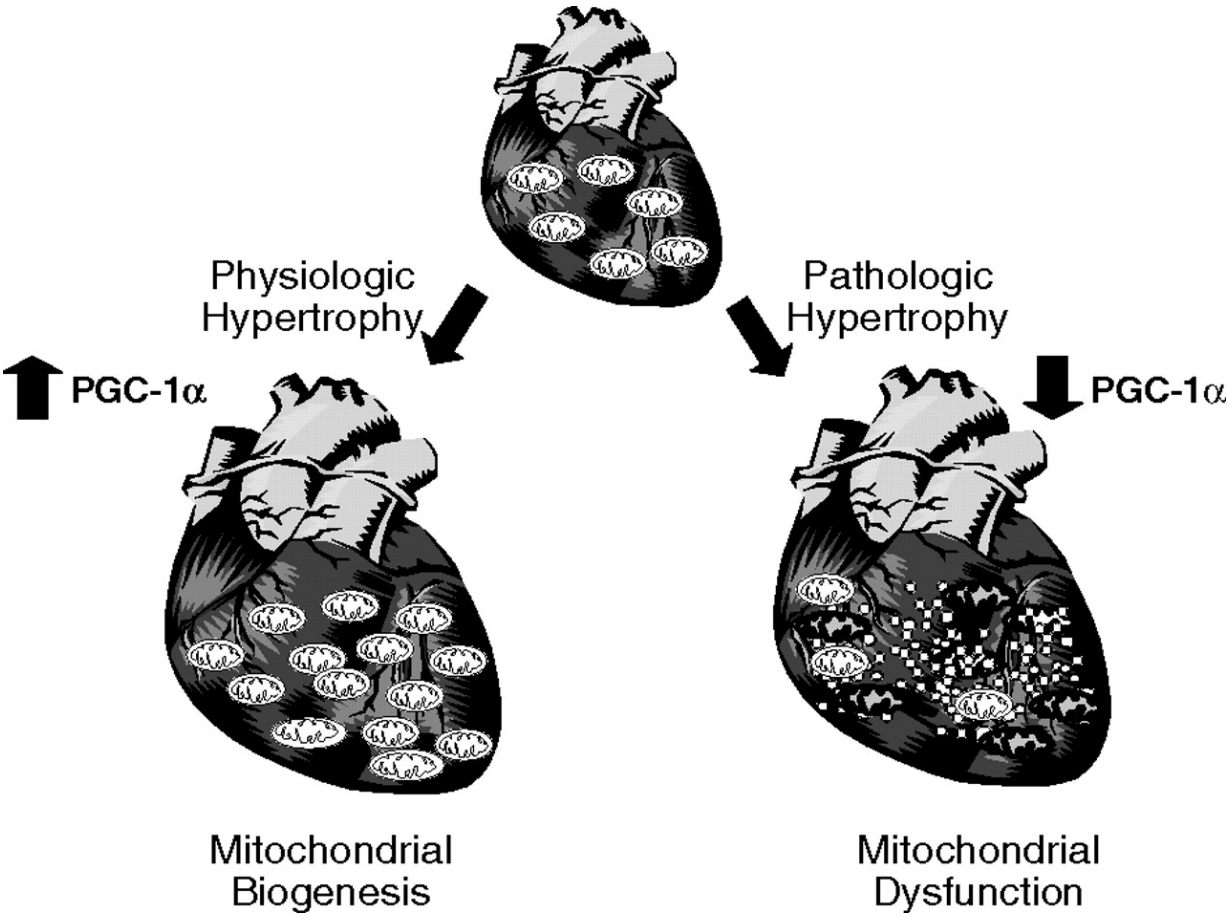

Figure 13. Post-natal maturation or under energy demanding conditions (i.e cold exposure, exercise) is characterized by increased PGC-1α expression and subsequently mitochondrial biogenesis and oxidative capacity. Cardiac hypertrophy is associated with decreased PGC-1α and mitochondrial impairment. Damaged and dysfunctional mitochondria lead to intracellular lipid accumulation and reactive oxygen species production. Mitochondrial dysfunction leads the cardiac muscle to an energy-deficient state. Modified by (Finck and Kelly, 2006)

3.4. Alterations of Cardiac FA Metabolism and Cardiac Dysfunction

Obesity, diabetes and other metabolic diseases lead to increased cardiac FA uptake and decreased oxidation. This phenotype is driven by circulating levels of FFAs and adipokines, the expression of fatty acid transporters and changes in the regulation of cardiac FAO at the enzymatic, as well as at the transcriptional level. These alterations in

cardiac FA metabolism can have a major impact on cardiac function and efficiency under pathological conditions (Atkinson et al., 2003) (Murthy and Shipp, 1977).

One of the crucial events, that is involved in the intramyocardial TG accumulation is the Increased fatty acid uptake which has been identified in obesity and diabetes.This could be also be dependent on higher expression of sarcolemmal fatty acid transporters. Cardiac fatty acid uptake is increased in the insulin-resistant, obese Zucker rats, which was associated with increased expression of FAT/CD36 localized in the sarcolemma with no significant change in total cellular content (Luiken et al., 2001; Murthy and Shipp, 1977). Increased translocation of FAT/CD36 to the sarcolemma has also been shown in hearts from db/db mice (Carley AN, 2007).

The mechanism resulting in the relocation of fatty acid transporters to the sarcolemma is unknown. It has been sugested that hyperinsulinemia is linked to obesity or diabetes-induced insulin resistance, as insulin induces the translocation of CD36/FAT to the sarcolemma in rat cardiac myocytes (Koonen et al., 2005) (Luiken et al., 2004).

In conclusion, obesity and diabetes increase intramyocardial TG stores, partially due to elevated circulating FFAs and TG, or increase in fatty acid uptake ,or increased intramyocardial TG synthesis due to increased myocardial CoA and long-chain acyl CoA synthesis (Reibel et al., 1981)..

Moreover a number of experimental studies suggested that reduced rates of fatty acid β -oxidation has a crucial role in the accumulation of intramyocardial lipid metabolites (How et al., 2005) (How et al., 2006) (Sharma et al., 2004; Young et al., 2002). Except the general preference of the heart to produce energy via the FAO process, Lopaschuk et al. have demonstrated that mice subjected to diet induced obesity result in fatty acid

β -oxidation being the major supplier of energy for the heart (Lopaschuk et al., 2010). Conclusively, decreased rates of fatty acid β-oxidation could probably lead to severe deficiency in energy-production which is accompanied by an excessive fuel storage that develops a toxic accumulative manner.and finally cardiac lipotoxicity.

CHAPTER FOUR

4. PPAR activation and Cardiac Lipotoxicity

4.1. Lipid-induced Pathology of Heart (“Cardiac Lipotoxicity”)

The cardiac pathology related to intramyocardial accumulation of lipid metabolites (acyl-carnitines, diacylglycerol, triaglycerides and ceramides) in obesity and diabetes is inked

to contractile dysfunction, cardiac fibrosis, left ventricular systolic dysfunction, and impaired diastolic volume (Finck et al., 2003; Hodanova, 1976; Schaffer, 2003; Yagyu et al., 2003).The investigation of this phenomenon in experimental studies by using rodent animal models generated the term which is noted as “cardiac lipotoxicity,” Elevated intramyocardial TG and ceramide concentration in hearts of obese Zucker diabetic rats led to cardiac dilatation and abnormal contractile function (Zhou et al., 2000). In this study, treatment of Zucker rats with the PPARγ agonist Troglitazone reduced plasma TAG levels and decreased cardiac ceramide accumulation, and finally restored cardiac function to normal levels.

Furthermore, other studies revealed that cardiac overexpression of fatty acyl coA synthase (FACS) or GPI-anchored lipoprotein lipase (LPL), resulted in lipid accumulation, cardiac hypertrophy, LV chamber enlargement and impaired contractility compared with wild-type subjects (Yagyu et al., 2003). It has been suggested that the downregulation of PPARα and/or PPARγ diminishes expression of FAO-related genes resulting in cardiac lipid accumulation that impairs the normal cardiac function (Young et al., 2002). In type 2 diabetic patients with heart failure, tremendous increase in cardiac lipid accumulation and impaired cardiac-FAO were reported (Kolwicz et al., 2013).

The contribution of reduced FAO to cardiac lipotoxicity in the setting of metabolic diseases, increases circulating levels of free fatty acids (FFAs) and very-low-density lipoprotein-triacylglycerol (VLDL-TAG) and leads cardiomyocytes to an excessive lipid supply. Increased accumulation of lipid metabolites in the cytosol such as TAG, long-chain acyl CoA, diacylglycerol (DAG), and ceramide induce apoptosis, resulting in in contractile dysfunction and cardiomyopathy. The alterations in FAO were finally linked to the decreased number of PPAR-regulated gene transcripts (Sharma et al., 2004).

The clinical impact of the above findings for cardiac lipotoxicity and the contribution of an impaired FAO was presented by epidemiological studies which verified that obese patients have lower life expectancy, and greater risk for cardiovascular events and heart failure (Kenchaiah et al., 2002).

4.2. Combined activation of PPARa and PPARg and Cardiac Lipotoxicity

Both PPARα and PPARγ activation have equal ability to induce the expression of genes involved in cardiac FAO (Finck et al., 2002) (Son et al., 2007). However, PPARγ can induce cardiac FAO-related gene expression (Son et al., 2007), particularly when PPARα is inhibited (Drosatos et al., 2013; Son et al., 2010). It seems paradoxical that combined activation of two positive regulators of FAO such as PPARα and PPARγ lead to an abnormal cardiac function and cardiac toxicity. It has been proposed that cardiac toxicity may be associated with lipo-gluco-toxicity due to combined increase in PPARγ-driven insulin sensitization and glucose uptake in the setting of higher PPARα-induced FA metabolism (Nolan et al., 2015)

Cardiomyocyte-specific overexpression of PPARγ causes intramyocardial lipid accumulation and cardiac dysfunction (Son et al., 2007), which has been attributed to cardiac arrhythmia. However, constitutive PPARγ expression in cardiomyocytes of Pparα-/- mice did not cause cardiac dysfunction, although myocardial lipids were still elevated (Son et al., 2010). Moreover, an interesting finding of this study was also that the mice which were overexpressing PPARγ in the heart and subsequently were treated with a PPARα agonist (WY 14643) exhibited decreased expression of the *Pgc1a* gene. This finding is consistent with another study, which showed that activation of

cardiomyocyte PPARγ in mice with LPS-induced downregulation of cardiac PPARα increased cardiac *Pgc1α* gene expression (Drosatos and Schulze, 2013).

These past studies suggest that there are overlapping PPAR actions and develop questions including the assessment of a potential competition for either promoter binding or co-activator/co-repressor binding which could may have clinical significance as it would define the mechanistic basis behind the Dual PPARα/γ agonist-induced cardiac dysfunction.

CHAPTER FIVE

5. Experimental analysis of the effects of combined activation of PPARa and PPARg in cardiac lipotoxicity in mouse models

5.1 SUMMARY AND OBJECTIVE

Peroxisome proliferator-activated receptor (PPAR) agonists target hyperlipidemia (PPARα) and hyperglycemia (PPARγ). Dual PPARα/γ agonists, such as Tesaglitazar that were developed to combine these benefits in type II diabetes patients, caused cardiac dysfunction despite lowering plasma glucose and lipids. We studied the

mechanisms that underlie the cardiotoxic effects of dual PPARα/γ activation with the aim to improve this failed therapy.

Wild type or diabetic mice were fed with chow and high fat diets containing a dual PPARα/γ agonist, Tesaglitazar, or combination of Tesaglitazar and Resveratrol for 6 weeks. We assessed cardiac function with 2D-echocardiography. PPARγ-coactivator (PGC)1α expression and acetylation, mitochondrial abundance and respiration were assessed in primary cardiomyocytes isolated from mice treated with Tesaglitazarglitazar or combination of Tesaglitazarglitazar and Resveratrol. Also, we assessed the mechanism via which combined PPARα and PPARγ activation downregulates *Pgc1α* expression.

Mice treated with Tesaglitazar developed cardiac dysfunction despite lower plasma triglyceride and glucose levels. Expression of PGC1α, a regulator of mitochondrial biogenesis, was most profoundly reduced among various cardiac fatty acid metabolism genes. Furthermore, mitochondrial abundance was lower and acetylation of PGC1α increased, which suggests deactivation of PGC1α. Sirtuin 1 (SIRT1), which deacetylates PGC1α, had lower expression in primary cardiomyocytes from Tesaglitazarr-treated mice. Combined activation of PPARα and PPARγ with simultaneous administration of single PPARα and PPARγ agonists in C57BL/6 mice lowered PGC1α expression and mitochondria abundance as observed with Tesaglitazar. Analyses in a human cardiomyocyte cell line showed that PPARα and PPARγ compete for binding on a PPAR element of the *Pgc1α* promoter as well as for protein-protein interaction with PGC1α. Activation of SIRT1 with resveratrol attenuated Tesaglitazar-induced cardiac dysfunction and corrected myocardial mitochondrial

respiration in C57BL/6 and diabetic *db/db* mice. The beneficial effect of resveratrol was abolished in cardiomyocyte-specific SIRT1$^{-/-}$ mice.

SIRT1-mediated activation of PGC1α blunts the cardiotoxic effect of combined activation of PPARα and PPARγ and improves the therapeutic potential of dual PPARα/γ agonist.

5.2 MATERIALS AND METHODS

Chemical reagents – All chemical reagents were obtained from SIGMA unless otherwise noted. Rosiglitazone and WY-14643 were purchased from Enzo Life Sciences.

Animals and Diets – C57BL/6 and *db/db* mice were obtained from the Jackson Laboratory and fed with CHOW of high fat diet supplemented with Tesaglitazar or combination of Tesaglitazar and Resveratrol. All procedures involving animals were approved by the Institutional Animal Care and Use Committees at Temple University and Columbia University. The mice were maintained under appropriate barrier conditions in a 12hr light-dark cycle and received food and water ad libitum. The *αMHC-Pparα* and *αMHC-Sirt1*$^{-/-}$ mice have been previously described (Finck et al., 2002; Hsu et al., 2010).

All diets were purchased from Bio-Serv and they were stored in cold-room (4^{o}C). Mice were fed with the Rodent Grain-based standard CHOW diet that contained 0.2mg/kg Tesaglitazar or both 0.2mg/kg Tesaglitazar and 0.067% Resveratrol. Mice were fed with HFD (Fat Calories: 60%) that contained 0.2mg/kg Tesaglitazar or both 0.2mg/kg Tesaglitazar and 0.067% Resveratrol. For the injection experiments mice were

administered with TESA (**0.5** µmol /kg) or combination of TESA and RSV (**100** mg/kg/day). Plasma TGs were measured with enzymatic assay kit (Infinity, Louisville) and blood glucose levels were assessed by glucometer. Prior to 2D-echocardiography or euthanasia mice were anesthetized by isofluorane inhalation. Mouse hearts were harvested, flash frozen and stored at -80°C until further use. All analyses involving animals were performed with at least 3-5 mice per experimental group.

Echocardiography analysis – Cardiac function of anesthetized mice was assessed by two-dimensional (2D) echocardiography as previously described (Drosatos et al., 2016; Joseph et al., 2017) (VisualSonics-Vevo2100).

Adenoviruses – Recombinant adenoviruses expressing human PPARγ cDNA (Ad-PPARγ) and control GFP (Ad-GFP) were generated as described previously (Bosma et al., 2014). Adenovirus expressing human PPARα cDNA (Ad-PPARα) was purchased from Vector Biolabs (Philadelphia, PA, USA). Infections of AC16 cells were performed as described previously (Bosma et al., 2014)

Transfection and luciferase assay – FuGENE 6 Transfection Reagent (Promega) was used to transfect AC16 cells, which were seeded in 96-well-plates (50,000 cells), with human *Pgc1α* promoter-driven pGL3-BV plasmids according to manufacturer's protocols. For transfection and luciferase assay analyses human PGC1α promoter deletion fragments were cloned into a pGL3 basic vector (pGL3-BV, Promega). The deletion fragments of Pgc1a promoter were amplified from the human genomic sequence using the common reverse primer +120R combined with -1631F, -1386F, -1020F, -754F, or -210F hPGC-1a primers that introduced KpnI and XhoI restriction sites in the 5' and 3' ends of the amplified fragments, respectively (**Table 7**). After

amplification, deletion fragments were purified through electrophoresis followed by gel extraction using the StrataPrep DNA Gel Extraction kit (Agilent Technologies). Purified hPGC1α promoter fragments were digested with KpnI and XhoI and cloned to the respective sites of the pGL3-BV. Sequencing of final pGL3-Bv hPGC1α plasmids were done to confirm proper sequence (GeneWiz).

Gene	Forward primer	Reverse primer
m18S	5'-CCATCCAATCGGTAGTAGCG-3'	5'-GTAACCCGTTGAACCCCATT-3'
m36B4	5'-GCGACCTGGAAGTCCAACTAC-3'	5'-ATCTGCTGCATCTGCTTGG-3'
mPgc1α	5'-CACGCAGCCCTATTCA-3'	5'-GTCGTACCTGGGCCTA-3'
mPgc1β	5´-AACCCAACCAGTCTCACAGG-3'	5'-CTCCTAGGGGCCTTTGTTTC-3'
mVlcad	5'-CCGGTTCTTTGAGGAAGTGAA-3'	5'-AGTGTCGTCCTCCACCTTCTC-3'
mPpara	5'-TGCAAACTTGGACTTGAACG-3'	5'-GATCAGCATCCCGTCTTTGT-3'
mCd36	5'-TGTGTTTGGAGGCATTCTCA-3'	5'-TGGGTTTTGCACATCAAAGA-3'
mCpt1	5'-CCCATGTGCTCCTACCAGAT-3'	5'-CCTTGAAGAAGCGACCTTTG-3'
mLpl	5'-GCTGGTGGGAAATGATGTG-3'	5'-TGGACGTTGTCTAGGGGGTA-3'
mPparg	5'-GAGTGTGACGACAAGATTTG-3'	5'-GGTGGGCCAGAATGGCATCT-3'
mMcad	5'-GATGCATCACCCTCGTGTAAC-3'	5'-AAGCCCTTTTCCCCTGAA-3'
mAox	5´-GGATGGTAGTCCGGAGAACA-3´	5´-AGTCTGGATCGTTCAGAATCAAG-3´
mErra	5´-CCTTCCCTGCTGGACCTC-3´	5´- CGACACCAGAGCGTTCACT-3´
mAngptl4	5´-GGAAAAGATGCACCCTTCAA-3´	5´-TGCTGGATCTTGCTGTTTTG-3'
mttfa	5'-CCGAAGTGTTTTTCCAGCAT-3'	5'-GGCTGCAATTTTCCTAACCA-3'
mLcad	5'-TTTCCGGGAGAGTGTAAGGA-3'	5'ACTTCTCCAGCTTTCTCCCA-3'
mUcp 3	5'-TGCTGAGATGGTGACCTACGA-3'	5'-CCAAAGGCAGAGACAAAGTGA-3'
mUcp 2	5'-TCATCAAAGATACTCTCCTGAAAGC-3'	5'-TGACGGTGGTGCAGAAGC-3'
mSirt1	5'-ATCGGCTACCGAGGTCCATA-3'	5'-ACAATCTGCCACAGCGTCAT-3'
hRPS13	5'-CCTTCACAGATCGGTGTAATCC-3'	5'-TCAGGAAGCAAGTCCCTTAGA -3'
hSirt1	5' -TGGCACAGATCCTCGAACAA -3'	5' -TGCCACAGTGTCATATCATCCA-'3'
hPGC1a +120	5'-AAAAAACTCGAGAAAAGCAAGGAGAAAGGGAA-3'	

RLuc	
hPGC1a -1631 FLuc	5’-AAAAAAGGTACCTACCCCCGAGGTTGTATTTTCCTG-3’
hPGC1a -1386 FLuc	5’-AAAAAAGGTACCTTTTTCTGTTTAAGGAGATGGACAA-3’
hPGC1a -1020 FLuc	5’-AAAAAAGGTACCAGTGTCATCATAAAACAGTTGCAC-3’
hPGC1a -754 FLuc	5’-AAAAAAGGTACCGGGAGCCTATGAGAGAAATGG-3’
hPGC1a -210 FLuc	5’- AAAAAAGGTACCTACCAAAGATTGCAGGGGATTTTG-3’

Table 7 - *Sequences of primers that were used for qRT-PCR or luciferase promoter analyses.*

96-well-plates were seeded with 50,000 AC16 cells. FuGENE 6 Transfection Reagent (Promega) was used to transfect them with 3µg hPgc1α fragment-containing pGL3-BV plasmids according to manufacturer's protocols. Renilla reporter vector (p-RL-Null, Promega) co-transfection was used for normalization. Cells were treated with rosiglitazone (50mM), WY 14643 (50mM), combination of rosiglitazone (50mM) and WY 14643 (50mM) 24h post-transfection. Control cells were treated with equivalent volume of dimethyl sulfoxide (DMSO, Sigma-Aldrich). Luciferase activities (Relative Luminescence Units, RLU) were quantified in cell lysates (Dual-Luciferase Reporter Assay System, Promega) by using the Infinite® M1000 PRO plate reader.from the aqueous phase by addition of 100% ethanol and centrifugation and washed twice with 75% ethanol. The DNA pellet was diluted in ddH2O. 20ng of DNA were used for PCR analysis

Mitotracker Red Staining – AC16 cells were plated on sterile glass chamber slides and were exposed to Mitotracker Red according to manufacturer's instructions (Molecular Probes). Imaging was performed with fluorescence microscope.(~550 nm excitation, ~570 nm emission). Cells were plated in sterile glass chamber slides (Thermo Scientific, nunc, 177380) that had been pre-coated with fibronectin/gelatin or laminin when ACMs were used. Cells were exposed to Mitotracker Red (200nM/well) per manufacturer's instructions (Molecular Probes). Hoechst (Thermo Fisher) was used as nuclear stain at 1:1000. Imaging was performed using Nikon Eclipse TI-RCP (20x objective; excitation 550 nm, emission 570 nm). Images were analyzed with ImageJ software. Corrected Total Cell Fluorescence (CTCF)-(analyzed particles/ total area) was calculated and expressed as fluorescence arbitrary units (AU).

RNA purification and gene expression analysis – Total RNA was purified from cells or hearts using the TRIzol reagent (Invitrogen). cDNA synthesis and analysis with SYBR Green Reagent and quantitative real-time PCR were performed as described previously (Drosatos et al., 2016). RNA purification was performed with the TRIzol reagent (Invitrogen) according to the instructions of the manufacturer. RNA was treated with DNase (Invitrogen) and cDNA was synthesized using the SuperScript III First-Strand Synthesis SuperMix (Invitrogen) and analyzed with quantitative real-time PCR that was performed with Brilliant II SYBR Green QPCR Reagents (Agilent Technologies). Incorporation of the SYBR green dye into the PCR products was monitored in real time with an Mx3000 sequence detection system (Stratagene). Samples were normalized against m18S or m36B4 or hRPS13.

Protein purification and analysis – Freshly isolated hearts and cells were homogenized in RIPA buffer containing protease/phosphatase inhibitors (Pierce-

Biotechnology) (online-only Data Supplement). Total protein extracts (30-40µg) were analyzed with SDS-PAGE and Western Blotting with antibodies from Abcam (PGC1a, SIRT1, ATP5A), Santa Cruz (β-actin, PPARα, PPARγ, pan-acetyl, TOM-20), and Cell Signaling (AMPKa, pAMPKa/Thr172),

Cells were homogenized in RIPA buffer containing protease inhibitors (1mM benzamidine, 1mM phenylmethylsulfonyl fluoride, 10µg/ml leupeptin, 10µg/ml aprotinin, 5mM ethylene glycol tetraacetic acid, 2mM ethylene diamine tetraacetic acid - SIGMA), as well as 1mM dithiothreitol and phosphatase inhibitors (Halt phosphatase inhibitor cocktail – Thermo Scientific). 25 µg of total protein extracts were analyzed with SDS-PAGE and transferred onto PVDF membranes with Trans-Blot-Turbo BioRad System for Western Blotting.

Isolation of crude mitochondrial fractions and overall-acetylation mitochondrial profile - Mouse hearts were rinsed in PBS, minced, and homogenized in isolation buffer (IBm1: ddH2O, 67mM Sucrose, 5mM Tris/HCL, 5mM KCL, 1mM EDTA,10% BSA, pH=7.2) using a Heidolph RZR2021 tissue homogenizer. Homogenate was centrifuged at 700g for 10min at 4C^{o} and the supernatant centrifuged at 7200g for 12min. The crude mitochondrial fraction was analyzed with western blotting.

Immunoprecipitation (IP) –. The protein lysates were purified from homogenized hearts in RIPA buffer after centrifugation at 14,000rpm for 15 mins at 4°C and the protein concentration was measured with a Pierce BCA Protein Assay Kit. Sepharose CL-48 beads (GE Healthcare Life Sciences) were used for the pre-clearing and immunoprecipitation steps. Sepharose beads were washed with distilled water) according to the instructions of the manufacturer and finally a slurry was prepared with

IP Mild Lysis Buffer (1% Triton, 20 mM Tris-Cl pH=7.5, 125mM NaCl, 1mg MgCl2, 1m M CaCl2, 1% Aprotinin, 1mM PMSF, 50mM NaF, 100μM sodium orthovanadate) in a concentration 25mg/ml. In order to reduce non-specific binding, a pre-clearing step was performed and 100μg of protein lysate were treeated with resin Sepharose beads in a rotating incubator for 1h at 4°C and then centrifugated at 14,000rpm for 2 mins. The flow was saved and added to the immobilized antibody for the IP. The antibody-coupled resin was washed twice with IP Mild Lysis Buffer. The protein mixture was added to the resin and was incubated with gentle mixing overnight at 4ºC. This was followed by 2 washes with IP Mild Lysis Buffer and 3 washes with RIPA buffer, addition of non-reducing protein loading buffer (for 1ml: 525μl ddH2O, 50μl 1M DDT, 125μl 0.5MTris-Cl pH=6.8, 200μl 10% SDS, 100μl Glycerol), incubation for 5 minutes on ice, and centrifugation. The flow was used for western blotting analysis.

Co-immunoprecipitation (Co-IP) – According to the user's manual instructions of the Co-IP kit (ThermoScientific, Rockford, lL, USA), antibody was immobilized on the Amino Link Plus coupling resin column. Culture medium was removed from cells and cells were washed with PBS. Ice-cold IP Lysis/Wash Buffer was added to the cells, which were incubated on ice for 5 minutes with periodic mixing. The lysate was centrifuged at 13,000×g for 10 minutes to pellet the cell debris and supernatant was used for further analysis. 1 mg lysate was pre-cleared with incubation (4oC for 30 min) with the control agarose resin and centrifugation at 1000 × g for 1 minute. The flow was saved and added to the immobilized antibody for the co-IP. All co-IP steps were performed at 4°C. The antibody-coupled resin was washed twice with IP Lysis/Wash Buffer. The protein mixture was added to the resin and was incubated with gentle mixing overnight at 4ºC. This was followed by 3 washes with IP Lysis/Wash Buffer, addition of elution buffer,

incubation for 5 minutes at room temperature and centrifugation. The flow from the elution step was used for western blotting analysis.

Adult Mouse Cardiomyocyte Isolation– Adult mouse cardiomyocytes (ACMs) were isolated from ventricles of C57BL/6 mice treated with CHOW diet or HFD containing TESA or combination of TESA and RSV. Hearts from heparinized mice (90 USP; ip) were cannulated through the aorta. Hearts were perfused with perfusion buffer (120.4 mM NaCl, 14.7 mM KCL, 0.6 mM NaH2PO4, 0.6 mM KH2PO4, 1.2 mM MgSO4, 10 mM Hepes, 4.6 mM NaHCO3, 30 mM taurine, 10 mM BDM, 5.5 mM glucose; pH 7.4) for 3 min followed by digestion with perfusion buffer containing 19250 units Collagenese type II (Worthington), 5-6 mg trypsin and 0.02 mM CaCl2 for 7 min. Ventricles were gently teared in small pieces, perfusion buffer containing 5 mg/ml BSA and 0.125 mM CaCl2 was added and filtered with 100 µm nylon. The filtrate was pelleted by gravity for 5 min, centrifuged for 30 sec at 700 rpm and the pellet resuspended in perfusion buffer containing 5 mg/ml BSA and 0.225 mM CaCl2. The cells were pelleted by gravity for 10 min, centrifuged for 30 sec at 700 rpm and the pellet resuspended in perfusion buffer containing 5 mg/ml BSA and 0.525 mM CaCl2. The cells were pelleted by gravity for 10 min, centrifuged for 30 sec at 700 rpm and the pellet was resuspended in perfusion buffer containing 5 mg/ml BSA and 1.025 mM CaCl2.

Seahorse Analysis – Isolated primary ACMs were counted with Hematocytometer. Dead cells were detected with Trypan Blue Dye staining. Cells were platted (3000 cells per well) in XF96 Seahorse® plates pre-coated with laminin with 20 µg/ml laminin (Invitrogen, 23017). In order to assess oxygen consumption rates (OCR) for fatty acid oxidation (FAO) recordings, cells were incubated in substrate limited medium (DMEM containing 10mM Glucose, 1.025mM CaCl2 , 0.5mM carnitine, pH=7.4) and assayed

with fatty acid oxidation medium as per manufacturer's protocol. Before starting the assay, 1mM palmitate conjugated with BSA was added in each well. Drugs used for maximal response during fatty acid oxidation were: Oligomycin (3μM) (Sigma, O4875), carbonyl cyanide-p-trifluoromethoxyphenylhydrazone (FCCP) (2μM) (Sigma, C2920), and Rotenone/Antimycin A (0.5μM) (Sigma, A8674)/ (Sigma, R8875). The pre-hydrated with XF assay calibrant, XF cartridges were filled with the drugs and the cartridge was calibrated for 30 minutes in XF96 Extracellular Flux Analyzer. All experiments were performed at 37^{o}C. Calculations were made as described in the Seahorse manual and XF Seahorse Mito Stress Test kit user guide. Briefly, basal respiration was calculated with subtraction of non-mitochondrial respiration rate from the last measurement prior to first injection. Maximal respiration was calculated by subtraction of the non-mitochondrial respiration measurement from maximum measurement after FCCP injection. ATP production-related OCR was obtained indirectly by measuring ATP-linked respiration in the presence of complex V inhibitor (Oligomycin). The decrease of oxygen consumption rate representing the portion of basal respiration that was used to drive ATP production was calculated with subtraction of the minimum measurement after Oligomycin injection from the last measurement prior to Oligomycin injection. Spare Respiratory Capacity was equal to (maximum respiration)-(basal respiration). Calculations were made with the Wave 2.3 Software.

Electron microscopy – Hearts from heparinized 12 weeks old mice fed with CHOW or CHOW-TESA or CHOW-TESA+RSV diets were excised and slowly perfused with cold PBS for 2 minutes and then with Fixation Buffer (Paraformaldehyde (EM grade) 2%, Glutaraldehyde (EM grade) 2.5%, Cacodylate buffer (Ted Pella Inc., Hartfield, PA) pH

7.4 0.1M, CaCl2 2mM, KCl 20mM) at 35^{o}C for 5 minutes. The hearts were dissected in 1mm x 1mm pieces with razor blade and incubated in fresh fixation buffer at 4 ^{o}C overnight. Tissues were washed 3 x 15 min each with 0.1M sodium cacodylate buffer pH 7.4 containing 2Mm calcium chloride and then fixed with freshly prepared 1% osmium tetroxide and 1.5% potassium ferrocyanide in 0.1M sodium cacodylate buffer pH 7.4 containing 2mM calcium chloride for 3 h on ice. A final wash of 4 x 15 min with water was performed and the tissues were stained en bloc with 1% uranyl acetate (aq) for 2 h. After the staining process tissues were washed for 3 x 15 min each with water. And then they were dehydrated in an ascending acetone series (25% acetone, 50% acetone, 75% acetone; 15 min. The next day, the tissues were dehydrated into 95% acetone for 15 min. and then again were dehydrated 2 x 15 min in 100% anhydrous acetone. Then the following steps below of transition and infiltration were followed:

1. Transition of tissues into 1 part 100% anhydrous acetone
2. Infiltration with 100% n-BGE for 30 minEMBed-812 resin as follows on a rotator:
3. Infiltration with Quetol-651/NSA resin as follows on a rotator:

a) 1 part Quetol-651/NSA resin: 3 parts n-BGE for 1 h

b) 1 part Quetol-651/NSA resin: 1 parts n-BGE for 1 h

c) 3 part Quetol-651/NSA resin: 1 part n-BGE for 1 h

d) 100% Quetol-651/NSA resin for 1 h

e) 100% Quetol-651/NSA resin for 1 h

f) 100% Quetol-651/NSA resin overnight

The last day of the experiment, the tissues were replaced in fresh Quetol-651/NSA resin for 1-2 h and then the samples were embed in aluminum dishes with fresh resin and

polymerize in a vacuum embedding oven for 1-2 days at 60˚C. Images taken by a Zeiss M 2BIO dissecting microscope..

For mitochondria number count, images analyzed with Image J Software. Number of mitochondria was counted and normalized with the total surface area. A frame of 4 squares (4.39''x 4.71'') was used in all of the pictures and the number of mitochondria that appeared in between the 4 squares were counted and compared between the 3 groups of (CTRL, TESA, TESA+RSV).So we calculated the amount of mitochondria per 133.35cm^2

(Delaware Biotechnology Institute).

Lipidomic analysis – Lipids were extracted via chloroform-methanol extraction, spiked with appropriate internal standards, and analyzed using a 6490 Triple Quadrupole LC/MS system (Columbia University). Glycerophospholipids and sphingolipids were separated with normal-phase HPLC using an Agilent Zorbax Rx-Sil column (inner diameter 2.1 x 100 mm) under the following conditions: mobile phase A (chloroform:methanol:1 M ammonium hydroxide, 89.9:10:0.1, v/v/v) and mobile phase B (chloroform:methanol:water:ammonium hydroxide, 55:39.9:5:0.1, v/v/v); 95% A for 2 min, linear gradient to 30% A over 18 min and held for 3 min, and linear gradient to 95% A over 2 min and held for 6 min. Quantification of lipid species was accomplished using multiple reaction monitoring (MRM) transitions that were developed in earlier studies (Chan et al., 2012) in conjunction with referencing of appropriate internal standards: ceramide d18:1/17:0 and sphingomyelin d18:1/12:0 (Avanti Polar Lipids, Alabaster, AL). Values are represented as mole fraction with respect to total lipid (% molarity). For this,

lipid mass (in moles) of any specific lipid is normalized by the total mass (in moles) of all the lipids measured (Chan et al, 2012). In addition, all of our results were further normalized by protein content.

Statistical Analysis – All group comparisons have been performed by 1-way ANOVA analysis or by non-paired two-tailed Student's t test. Values represent means ± SEM. Sample size and p values are provided in the figure legends.

5.3 RESULTS

5.3.1 Tesaglitazar causes cardiac dysfunction in C57BL/6 mice

Six weeks-old C57BL/6 male mice were fed with standard diet (CHOW) or high fat diet (HFD) supplemented with tesaglitazar for 6 weeks. After completion of the treatment, tesaglitazar feeding led to a 34% decrease in plasma triglycerides (TGs) and an 18% decrease in glucose levels in the HFD-fed group **(Figure 14A, 14B)**, without any significant difference in weight gain rate or food consumption (**Figure 15A-15D**).

CHOW/tesaglitazar-treated mice did not show differences in plasma-TG or glucose levels but as the HFD-groups, they also did not have differences in weight and food consumption compared to control group **(Figure 14A, 14B)**. Despite the beneficial effects of tesaglitazar on the impaired metabolic parameters of the HFD group, 2D-echocardiography revealed cardiac dysfunction in CHOW/tesaglitazar- and HFD/tesaglitazar-fed groups **(Figure 14C).** HFD itself had its own effect in reducing fractional shortening (FS) (18%) compared to CHOW-fed mice (**Figure 14D**). Tesaglitazar reduced FS% by ~20% and increased systolic left ventricular internal diameter during systole (LVIDs) (30%) compared to control mice **(Table 8**). The tesaglitazar-induced reduction in FS% was more profound inCHOW-fed than HFD-fed mice, as HFD-fed mice had already impaired cardiac function (lower FS% by 18%) compared to CHOW-fed control group.

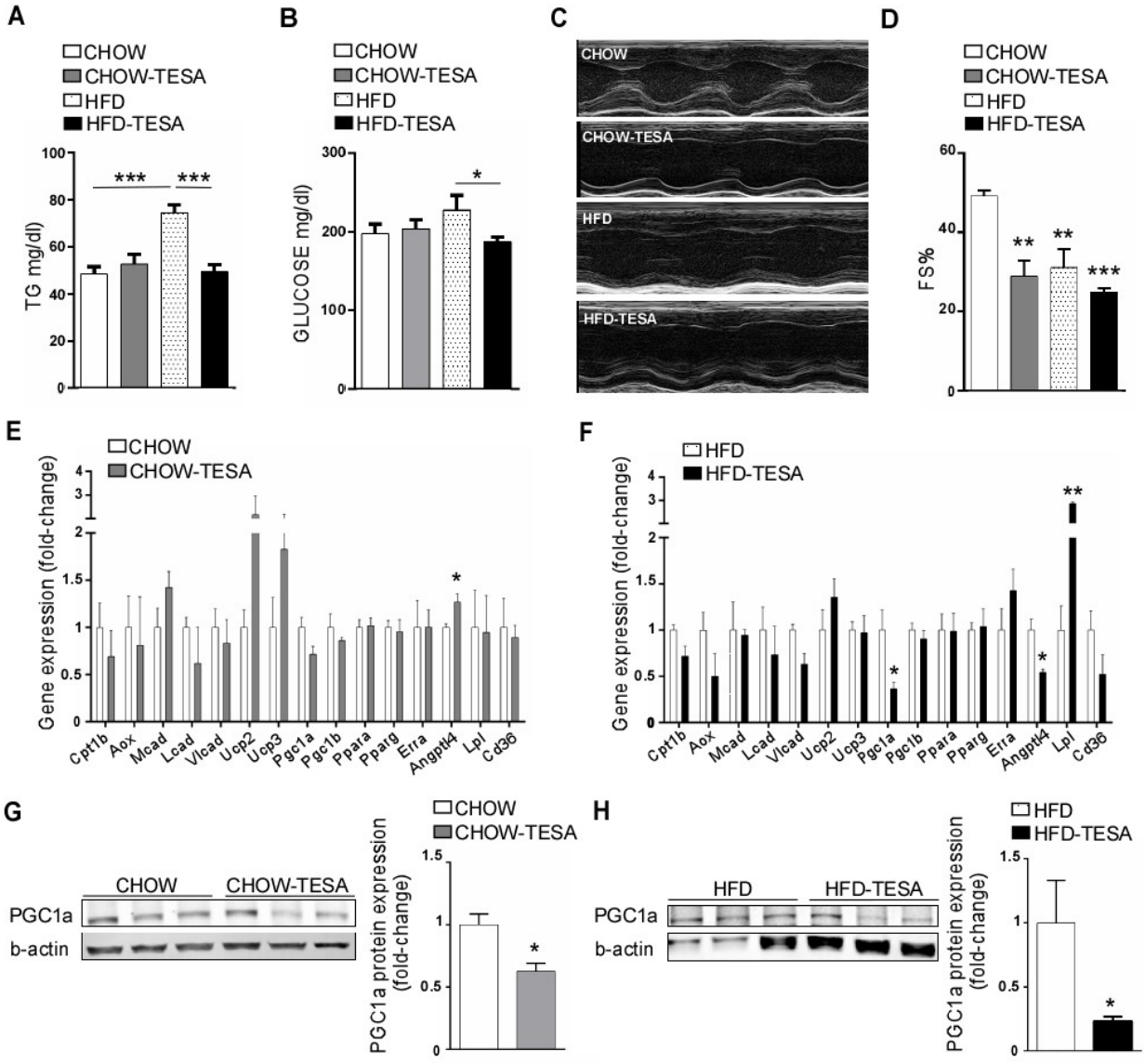

Figure 14. A-H: Plasma TG (A), plasma glucose (B), representative short-axis M-mode echocardiography images (C), fractional shortening (%) (D) cardiac CPT1β, AOX, MCAD, LCAD, VLCAD, UCP2, UCP3, PGC1α, PGC1β, PPARα, PPARγ, ERRα, ANGPTL4, LPL, and CD36 mRNA levels (E, F), immunoblot (G, I) and densitometric analysis (H, J) of cardiac PGC1α and β-actin of C57BL/6 mice treated with CHOW (A-D, E, G, H) or HFD (A-D, F, I, J) containing tesaglitazar (0.5 μmol/kg body weight) for 6 weeks. Statistical analysis was performed using 1-way ANOVA or unpaired 2-tailed Student's t-test *P,0.05, **P,0.01, ***P<0.001, (n=3-5). Error bars represent SEM.

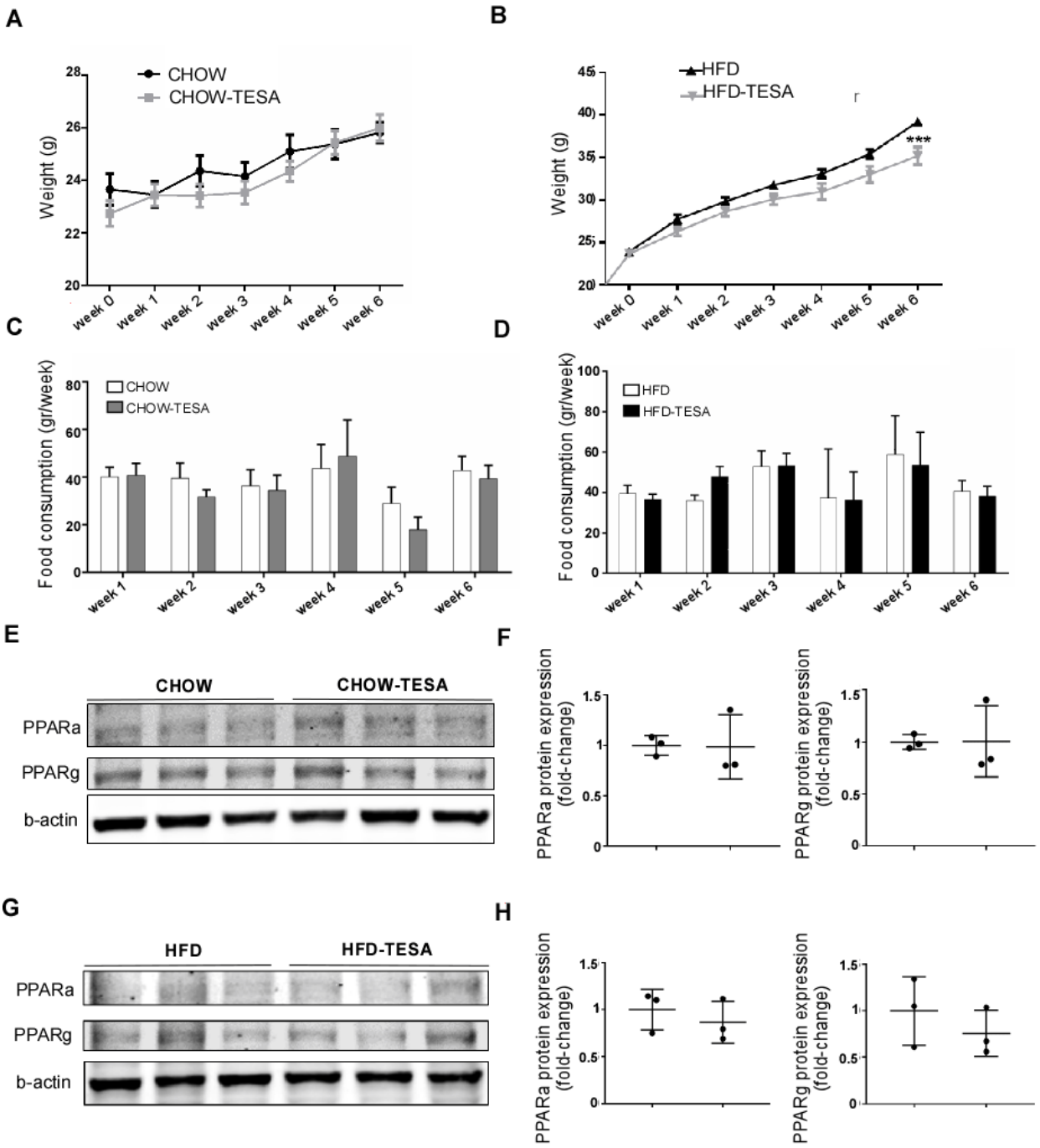

Figure 15 - A-H: Weight gain rate curves (A,B), Food consumption rates (C,D), immunoblot (E, G) and densitometric analysis (F, H) of cardiac PPARα , PPARγ and β-actin of C57BL/6 mice treated with CHOW (A, C, E, F) or HFD (B, D, G, H) containing TESA (0.5 μmol/kg body weight) for 6 weeks. Statistical analysis was performed using Student's t-test, ***P<0.001, (n=3-5). Error bars represent SEM.

Parameters	Groups			
	CHOW	CHOW-TESA	HFD	HFD-TESA
EF	80.8	55.53**	55.5	49.3
FS	49.2	28.93**	28.9	24.8
LV Mass	103.4	98.2	98.2	106.0
LV Mass (Cor)	82.7	78.5	78.5	84.8
LV Vol;d	80.9	59.1	59.1	84.82*
LV Vol;s	15.6	27.1	27.1	42.9
IVS;d	0.7	0.8	0.8	0.7
IVS;s	1.3	1.1	1.1	1.0391*
LVID;d	4.2	3.9	3.9	4.33*
LVID;s	2.1	2.79*	2.8	3.3
LVPW;d	0.7	0.7	0.7	0.585*
LVPW;s	1.4	0.946*	0.9	0.853*

Table 8 - Table of 2D-echocardiography parameters of C57BL/6 mice treated with CHOW or HFD containing TESA (0.5 µmol/kg body weight) for 6 weeks. Statistical analysis was performed with unpaired 2-tailed Student's t-test between groups, *p>0.05, (n=5).

5.3.2 Tesaglitazar-mediated cardiac dysfunction is associated with lower PGC1α expression

Because tesaglitazar is a dual agonist for both PPARα and PPARγ, we examined expression of cardiac FAO-genes in mice treated with tesaglitazar-containing CHOW or HFD **(Figure 14E, 14F)**. The most profound difference found with tesaglitazar was the reduction of PGC1α expression, which encodes for the common key transcriptional co-activator of PPARs (Finck and Kelly, 2006) and regulates mitochondrial biogenesis. Tesaglitazar decreased PGC1α mRNA levels (64%) in HFD-fed mice and showed the same trend (30%) in CHOW-fed mice (**Figure 14F).** Tesaglitazar treatment showed

trends of reduced expression for most of the FA metabolism genes, except Angiopoietin-like 4 (ANGPTL4) that was increased in CHOW/tesaglitazar-fed group (27%). A similar increase in ANGPTL4 mRNA occurred in CHOW or HFD-fed mice (16- and 4.2 -fold, respectively) injected with tesaglitazar, compared to controls (**Figure 16A, 16B**). On the other hand, ANGPTL4 mRNA levels were decreased (45%) in HFD/tesaglitazar-fed group compared to HFD-controls. Moreover, mRNA levels of lipoprotein lipase (LPL), which is inhibited by ANGPTL4, was significantly increased (2.8-fold) in the HFD-treated group. The observed reduction in PGC1α mRNA levels paralleled reduction in cardiac protein levels in CHOW/tesaglitazar (40%) (**Figure 14G, 14H**) and HFD/tesaglitazar (77%) (**Figure 14I, 14J**) mice. In contrast to these changes in PGC1α, no significant differences in cardiac PPARα and PPARγ protein levels were found with tesaglitazar treatment (**Figure 15E,15H**).

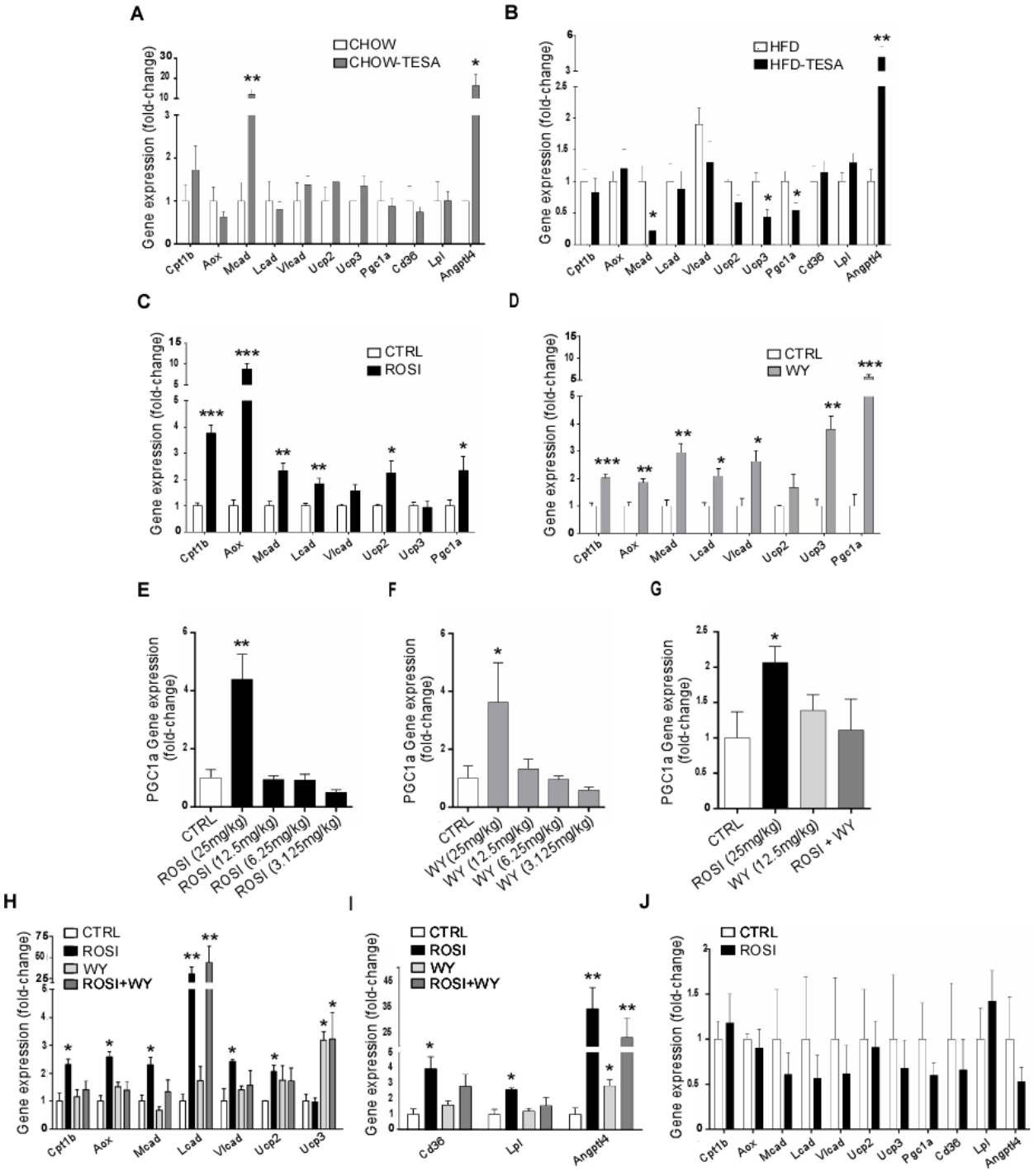

Figure 16. **A, B:** CPT1B, AOX, MCAD, LCAD, VLCAD, UCP2, UCP3, PGC1A, ANGPTL4, LPL, CD36 mRNA levels in hearts of CHOW-fed (A) or HFD-fed (B) C57BL/6 mice treated intraperitoneally with 2 mg/kg tesaglitazar for 7 days. Control mice were treated with DMSO; (unpaired 2-tailed Student's t-test; *p<0.05 vs CTRL, **p<0.01 vs. CTRL, (n=4-6). **C, D:** CPT1B, AOX, MCAD, LCAD, VLCAD, UCP2, UCP3, and PGC1α mRNA levels in hearts of C57BL/6 mice treated intraperitoneally (i.p.) with PPARγ agonist, rosiglitazone (33 mg/kg) (C) or PPARα agonist, WY-14643 (30 mg/kg) (D) for 8h. Control mice were treated with DMSO; n=4-6; *p<0.05 vs CTRL, **p<0.01 vs. CTRL, ***p<0.001 vs. CTRL. (**E-G):** PGC1α mRNA levels in

hearts obtained from C57BL/6 mice treated with 25 mg/kg, 12.5 mg/kg, 6.25 mg/kg, and 3.125 mg/kg rosiglitazone (E), 25 mg/kg, 12.5 mg/kg, 6.25 mg/kg, and 3.125 mg/kg WY-14643 (F) or combination of rosiglitazone (25 mg/kg) and WY-14643 (12.5 mg/kg) (G)**. H,I:** CPT1B, AOX, MCAD, LCAD, VLCAD, UCP2, UCP3, and PGC1α (H) CD36, LPL and ANGPTL4 (I) mRNA levels in hearts of C57BL/6 mice treated intraperitoneally with 25 mg/kg rosiglitazone, 12.5 mg/kg WY-14643 or combination of rosiglitazone (25 mg/kg) and WY-14643 (12.5 mg/kg). Control mice were treated with DMSO; n=4-6; *p<0.05 vs CTRL, **p<0.01 vs. CTRL. **J:** Cpt1β, AOX, MCAD, LCAD, VLCAD, UCP2, UCP3, AND PGC1A, CD36, LPL, and ANGPTL4 mRNA levels in hearts of αMHC-PPARα mice treated intraperitoneally with 25 mg/kg rosiglitazone. Statistical analyses were performed with unpaired 2-tailed Student's t-tests. Error bars represent SEM.

5.3.3 Activation of either PPARα or PPARγ increased cardiac PGC1α and FAO-related gene expression

We then tested if the actual activation of PPARα and PPARγ and no other off-target effects of the drug drive the inhibitory effect of the dual PPARα/γ agonist on the expression of PGC1α. Thus, we compared the effects of direct intraperitoneal (i.p.) administration of tesaglitazar and combination of single PPARα and PPARγ agonists in C57BL/6 mice. Daily injections of mice with tesaglitazar for 7 days reduced cardiac PGC1α expression in HFD-fed mice (45%) but not in CHOW-fed mice (**Figure 16A, 16B**). In addition, tesaglitazar increased cardiac *Angptl4* expression in both CHOW- (4.2-fold) and HFD-fed (16-fold) mice. On the other hand, medium-chain acyl-CoA dehydrogenase (*Mcad)* expression was increased (12-fold) in mice fed with CHOW/tesaglitazar (**Figure 16A**), while HFD/tesaglitazar treatment had the opposite effect (**Figure 16B**).

We then administered i.p. PPARα agonist, WY-14643 (30mg/kg), or PPARγ agonist, rosiglitazone (33mg/kg) in C57BL/6 (Drosatos et al., 2013). Rosiglitazone increased the expression of cardiac carnitine palmitoyl-transferase 1β (*Cpt1β*) (3.7-fold),

acetyl-CoA oxidase (*Aox*) (8.7-fold), *Mcad* (2.3-fold), long chain acyl-CoA dehydrogenase (*Lcad*) (1.8-fold), uncoupling protein 2 (*Ucp2*) (2.3-fold), and *Pgc1α* (2.4-fold) **(Figure 16C).** The expression levels of very long-chain acyl-CoA dehydrogenase (*Vlcad*) and *Ucp3* did not change significantly **(Figure 16C).** The PPARα agonist, WY-14643, increased the expression levels of *Cpt1β* (2-fold), *Aox* (1.9-fold), *Mcad* (3-fold), *Lcad* (2.1-fold), *Vlcad* (2.6-fold), *Ucp3* (3.8-fold), and *Pgc1α* (5.7-fold), while it did not alter significantly the expression of *Ucp2* **(Figure 16D).**

5.3.4 PPARα activation compromised PPARγ-mediated induction of PGC1α and FAO-related gene expression

Both PPARα and PPARγ activation by WY14643 and rosiglitazone, respectively increased PGC1α mRNA levels. In order to investigate whether PPARα and PPARγ compete for regulating *Pgc1α* expression, we performed dose titration experiments to identify the minimum dose of rosiglitazone that increases cardiac PGC1α levels and the maximum dose of WY-14643 that does not. I.p. administration of a series of doses of rosiglitazone and WY-14643 (25mg/kg, 12.5mg/kg, 6.25mg/kg, 3.125mg/kg) in C57BL/6 mice showed that 25mg/kg is the lowest dose of rosiglitazone that induces cardiac Pgc1α expression **(Figure 16E)** and 12.5mg/kg the highest dose of WY-14643 that does not **(Figure 16F).** C57BL/6 mice were then injected with combination of 25mg/kg rosiglitazone and 12.5mg/kg WY-14643. The combined treatment prevented rosiglitazone-mediated upregulation of cardiac Pgc1α gene expression **(Figure 16G).** Accordingly, while rosiglitazone increased CPT1β (2.3-fold), AOX (2.6-fold), MCAD (2.3-fold), VLCAD (2.4-fold), and UCP2 (2.1-fold) mRNA levels, combined injection with both

PPARα and PPARγ agonists in C57BL/6 mice blocked the effects of rosiglitazone **(Figure 16H).** Conversely, treatment of C57BL/6 mice with WY-14643 did not prevent rosiglitazone-mediated increase of LCAD (~25-fold) **(Figure 16H).** Cardiac *Ucp3* gene expression was increased (3.2-fold) by WY-14643 and retained the same levels in mice treated with the combination **(Figure 16H).** Similarly, combined administration of rosiglitazone and WY-14643 prevented PPARγ-mediated upregulation of the expression of lipid uptake-related genes, such as cluster of differentiation 36 (*Cd36*) and *Lpl* **(Figure 16I).** On the other hand, both agonists, as well as their combined administration increased the expression of *Angptl4* with rosiglitazone being the major inducer (single treatment: 35-fold and combined treatment: 25-fold), compared to WY-14643 single treatment (2.5-fold) **(Figure 16I).** Thus, although combined-PPARα/γ activation led to greater expression of some FAO-related genes, the expression of other downstream PPAR targets was either not increased or in some cases reduced.

To assess further the inhibitory effect of PPARα on PPARγ-mediated stimulation of cardiac FA metabolism-related gene expression, we injected rosiglitazone i.p. in mice with constitutive cardiomyocyte-specific expression of *Pparα* (*αMHC-PPARα*) (Finck et al., 2002) and tested for cardiac expression of *Pgc1α* and other FA metabolism-related genes. While treatment of C57BL/6 mice with rosiglitazone increased CD36, LPL, ANGPTL4, CPT-1B, AOX, MCAD, LCAD, VLCAD and UCP2 mRNA levels **(Figure 16H, 3I),** it did not have the same effect in *αMHC-PPARα* mice. Cardiac PGC1α mRNA showed a trend for lower levels (40%) and CPT-1B, AOX, MCAD, LCAD, VLCAD, UCP2, UCP3, CD36, LPL, and ANGPTL4 mRNA levels were not upregulated in rosiglitazone-treated *αMHC-Pparα* mice **(Figure 16J).** In conclusion, combined

activation of PPARα and PPARγ either pharmacologically or via overexpression reduced cardiac PGC1a expression.

5.3.5 Combined PPARα/PPARγ activation decreased cardiac mitochondria abundance and affected mitochondrial respiration

PGC-1α regulates mitochondrial biogenesis (Lehman et al., 2000) by controlling the mitochondrial transcription factor A (mtTFA) expression (Wu et al., 1999). Given that combined administration of single PPARα and PPARγ agonists, as well as administration of PPARγ agonist in *αMHC-PPARα* mice, and treatment with dual-PPARα/γ agonist, tesaglitazar, had the same inhibitory effect on cardiac PGC1A levels, we focused on determining whether combined PPARα and PPARγ activation have other PGC1α-dependent effects, such as modulation of mitochondrial abundance and function.

Cardiac mtTFA mRNA levels were increased (2-fold) in rosiglitazone-treated C57BL/6 mice but combined treatment with rosiglitazone and WY-14643 prevented this increase **(Figure 17A).** This finding was consistent with reduced number of mitochondria in hearts from mice treated with the combination of rosiglitazone and WY-14643. Electron microscopy (EM) analysis (magnification: 4,000x and 10,000x) **(Figure 17B)** and assessment of mitochondrial number **(Figure 17C)** confirmed that cardiac myocyte mitochondria abundance was reduced in mice treated with both rosiglitazone and

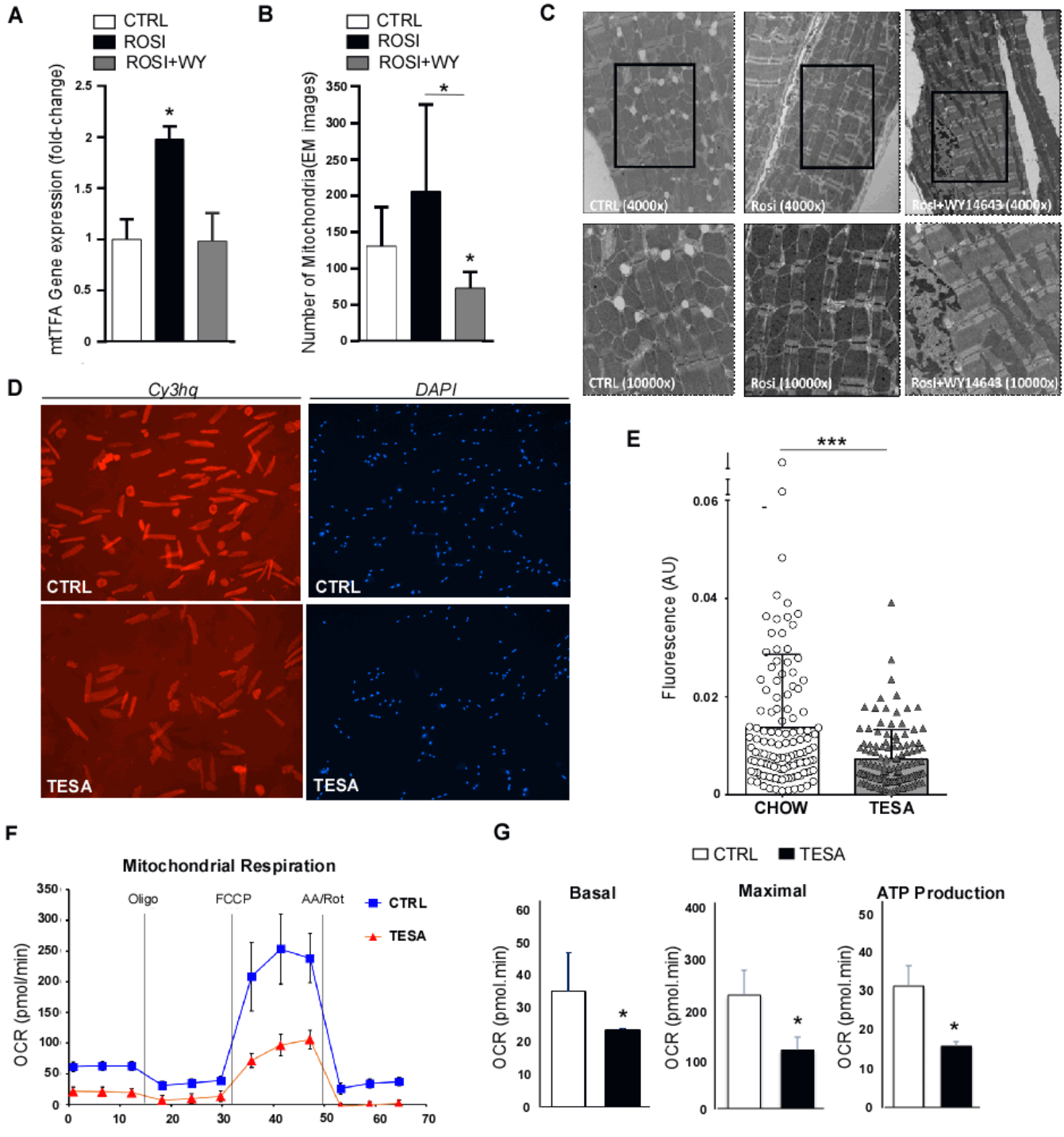

Figure 17. **A-C**: Cardiac mtTFA mRNA levels (A), representative electron microcopy images (4000x and 10000x) (B) and quantitation of mitochondria normalized with total surface area (mito-number/133.35cm^2) (C) in C57BL/6 mice treated intraperitoneally with 25 mg/kg Rosiglitazone, 12.5 mg/kg WY-14643 or combination of Rosiglitazone (25 mg/kg) and WY-14643 (12.5 mg/kg). Control mice were treated with DMSO; *p<0.05 vs CTRL, **p<0.01 vs. CTRL. (n=4-6) **D, E:** Representative images obtained from fluorescence microscopy of isolated adult mouse cardiomyocytes (ACMs) stained with Mitotracker Red and quantitation of mitochondrial number/total area. ACMs were obtained from C57BL/6 mice treated

intraperitoneally with 2mg/kg tesaglitazar for 7 days with daily injections (n=3)(number of analyzed cells: CTRL:127, tesaglitazar:125). **F**. Oxygen Consumption Rate (OCR), basal respiration, maximal respiration and ATP production-related OCR measured with XF96 Seahorse Analyzer in ACMs isolated from C57BL/6 mice treated intraperitoneally with 2mg/kg tesaglitazar for 7 days. Oligo indicates oligomycin (3μM), FCCP indicates Carbonyl cyanide-p-trifluoromethoxyphenylhydrazone (2μM), AA/Rot indicates Antimycin A/ Rotenone (0.5μM). Statistical analyses were performed with unpaired 2-tailed Student's t-tests. *p<0.05 , ***p<0.0001, (n= 3 wells-Representative experiment of 3 independent experiments); error bars represent SEM.

WY-14643 (45% reduction compared to control DMSO-treated mice and 65% compared to rosiglitazone-treated animals)**.** These results suggested that combined activation of PPARα and PPARγ, which prevents rosiglitazone-mediated upregulation of *Pgc1α* expression, also reduces mitochondria abundance.

Consistent to the previous finding, mitochondrial mitotracker red staining **(Figure 17D)** of primary ACMs isolated from mice subjected to daily i.p. injections with tesaglitazar (2mg/kg) for 7 days, showed lower mitochondria abundance (45%) compared to the ACMs derived from control mice (DMSO-injected) **(Figure 17E)**. Accordingly, treatment of AC16 cells (human cardiomyocyte cell line) with tesaglitazar (50 □M and 100 □M) for 24 h decreased mitochondria abundance as determined by mitotracker staining (20% reduction in cells treated with 50 μM tesaglitazar and 25% reduction for cells treated with 100 μM tesaglitazar) (**Figure 18A, 18B**).

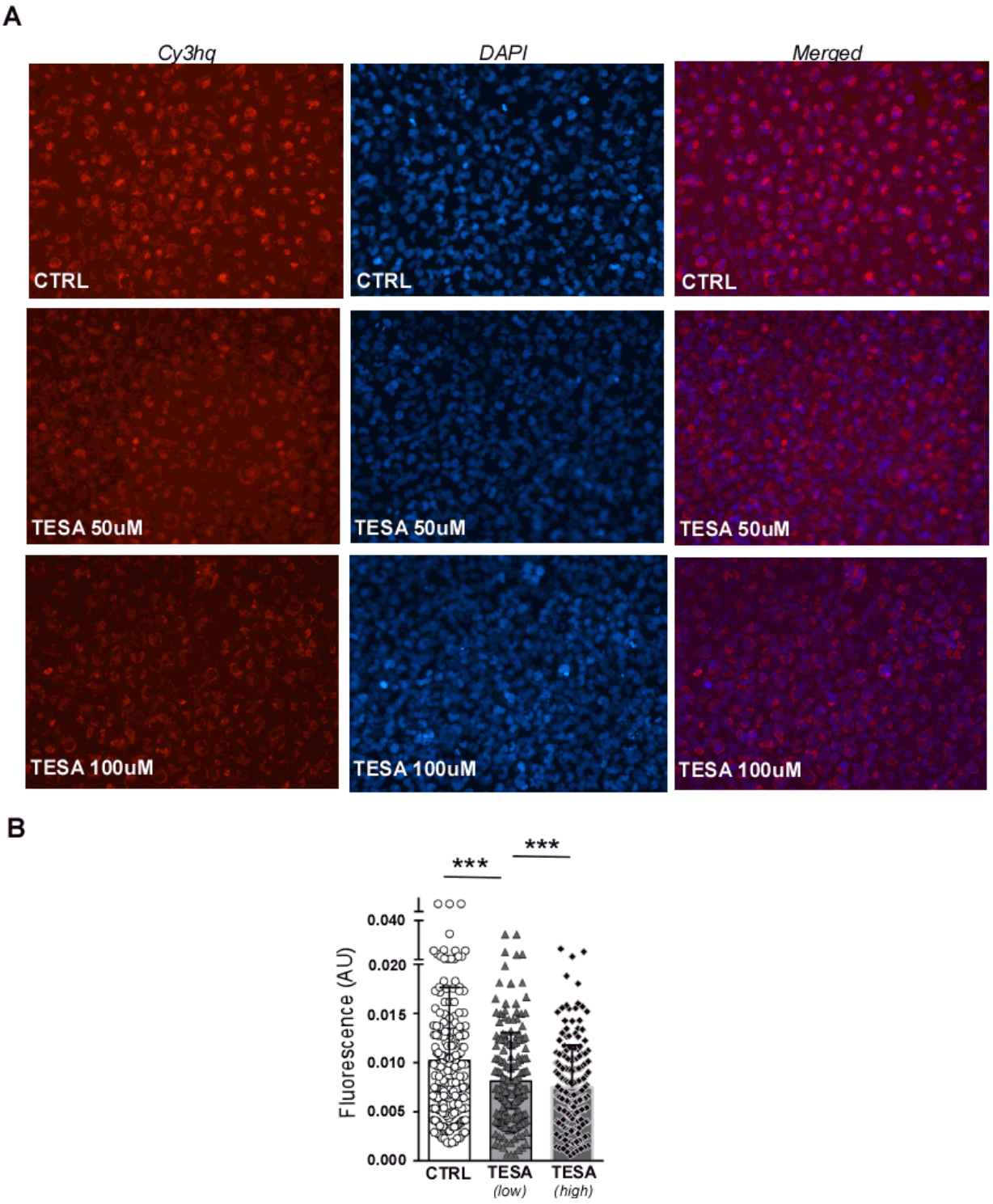

Figure 18 - A, B: Representative images obtained from fluorescence microscopy of AC16 cells stained with Mitotracker Red (A) and quantitation (B) of mitochondrial number/total area. AC16 cells were treated prior staining with 50Mm (low) or 100Mm (high) TESA for 24h (number of analyzed cells: CTRL:206, TESA 50μM: 214, TESA 100μM: 201. Statistical analysis was performed with unpaired 2-tailed Student's t-test between groups, **P,0.01, ***P<0.001. Error bars represent SEM.

In order to assess whether the reduction in mitochondrial number had an effect in the respiratory capacity of cardiomyocytes, we performed Seahorse analysis in primary ACMs derived from mice treated with tesaglitazar. This analysis showed impaired mitochondrial respiration as shown by lower OCR for basal respiration, maximal respiration and ATP production. This indicates lower capability of the tesaglitazar-treated ACMs to respond to energetic demands **(Figure 17F, 17G).**

5.3.5 PPAR element (PPRE) of the -1631/-1609bp Pgc1α promoter region was critical for the inhibitory effect of PPARα on PPARγ-mediated activation of Pgc1α promoter As combined PPARα and PPARγ activation inhibited PGC1α expression, we tested whether this effect is driven by altered *Pgc1α* promoter activity. In order to map the regions of the human *Pgc1α* promoter (obtained from UCSC Genome Browser) that contain PPREs that PPARs may bind on, we used Genomatix software and analyzed the *Pgc1α* promoter sequence up to 2,000bp prior to the transcription initiation site **(Figure 19A)**. We compared the sequence of the human *Pgc1α* promoter and the mouse *Pgc1α* promoter sequence with the CLUSTAL O (1.2.0) sequence alignment software **(Figure 20**). This analysis identified 5 conserved PPREs that span regions -1631/-1609bp, -1386/-1362bp, -1012/-991bp, -634/-612bp, and -210/-189bp of the human *Pgc1α* promoter. To map the region of the human *Pgc1α* promoter that is


A
-2000 TAGCATTGGATAAACACAAATAAAGGTATCAGTGAATATCACAATGGAAGAATCACATGA
-1940 TAATAATTAATAAACATTGACTCTTCTTGGCCAGGTGACCAATATTATTTCACAGTTGAT
-1880 CCTTGAGGGCAGAGCCAATGACCTTTGTCCTGAATTTTAATAATTTACTGAAGTTTTACA
-1820 TTAAATCAGAATATAATTGGGAAGAAAATTAGTGTTTCTTTGTGGGGAGTGCAGAGTAAT
-1760 GCCACTAATTGCTTGTATAAAAGCATTCCCGAGGTTGTATTTTCCTGTTCTTTCATTAGA
-1700 AAATTAAAACTACAGTAATTTTCTGCTGTTTATAAAAGGGAAAATGTGCTGGTGAACTGT
-1640 ATTCAGCAAACTTAAAATGTCAAAGCTCTTGGCCACCTTTTTATGCCCAGTAATGATAAA
-1580 CTGTCAACTTCCTTACATTATTTGGGAATTTACTAGCAACTTGTTGCAGCTCTCACAGCA
-1520 CACAAATCTCTTATAATATGTATGGTCTGAAAGAAGCAGCAGTCTGCTGGTATTTTGTTT
-1460 CTTTTGTTCTTTCTTTCACTTTAATATTTGAGCAATTTAATATTTAAAATATGTGTTAGG
-1400 GCAAATAACCATGTTTTTCTGTTTAAGGAGATGGACAATGAAGAACAGTGTAAATTAACC
-1340 TCAGTAGAATAATGCTTTACAAATTATATTTAGGTAACTGGGGGATTGTTTTCAGGTAAA
-1280 TTATTATCAAGTAAAAGAATTGAGCTGATTCTAAAAGTATATTGGGTTTAACATTTTATG
-1220 AAAACATGTTTATTCACACAGATACATACACGTGTACATCTCCTGGGAACTTGGAAGGGT
-1160 TAAGTCAGACCACTGTCATGTTACAGGAAGTGTTTTTCCACTGTGTCCAGTACCTTGAGT
-1100 TTGTTATGTATTCAATATGTAGTGTCATCATAAAACAGTTGCACCTACCTGCATTAGCCC
-1040 TCATTGTCTCAAGGTACAAGCTGAAAAATAATAGAAAGTAAAGCTCAGGAATTGAATATT
-980 TCTGCTAATAGTGTGTTGGTATTTTTCCCTCAGTTCACAGACATTCTTGATTTCAAAACG
-920 CAAACTACACAACCCAGGGCACTAGGGTTGGAATTCAATGTTTATTCAAAAAGGCACCCT
-860 AAGGCAGTTAGGGAGGAAACGCTACATGTATGAAAAATAGGAGCCGGGAATCAAAGCTGA
-800 TCTGAGCAGAGCAGCAGCGACTGTATTTACTAACACTTGTTTTCTGGGAGCCTATGAGAG
-740 AAATGGAAATAATTAGAAGGAAGCTGAAAGGATGGGGTTTTGTGGCTTGTTCTCCTTATA
-680 TGGAGCAAAGAAAACTGCAGCAACTCTTCGGGAGCTGGTATTCCCTACTGCCATGGGGGC
-620 AGCCGAATTCTGGGTGGAGGAGTTTGTTTATACCTTAACACATACAGGCTATTTTGTTGA
-560 TTAAACAAGCAAAAAAAAAAAAAAAAAAAAAAAAAAAAAGCCCCGTTTGCGCTTTCAAACACTC
-500 CCTCAATGAGAAAATGTCTCATAAAAATGCATCATGTGATAAGCTCTTGCTTTAGTCCCA
-440 AACTGAGCTTGAGTCCACTTGGAGATCTTAGAATTAAAGAGTTCTTAGGGAATACACGTT
-380 TTAGCTAAGAATATAGTTACTCTGTCATGAAACAGGGAGCTTTGCCACTTGCTTGTTTTG
-320 GAAGGAAAATAAATTAAAAAAAGATTGCAGGGGATTTTGGTTATTATATGGCCAGGGCTC
-260 CGTTTAGAGTCTGTGGCATTCAAAGCTGGCTTTAATCACAGCATGATGCTTGAAGCCTCC
-200 AAAAGTCTAAGTGTTTCCTTTCTTTCTTTCTTTTCTTTTTCTTTCTTTTTTTTTTTTTTT
-140 AAAGCGTTACTTCACTGAAGCAGAGGGCTGCCTTTGAGTGACGTCACGAGTTAGAGCAGC
-80 AAGCTGCACAGGGGAAGGGAGGCTGGGTGAGTGACAGCCCAGCCTACTTTTTAATAGCTT
-20 TGTCATGTGACTGGGGACTG
B
KpnI
XhoI
hPGC-1α promoter -1631
hPGC-1α promoter -1386
hPGC-1α promoter -1012
hPGC-1α promoter -210
C
CTRL
ROSI
WY
ROSI+WY
Pgc1a gene expression (fold-change)
D
CTRL
ROSI
WY
ROSI+WY +MK
Pgc1a gene expression (fold-change)
E
CTRL
ROSI
WY
ROSI+WY
hPgc1a promoter activity (-1631)
F
CTRL
ROSI
WY
ROSI+WY
hPgc1a promoter activity (-1386)
G
CTRL
ROSI
WY
ROSI+WY
hPgc1a promoter activity (-1012)
H
CTRL
ROSI
WY
ROSI+WY
hPgc1a promoter activity (-210)
I
Ad-GFP
Ad-PPARa
Ad-PPARg
Ad-PPARa +Ad-PPARg
Gene expression (fold-change)
PPARa
PPARg
PGC1a
J
Ad-GFP
Ad-PPARa
Ad-PPARg
Ad-PPARa Ad-PPARg
PPARg
PPARg
PGC1a
PPARa
PPARa
PGC1a

Figure 19. **A**: Predicted PPREs in the promoter of human *Pgc1α* gene. **B:** Schematic representation of *Pgc1α* promoter deletion mutants cloned in pGL3-BV luciferase reporter plasmid for luciferase promoter assays. **C, D:** PGC1α mRNA levels in AC16 cells treated with 50 μM rosiglitazone (C, D), 50 μM WY-14643 (C, D), combination of Rosiglitazone and WY-14643 (C, D) or combination of Rosiglitazone, WY-14643 and the PPARα antagonist, MK886 (D). **E-H:** Luciferase activity in AC16 cells transfected with reporter plasmids containing *Pgc1α* promoter deletion fragments, *pGL3BV-hPgc1α-1631* (E)**,** *pGL3BV-hPgc1α-1386* (F), *pGL3BV-hPgc1α-1012* (G), and *pGL3BV-hPgc1α-210* (H), followed by treatment with 50 μM Rosiglitazone, 50 μM WY-14643 or combination of both *(n=6-12*); **I:** PPARα, PPARγ and PGC1α mRNA levels in AC16 cells infected with recombinant adenoviruses expressing PPARα or PPARγ; *(n=6).* **J:** Co-immunoprecipitation of PGC1α with PPARγ or PPARα purified from protein lysates obtained from AC16 cells infected with recombinant adenoviruses expressing PPARα and PPARγ. Statistical analyses were performed with unpaired 2-tailed Student's t-tests, *p<0.05, ***p<0.001 vs CTRL. Error bars represent SEM**. Experiments provided by Konstantinos Drosatos, MSc, PhD, Melissa J. Lieu, BS and Yujia Yue, BS.**

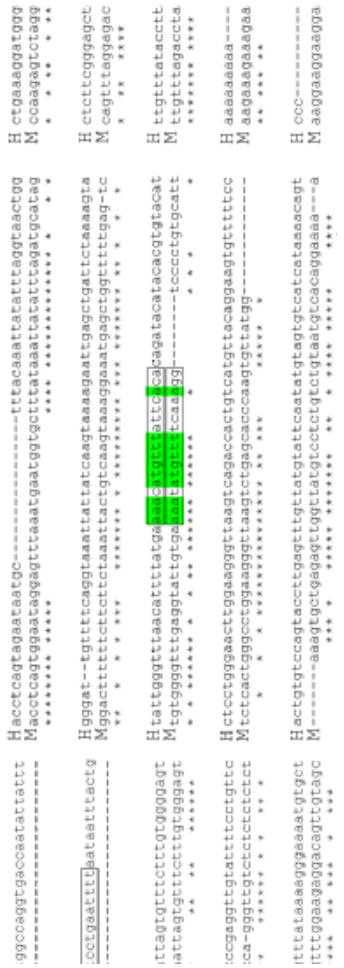

Figure 20 - Comparison of the sequence of the human and the mouse PGC1α promoter sequence with the CLUSTAL O (1.2.0) sequence alignment software. Conserved PPREs that span regions -1631/-1609 bp, -1386/-1362 bp, -1012/-991 bp, -634/-612 bp, and -210/-189 bp of the PGC1α

responsible for the inhibitory effect of PPARα on PPARγ-mediated upregulation of *Pgc1α* gene expression, we generated a panel of *Pgc1α* promoter deletion mutants **(Figure 19B)** that we cloned in pGL3-BV luciferase reporter plasmid for luciferase promoter assays in AC16 cells. We first treated AC16 cells with increasing doses of rosiglitazone (25, 50 and 100μM) and WY-14643 (25, 50 and 100μM) (**Figure 21A-F**) to identify the minimum dose of rosiglitazone that increases *Pgc1α* expression and the maximum dose of WY-14643 that does not. This analysis prompted us to select 50μM rosiglitazone and 50μM WY-14643 (**Figure 21B, 21F**) for our *in vitro* experiments. Treatment of AC16 cells with 50μM rosiglitazone, increased PGC1α mRNA levels (2.8-fold) **(Figure 21C)**. The same dose, however, did not increase PGC1α mRNA levels after combination with 50μM WY-14643 **(Figure 19C)**. The inhibitory effect of PPARα agonist on rosiglitazone-mediated increase of *Pgc1α* expression was abolished upon co-administration of 10μM PPARα antagonist (MK886) **(Figure 19D).**

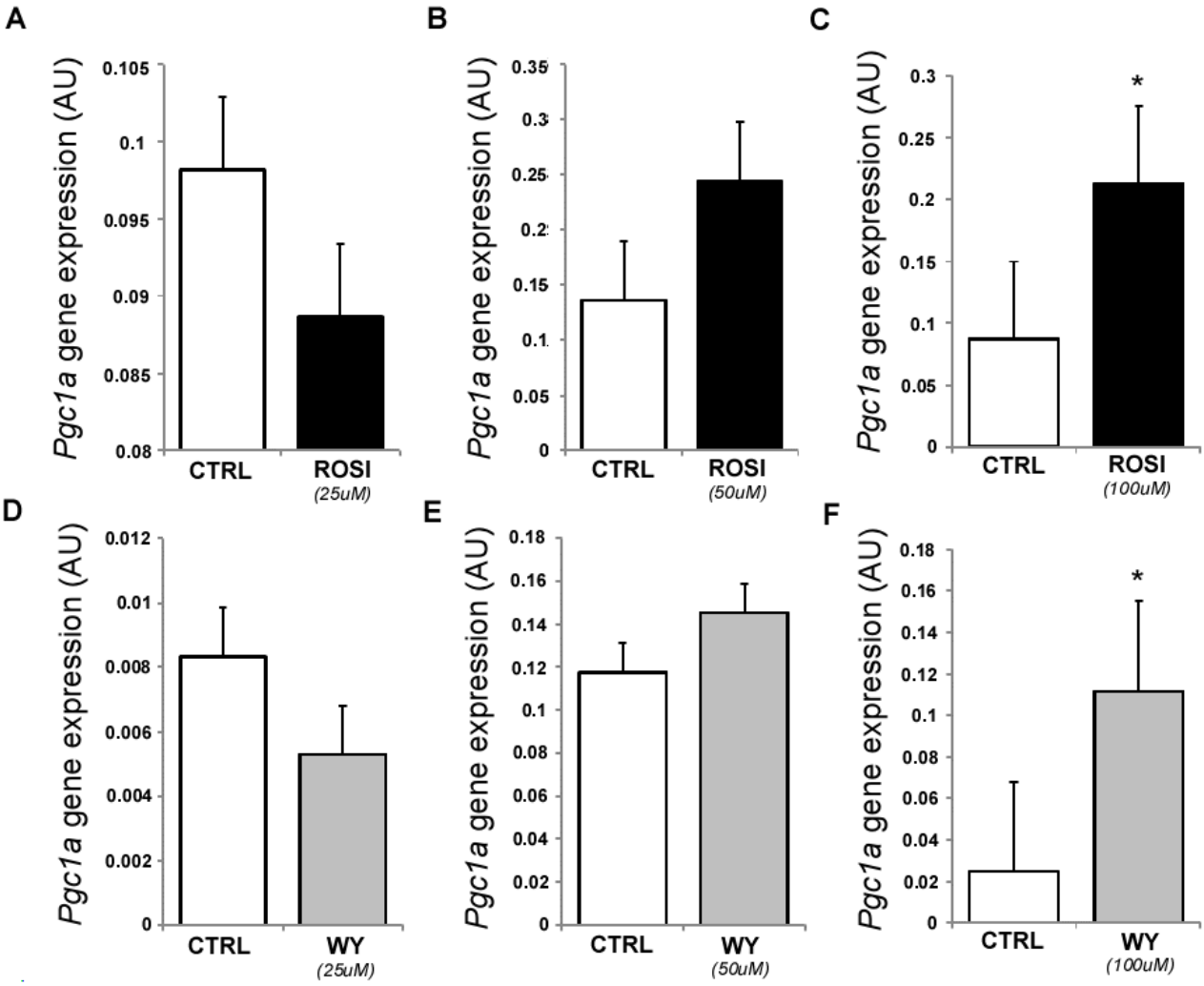

Figure 21 - A-F: PGC1α mRNA levels in AC16 cells treated with increasing doses of rosiglitazone (25, 50 and 100 μM) (A-C) and WY-14643 (25, 50 and 100 μM) (D-F); n=4, *p<0.05 vs. CTRL. Statistical analysis was performed with unpaired 2-tailed Student's t-test *p<0.05, Error bars represent SEM

AC16 cells were transfected with reporter plasmids containing *Pgc1α* promoter deletion mutants, *pGL3BV-hPgc1α-1631*, *pGL3BV-hPgc1α-1386, pGL3BV-hPgc1α-1012*, and *pGL3BV-hPgc1α-210*, followed by treatment with 50μM rosiglitazone, 50μM WY-14643 or combination of both. Rosiglitazone increased luciferase activity of the *pGL3BV-hPgc1α-1631* **(Figure 19E)** and *pGL3BV-hPgc1α-1386* **(Figure 19F)** vectors, while it did not have any effect on *pGL3BV-hPgc1α-1012* **(Figure 19G)** and *pGL3BV-*

hPgc1α-210 **(Figure 19H**). On the other hand, WY-14643 did not increase luciferase activity in any of the groups (**Figure 19E-H**). However, the combined treatment with rosiglitazone and WY-14643 prevented rosiglitazone-mediated increase in the activity of the *hPgc1α-1631* promoter fragment **(Figure 19E).** Thus, activation of PPARα prevents PPARγ-mediated induction of *Pgc1α* promoter activity when the PPRE of the -1631/-1609bp region is present.

5.3.6 PPARα activation blocked PPARγ protein-protein interaction with PGC1α

It has been previously shown that PGC1α can bind and activate both PPARγ (Wu et al., 1999) and PPARα (Vega et al., 2000) Thus, we tested whether activation of PPARα interferes with protein-protein interaction of PPARγ with PGC1α in AC16 cells infected with recombinant adenoviruses expressing human PPARα (Ad-PPARα) and PPARγ (Ad-PPARγ). In a similar manner with pharmacologic activation of PPARα and PPARγ, PGC1α mRNA levels were upregulated (2.6-fold) in cells treated with Ad-PPARγ **(Figure 19I).** The positive effect of PPARγ on *Pgc1α* gene expression was blocked in cells infected with the combination of Ad-PPARα and Ad-PPARγ (**Figure 19I)**. Immunoprecipitation(IP) of either PPARα or PPARγ and WB analysis for PGC1α in protein lysates obtained from AC16 cells treated with Ad-PPARα, Ad-PPARγ or combination of both showed that overexpression of PPARα increased protein-protein interaction of the latter with PGC1α and reduced the binding of PPARγ on PGC1α (**Figure 19J)**.

Thus, PPARα and PPARγ compete for regulation of *Pgc1α* gene expression and the PPRE of the -1631/-1609bp region of h*Pgc1α* promoter is critical for this regulation. Also, PPARα and PPARγ compete for protein-protein interaction with PGC1α.

5.3.7 Tesaglitazar- decreased cardiac SIRT1 expression and increased PGC1α acetylation

PGC1α activation is controlled via deacetylation of lysine residues by the deacetylase SIRT1 (Rodgers et al., 2005). We thus determined whether tesaglitazar-mediated cardiac dysfunction is also associated with altered acetylation of PGC1α. The ratio of acetylated PGC1α (Ac-PGC1α) to PGC1α input was increased in hearts of mice fed with either CHOW or HFD supplemented with tesaglitazar. Specifically, Ac-PGC1α/PGC1α input ratio was increased in both CHOW- (3.3-fold) and HFD-fed (1.6-fold) mice **(Figure 22A, 22B)**, respectively**.** In accordance with the increased Ac-PGC1α levels, SIRT1 protein levels were decreased in tesaglitazar-treated mice that were fed with CHOW (40%) and HFD (60%) **(Figure 22C, 22D)**.

5.3.8 Tesaglitazar decreased SIRT1 in primary ACMs and increased total acetylome in primary ACMs

We then assessed whether downregulation of cardiac SIRT1 is accounted for by altered expression in primary ACMs and no other cell types of the cardiac muscle, such as fibroblasts or endothelial cells. Thus, we isolated ACMs from mice that had undergone daily i.p, injections with tesaglitazar (2mg/kg) for 7 days. Western blotting analysis showed that there was significant decrease in SIRT1 protein levels (68%) **(Figure 22E,**

22F), which was accompanied by increased (20%) total protein acetylome levels **(Figure 22E, 22F)**.

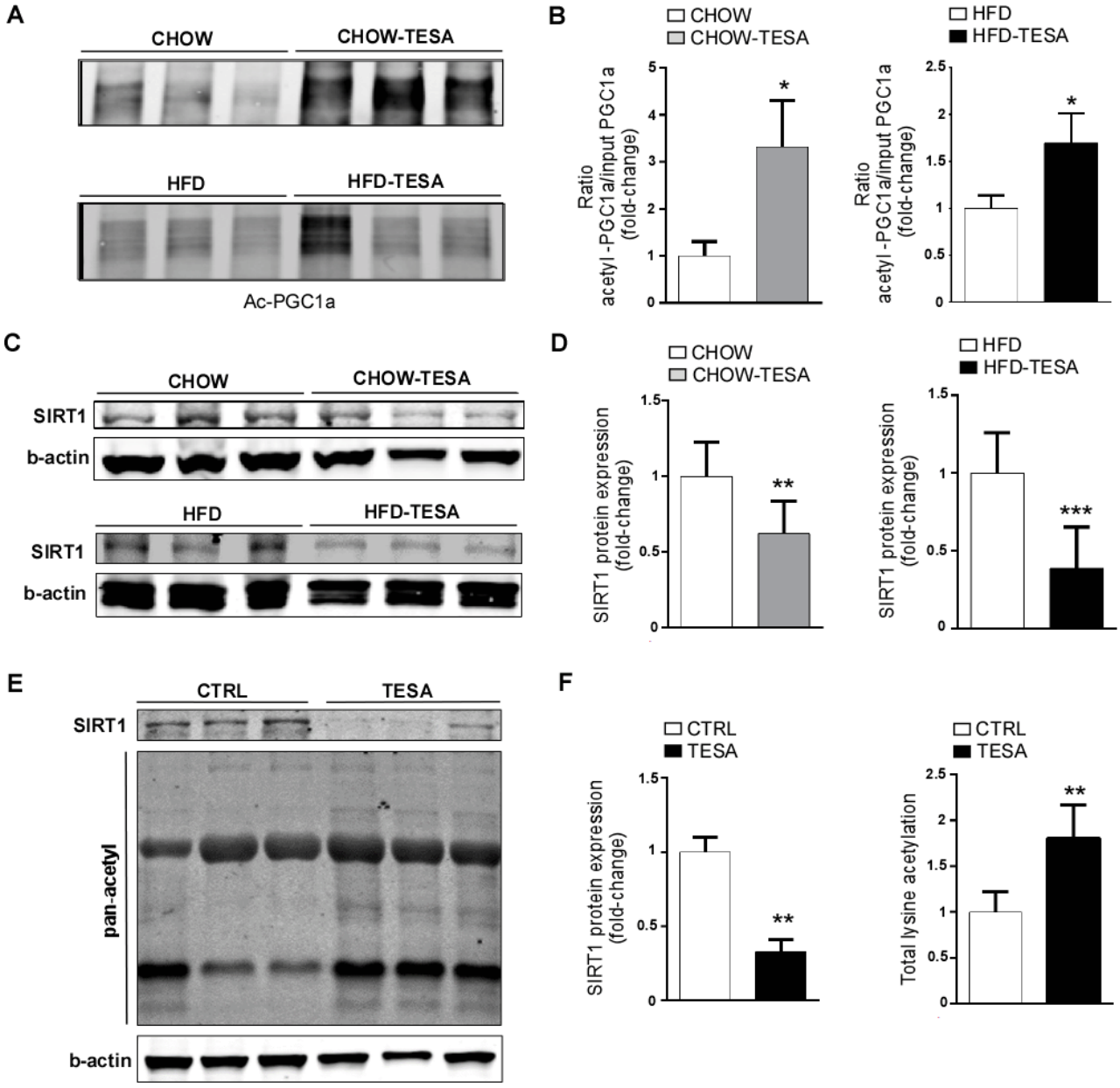

Figure 22. A, B: Immunoblot following immunoprecipitation (A) and densitometric analysis (B) of acetylated-PGC1a (Ac-PGC1a) normalized to total PGC1α protein expression (shown in Figures 1G and 1H) in hearts obtained from C57BL/6 mice fed with CHOW/tesaglitazar or HFD/tesaglitazar *(n=3)*. **C, D:** Immunoblot (C) and densitometric analysis (D) of SIRT1 and β-actin protein levels in hearts obtained from CHOW/tesaglitazar-fed or HFD/tesaglitazar-fed

C57BL/6 mice for 6 weeks. **E, F:** Immunoblot (E) and densitometric analysis (F) of SIRT1, β-actin expression and total acetylome in ACMs isolated from C57BL/6 mice treated intraperitoneally with 2mg/kg tesaglitazar for 7 days *(n=3)* Statistical analyses were performed with unpaired 2-tailed Student's t-tests, *p<0.05, **p<0.01, ***p<0.001. Error bars represent SEM.

5.3.9 Combined treatment with tesaglitazar and resveratrol, which activates SIRT1, ameliorated cardiac dysfunction while it maintained the anti-hyperglycemic and anti-hyperlipidemic effects

As tesaglitazar decreased SIRT1 expression and increased Ac-PGC1α levels we aimed to improve the failed therapy with tesaglitazar by adding resveratrol that activates SIRT1 and eventually PGC1α. Thus, we treated C57BL/6 mice with CHOW diet or HFD containing tesaglitazar (0.5μmol/kg) or combination of tesaglitazar (0.5μmol/kg) and resveratrol (100mg/kg/day) for 6 weeks. Both CHOW- and HFD-fed mice did not have significant differences in weight gain rates regardless of the treatment with tesaglitazar or combination of tesaglitazar and resveratrol (**Figure 23A, 23B**). Plasma glucose and TGs were significantly lower both in mice that were fed with HFD and tesaglitazar (26%) or with tesaglitazar and resveratrol (48%) compared to control mice on the same diet without tesaglitazar **(Figure 24A, 24B).** Thus, the beneficial metabolic effects of tesaglitazar were maintained after treatment with combination of tesaglitazar

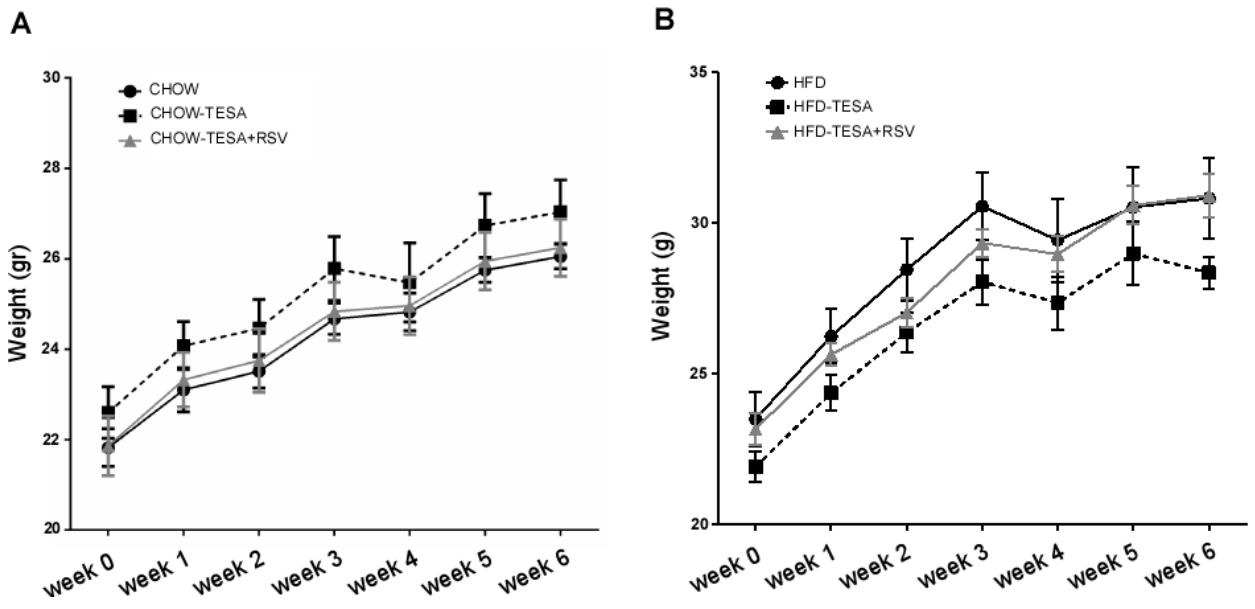

Figure 23 - A,B: Weight gain rate curves of C57BL/6 mice treated with CHOW (A) or HFD (B) containing TESA (0.5 μmol/kg body weight) or TESA (0.5 μmol/kg body weight) and RSV (100 mg/kg/day) for 6 weeks.

and resveratrol**.** Plasma glucose and TG levels did not change significantly in CHOW-fed mice. 2D-echocardiography confirmed significant cardiac dysfunction in mice treated with CHOW/tesaglitazar or HFD/tesaglitazar 4 weeks **(Figure 24C, 24D)** and 6 weeks **(Figure 24E- 24F)** after the beginning of the treatment. However, mice treated with combination of tesaglitazar and resveratrol showed significant improvement in cardiac function (FS%) compared to mice treated with tesaglitazar alone at both 4 weeks **(Figure 24C, 24D and Table 9)** and 6 weeks **(Figure 24E, 24F and Table 9)** after the beginning of the treatment**.** These findings, showed that resveratrol attenuated the tesaglitazar-mediated cardiac dysfunction in WT mice.

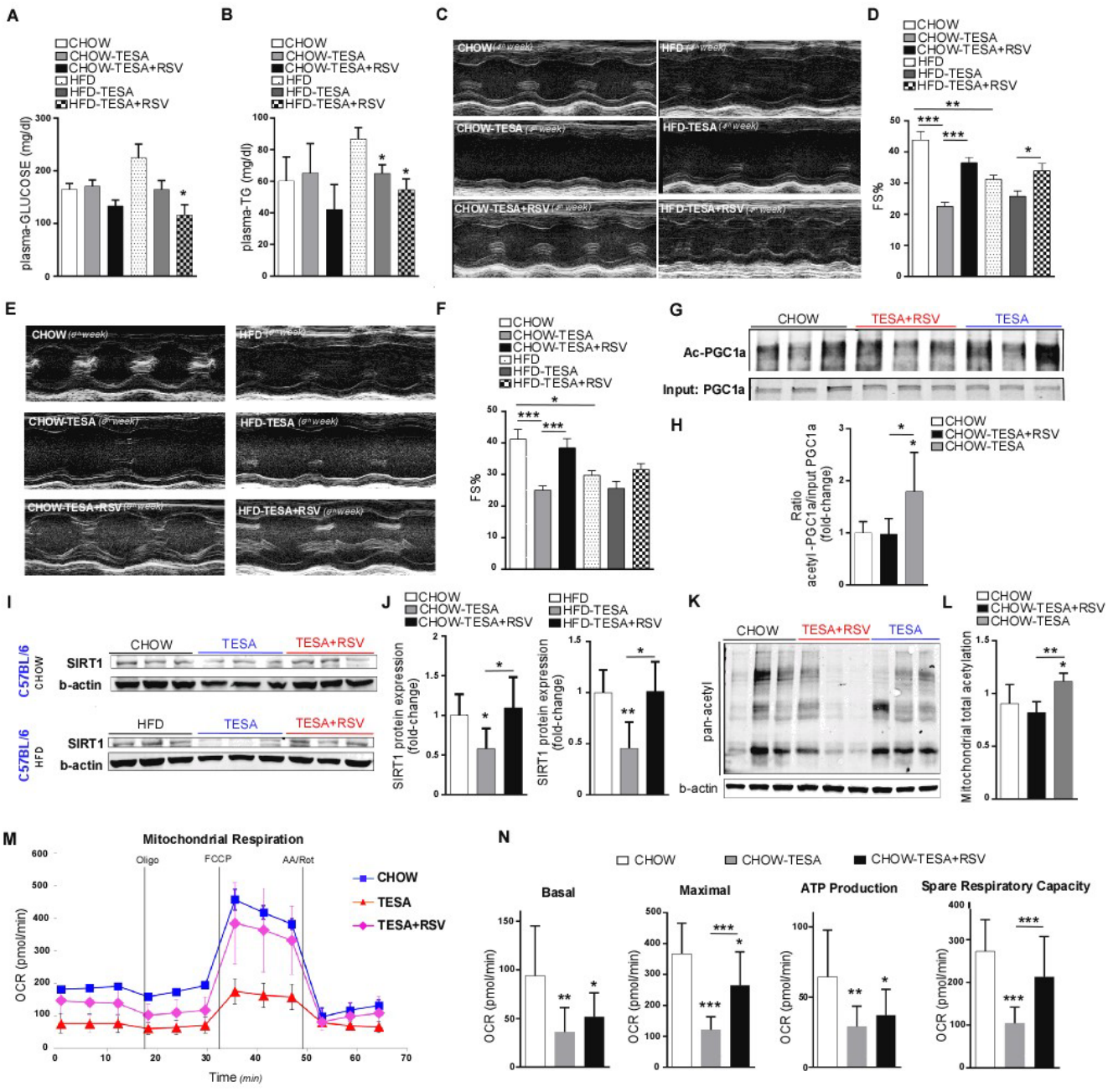

Figure 24. A-I: Plasma glucose (A), plasma TG (B), representative short-axis M-mode echocardiography images (C, E), fractional shortening (%) (D, F), immunoblots (G, I) and densitometric analysis (H, J) of cardiac acetylated-PGC1a (Ac-PGC1a) (G,H), total PGC1a (G,H), SIRT1 (I, J), and β-actin (I, J) of C57BL/6 mice treated with CHOW or HFD containing tesaglitazar (0.5 μmol/kg) or combination of tesaglitazar (0.5 μmol/kg) and resveratrol (100 mg/kg/day) for 4 weeks (C, D) or 6 weeks (A, B, E-J). **K, L**: Immunoblot (K) and densitometric analysis (L) of total acetylome and ATP5A of cardiac mitochondrial lysates obtained from C57BL/6 mice fed with CHOW diet containing tesaglitazar (0.5 μmol/kg) or combination of tesaglitazar (0.5 μmol/kg) and resveratrol (100 mg/kg/day) for 6 weeks, (n=5). **M-Q**: Oxygen Consumption Rate (OCR), basal respiration, maximal respiration, ATP production-related OCR and spare respiratory capacity measured with XF96 Seahorse Analyzer in ACMs isolated from

C57BL/6 mice fed with CHOW/tesaglitazar diet for 6 weeks. Oligo indicates oligomycin (3uM), FCCP indicates Carbonyl cyanide-p-trifluoromethoxyphenylhydrazone (2uM), AA/Rot indicates Antimycin A/ Rotenone (0.5uM) oligomycin. Statistical analyses were performed with unpaired 2-tailed Student's t-tests between groups, (n=3) *p<0.05, **p<0.01, ***p<0.001. Error bars represent SEM.

Parameters	Groups					
	CHOW	CHOW-TESA	CHOW-TESA+RSV	HFD	HFD-TESA	HFD-TESA+RSV
EF	**72.0**	**49.6**	**68.5**	**56.9**	**50.6**	**59.6**
FS	**41.2**	**25.0**	**38.5**	**29.8**	**25.7**	**31.6**
LV Mass	127.1	162.8	210.0	156.9	151.1	150.7
LV Mass (Cor)	101.7	130.3	168.0	125.5	120.9	120.5
LV Vol;d	76.4	86.1	89.6	88.5	77.5	82.6
LV Vol;s	21.6	43.9	28.1	38.4	39.4	33.7
IVS;d	1.0	1.1	1.5	0.9	1.1	0.9
IVS;s	1.6	1.5	2.0	1.5	1.4	1.5
LVID;d	4.1	4.3	4.4	4.4	4.1	4.3
LVID;s	2.4	3.3	2.7	3.1	3.1	2.9
LVPW;d	0.7	0.8	0.7	0.8	0.8	0.8
LVPW;s	1.2	0.9	1.2	1.2	1.0	1.2

Table 9 - Table of 2D-echocardiography parameters of C57BL/6 mice treated with CHOW or HFD containing TESA (0.5 µmol/kg body weight) or TESA (0.5 µmol/kg body weight) and RSV (100 mg/kg/day) for 6 weeks. Statistical analysis was performed with unpaired 2-tailed Student's t-test between groups, *p>0.05, **p<0.005, (# P<0.05, ## P<0.005, ### P<0.0005 TESA vs TESA+RSV) (n=7-8).

We then tested whether improved cardiac function in mice treated with combination of tesaglitazar and resveratrol was accompanied by changes in cardiac PGC1α acetylation and regulation. Immunoprecipitation assays showed that treatment

with tesaglitazar increased Ac-PGC1α (48%), while combined treatment with tesaglitazar and resveratrol restored PGC1α acetylation to normal levels **(Figure 24G, 24H).** We observed a similar trend towards reduced Ac-PGC1α/total PGC1α ratio for the respective HFD-treated group, which did not reach statistical significance **(Figure 25A,25B)**. Assessment of cardiac SIRT1 protein levels showed that combined tesaglitazar and resveratrol treatment increased SIRT1 expression in both CHOW- (47%) and HFD-fed (55%) mice compared to mice that received tesaglitazar alone **(Figure 24I, 24J**). Restoration of cardiac SIRT1 expression was associated with reduced (27%) total acetylome of proteins isolated from cardiac mitochondrial lysates of mice fed with CHOW diet and tesaglitazar or combination of tesaglitazar and resveratrol (**Figure 24K, 24L**). We didn't observe significant differences in total acetylome of mitochondria isolated from HFD-fed mice tesaglitazar or combination of tesaglitazar and resveratrol **(Figure 25C, 25D).** Furthermore, although previous studies have reported increased phosphorylation/activation of 5'AMP-activated protein kinase (AMPK) by RSV (Canto and Auwerx, 2009), Western Blotting analysis for p-AMPK (Thr172) didn't display obvious differences among treated groups **(Figure 26A-D).**

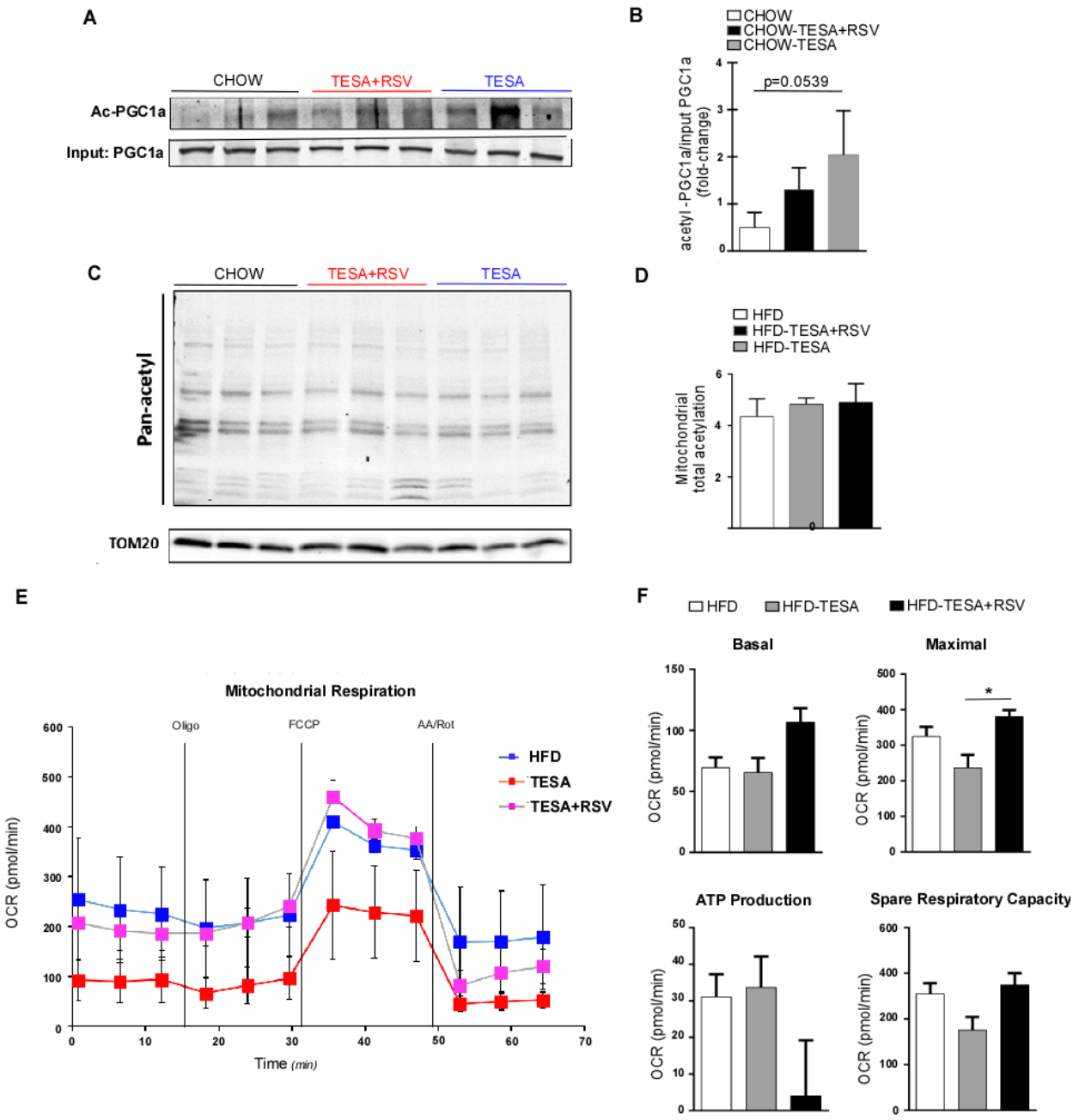

Figure 25 - A,B: Cardiac Ac-PGC1α, total PGC1α, β-actin immunoblots (A) and densitometric analysis (B) of *C57BL/6* mice treated with HFD containing TESA (0.5 μmol/kg body weight) or combination of TESA (0.5 μmol/kg body weight) and RSV (100 mg/kg/day) **C, D:** Immunoblot (C) and densitometric analysis (D) of total acetylome and ATP5A of cardiac mitochondrial lysates obtained from C57BL/6 mice fed with HFD containing TESA (0.5 μmol/kg body weight) or combination of TESA (0.5 μmol/kg body weight) and RSV (100 mg/kg/day) for 6 weeks, (n=3). **E, F:** Oxygen Consumption Rate (OCR), basal respiration, maximal respiration, ATP production-related OCR and spare respiratory capacity measured with XF96 Seahorse Analyzer in ACMs isolated from C57BL/6 mice fed with HFD/TESA diet for 6 weeks. Oligo indicates oligomycin (3uM), FCCP indicates Carbonyl cyanide-p-trifluoromethoxyphenylhydrazone (2uM), AA/Rot indicates Antimycin A/ Rotenone (0.5uM) oligomycin. Statistical analyses were

performed with unpaired 2-tailed Student's t-tests between groups, (n=3). Error bars represent SEM.

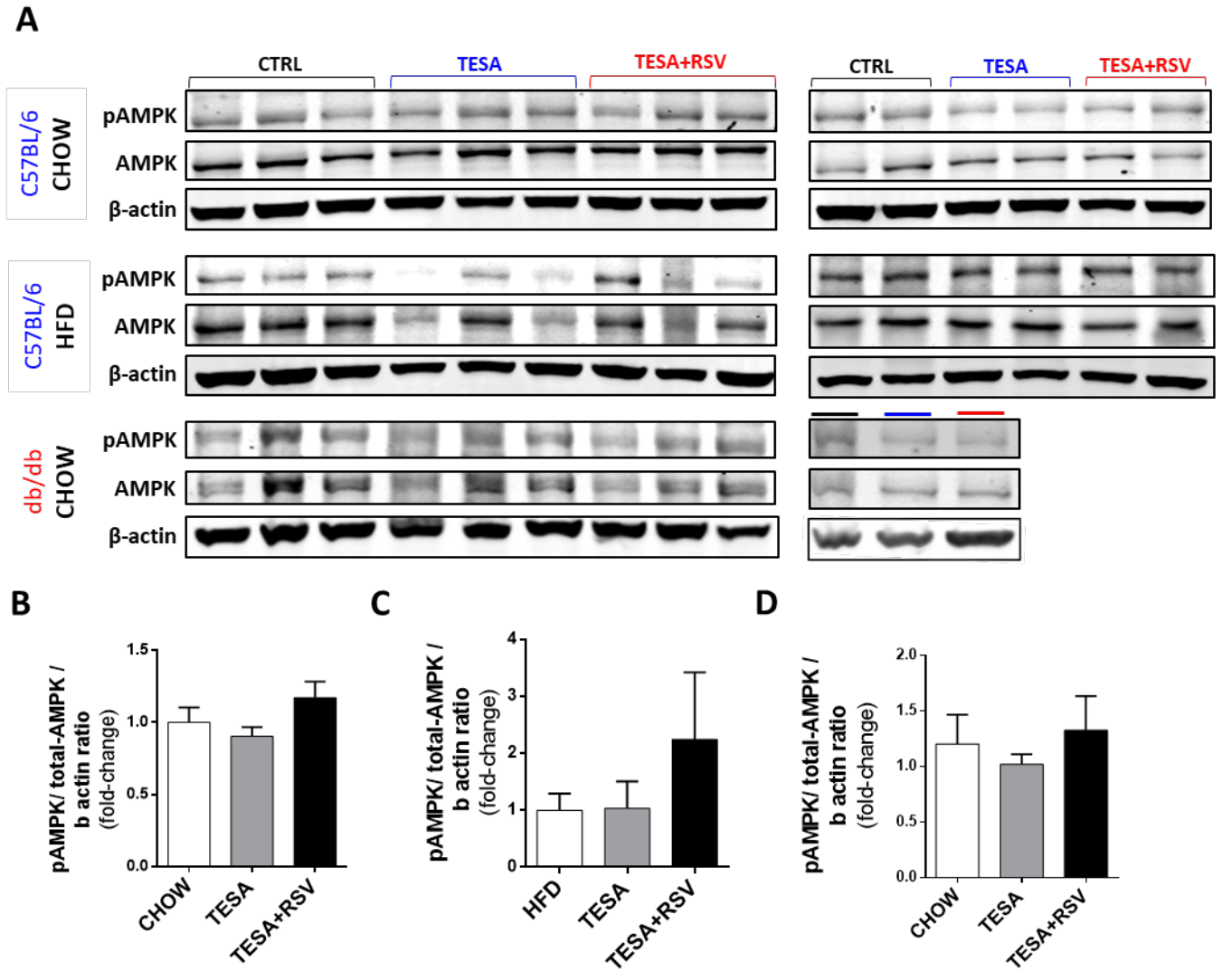

Figure 26 - A. phosphor-AMPK (pAMPK), total-AMPK (tAMPK) and β-actin (loading control) protein expression in hearts from CHOW or HFD/TESA or TESA+RSV-fed C57BL/6 mice for 6 weeks or CHOW/TESA or CHOW/TESA+RSV **B-D.** and respective quantitative densitometry analysis (n=5)

5.3.10 Combined tesaglitazar and resveratrol treatment improved respiratory capacity, increased mitochondria abundance and altered cardiac lipid content

SIRT1 and PGC1α are regulators of mitochondrial biology. Therefore, we analyzed mitochondrial respiration with the Seahorse system in isolated primary ACMs from C57BL/6 mice treated with CHOW diet containing tesaglitazar or combination of tesaglitazar and resveratrol. This analysis showed that combined tesaglitazar and resveratrol treatment restored OCR to normal levels (**Figure 24M**) as shown by improved basal respiration, maximal respiration, OCR for ATP production and spare respiratory capacity (**Figure 24N**). Respective differences in the HFD-fed mice treated with tesaglitazar or tesaglitazar and resveratrol were similar with those observed in CHOW-fed mice but did not reach statistical significance **(Figure 25E, 25F)**.

We next performed mitotracker staining to assess mitochondria abundance in primary ACMs obtained from mice that received daily i.p. injections with tesaglitazar (2mg/kg/day) and resveratrol (100mg/kg/day) for 7 days (**Figure 27A,27C)**. This analysis showed an 80% reduction in mitochondria abundance of ACMs obtained from mice treated with tesaglitazar alone and a 60% increase in ACMs from mice treated with tesaglitazar and resveratrol **(Figure 27A,27C)**. The same analysis in AC16 cells that were treated with 100 μM tesaglitazar or combination of 100 μM tesaglitazar and 100 μM resveratrol for 24h showed reduction (55%) of mitochondrial number in cells treated with tesaglitazar that was restored with combined tesaglitazar and resveratrol treatment (**Figure 28A, 28B)**.

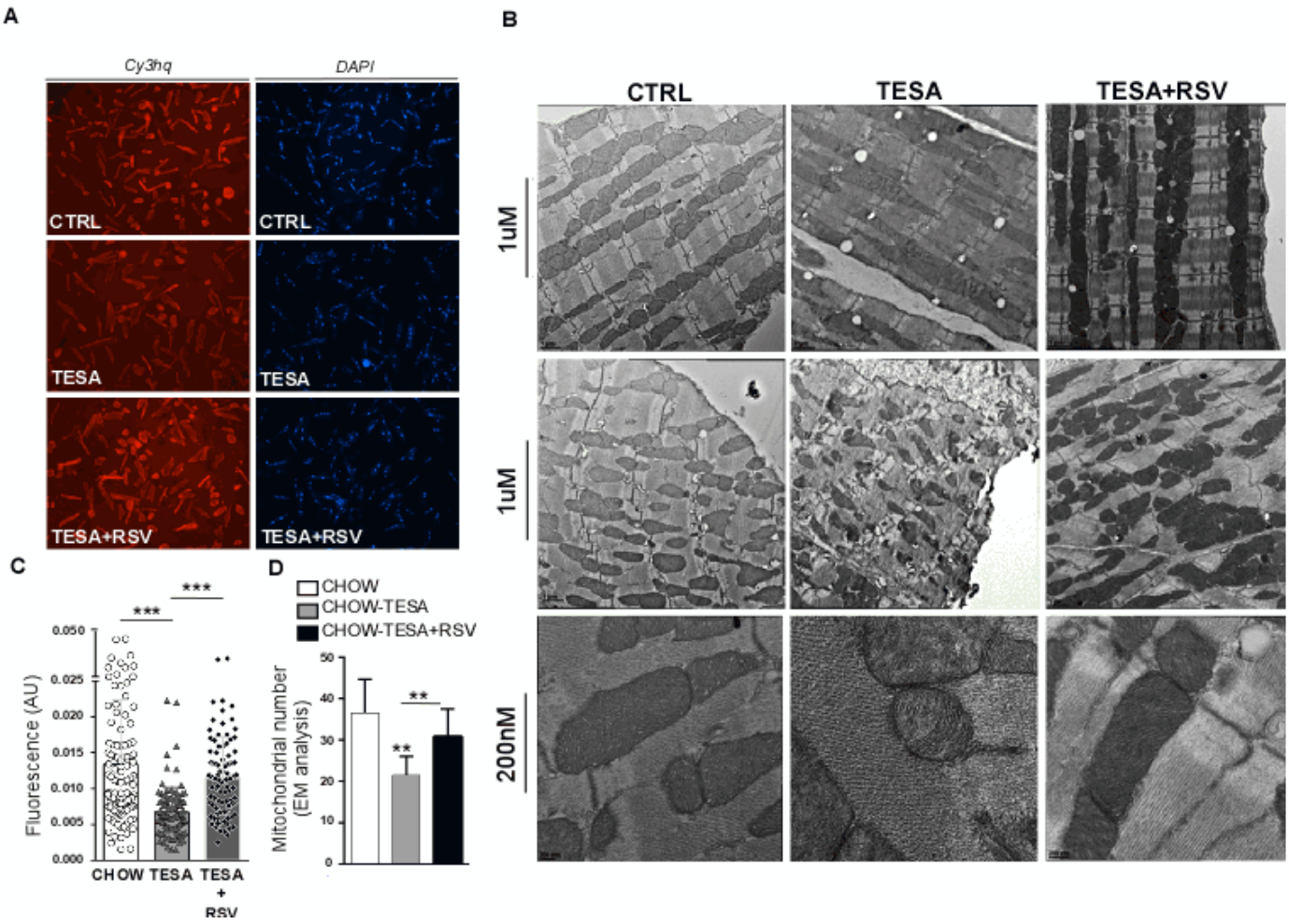

Figure 27. A, B: Representative images obtained from fluorescence microscopy (A) of isolated adult mouse cardiomyocytes (ACMs) stained with Mitotracker Red and quantitation (B) of mitochondrial number/total area. ACMs were obtained from C57BL/6 mice treated with intraperitoneal daily injections of tesaglitazar (2mg/kg) or combination of tesaglitazar (2mg/kg) and resveratrol (100mg/kg) for 7 days (*n=3)* (number of analyzed cells: CTRL: 158, Tesaglitazar: 157, Tesaglitazar+Resveratrol: 157). **C, D.** Quantitation of mitochondrial number normalized with total surface area (mito-number/133.35cm^2) (C) and representative electron microcopy images (resolution: 1um,200nm) (D) in hearts obtained from C57BL/6 mice fed with CHOW diet containing tesaglitazar or combination of tesaglitazar and resveratrol for 6 weeks. Statistical analyses were performed with unpaired 2-tailed Student's t-test between groups, *p<0.05, **p<0.005, ***p<0.0005 . Error bars represent SEM

The improvement in mitochondria abundance of AC16 cells treated with combination of tesaglitazar and resveratrol was accompanied by increased SIRT1 expression **(Figure 28C).**

We then performed EM analysis (image resolution: 1μm and 200nm), which confirmed that cardiac mitochondria abundance was reduced (40%) in tesaglitazar-treated mice and restored in mice treated with tesaglitazar and resveratrol **(Figure 27B, 27D).** Morphological analysis of mitochondria from EM images showed that hearts of tesaglitazar-treated mice displayed more spherical mitochondria with abnormal morphology compared to control mice that had regular arrangement of myofibrils and mitochondria with abundant regular cristae in between. EM images from mice treated with tesaglitazar and resveratrol showed organized myofibrils with numerous mitochondria in between, which retained normal structure and organized cristae compared to tesaglitazar-treated group **(Figure 27B)**.

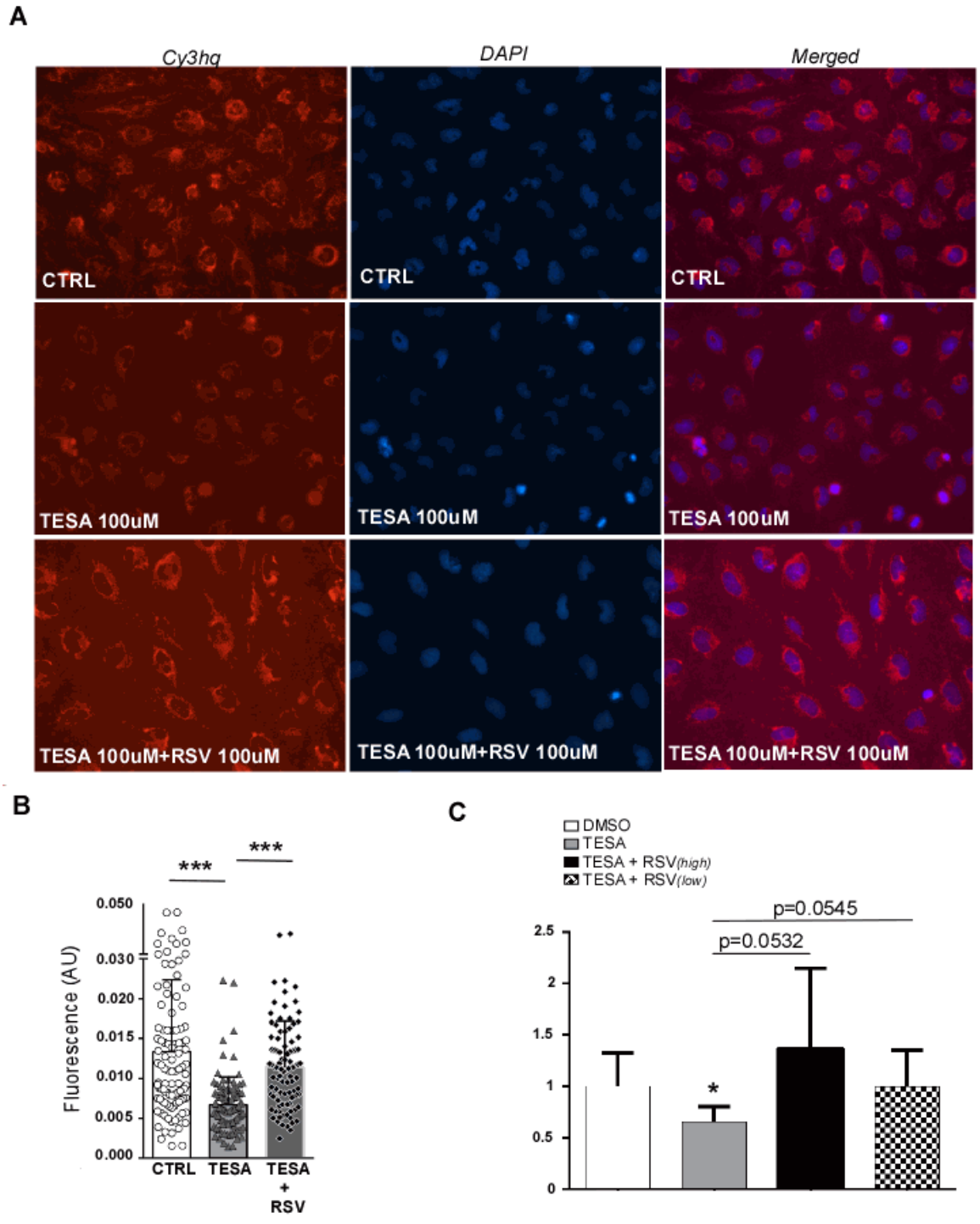

Figure 28- A, B: Representative images obtained from fluorescence microscopy of AC16 cells stained with Mitotracker Red (A) and quantitation (B) of mitochondrial number/total area. AC16 cells were treated prior staining with 100μM TESA or 100μM TESA and 100μM RSV for 24h (number of analyzed cells: CTRL:103, TESA 100μM: 100, TESA 100μM+ RSV 100 μM: 100. **C**. SIRT1 mRNA levels of AC16 cells treated with 100μM TESA or 100μM TESA and 100μM RSV (high) or 100μM TESA and 50μM RSV (low). Statistical analysis was performed with unpaired 2-

tailed Student's t-test between groups, *P<0.05, **P<0.01, ***P<0.001. Error bars represent SEM

5.3.11 Mice treated with tesaglitazar or combination of tesaglitazar and resveratrol had distinct lipidomic signatures

As treatment with tesaglitazar reduced mitochondria abundance and respiratory capacity, we tested whether it also affects cardiac lipid content. Lipidomic analysis revealed significant differences in most of the lipid classes we assessed. Heat map analysis for the lipid species that we tested followed by hierarchical clustering of those that changed significantly ($p<0.05$) indicated distinct cardiac lipidomic signatures between the three groups of mice (control CHOW-fed vs. Tesaglitazar vs. Tesaglitazar+resveratrol) (**Figure 29**). This analysis showed that tesaglitazar increased cardiac TG (6.8-fold), acyl-carnitines (2.3-fold), diacylglycerols (3.1-fold), and phosphatidic acid (30%), reduced phosphatidyl-choline (37%), while there was a strong trend of reduction for monoacyl-glycerols (40%; $p=0.053$) and ceramides (27%; $p=0.08$). Combined treatment with TESAGLITAZAR and RESVERATROL restored normal levels of acyl-carinitines, phosphatidic acid, phosphatidyl-choline, monoacyl-glycerols, and ceramides (**Table 10**).

LIPIDS	Normalized Average	Normalized Standard Error	P value

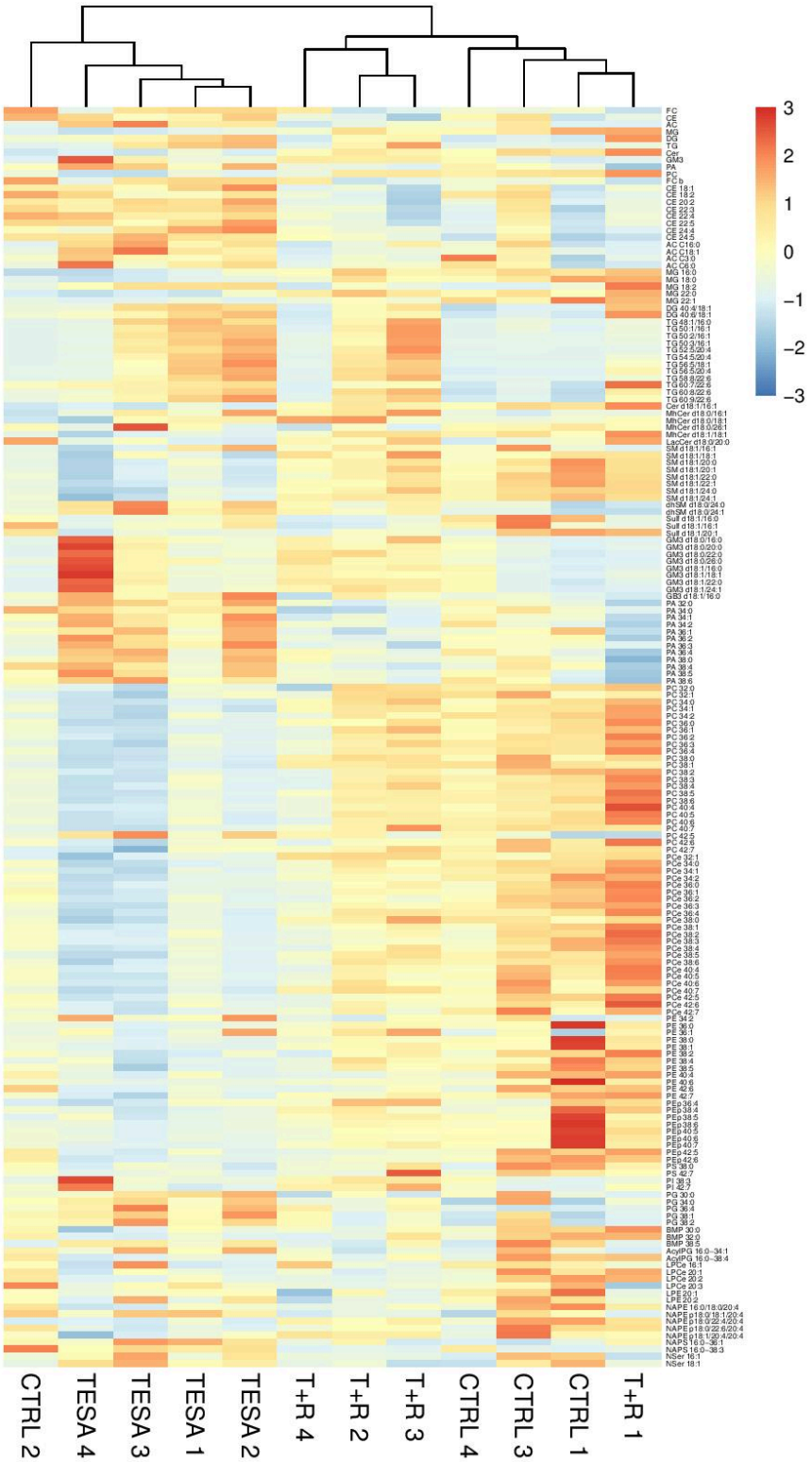

Figure 29. Heat map and correlation clustering following lipidomic analysis of hearts obtained from C57BL/6 mice fed with CHOW diet containing tesaglitazar or combination of tesaglitazar and resveratrol for 6 weeks.

	CTRL	TESA	T+R	CTRL	TESA	T+R	CTRL vs TESA	CTRL vs T+R	TESA vs T+R
FC	1.00	1.03	0.93	0.04	0.03	0.03	0.589	0.275	0.094
CE	1.00	1.09	0.60	0.17	0.09	0.07	0.678	0.095	0.009
AC	1.00	2.27	0.65	0.28	0.29	0.17	0.030	0.383	0.005
MG	1.00	0.61	1.06	0.14	0.04	0.12	0.054	0.763	0.018
DG	1.00	3.09	2.61	0.21	0.44	0.74	0.009	0.111	0.635
TG	1.00	6.79	4.75	0.09	1.77	2.08	0.027	0.158	0.528
Cer	1.00	0.73	1.14	0.11	0.04	0.09	0.082	0.397	0.010
GM3	1.00	2.72	2.25	0.35	0.92	0.45	0.169	0.095	0.697
PA	1.00	1.30	0.74	0.04	0.09	0.07	0.040	0.030	0.005
PC	1.00	0.63	1.07	0.07	0.05	0.12	0.008	0.662	0.019
FC b	1.00	1.03	0.93	0.04	0.03	0.03	0.589	0.275	0.094
CE 18:1	1.00	1.35	0.77	0.14	0.13	0.08	0.150	0.258	0.014
CE 18:2	1.00	0.94	0.51	0.17	0.09	0.07	0.787	0.057	0.018
CE 20:2	1.00	1.32	0.71	0.12	0.08	0.07	0.099	0.110	0.002
CE 22:3	1.00	1.38	0.79	0.22	0.07	0.09	0.184	0.452	0.003
CE 22:4	1.00	1.30	0.75	0.21	0.07	0.10	0.280	0.369	0.006
CE 22:5	1.00	1.44	0.75	0.19	0.13	0.08	0.144	0.326	0.007
CE 24:4	1.00	2.49	0.97	0.28	0.45	0.14	0.047	0.946	0.029
CE 24:5	1.00	1.58	0.96	0.22	0.06	0.11	0.063	0.902	0.004
AC C16:0	1.00	2.11	0.81	0.40	0.23	0.28	0.073	0.739	0.018
AC C18:1	1.00	2.42	0.54	0.21	0.37	0.11	0.023	0.125	0.005
AC C3:0	1.00	1.15	0.63	0.31	0.11	0.06	0.704	0.332	0.011
AC C6:0	1.00	1.71	0.78	0.28	0.29	0.12	0.170	0.532	0.039
MG 16:0	1.00	0.77	1.10	0.10	0.05	0.06	0.118	0.466	0.008
MG 18:0	1.00	0.56	1.04	0.15	0.04	0.13	0.046	0.854	0.017
MG 18:2	1.00	2.52	1.86	0.13	0.20	0.69	0.001	0.314	0.441
LIPIDS	**CTRL**	**TESA Average**	**T+R Average**	**CTRL**	**TESA**	**T+R**	**CTRL vs**	**CTRL vs T+R**	**TESA vs T+R**

	Average			SE	SE	SE	TESA		
MG 22:0	1.00	0.74	1.27	0.10	0.06	0.06	0.088	0.077	0.001
MG 22:1	1.00	0.36	0.76	0.23	0.03	0.17	0.046	0.470	0.086
szDG 40:4/18:1	1.00	3.02	2.55	0.21	0.43	0.58	0.010	0.065	0.583
DG 40:6/18:1	1.00	3.10	2.62	0.22	0.45	0.77	0.010	0.119	0.645
TG 48:1/16:0	1.00	3.36	2.35	0.11	0.70	0.88	0.025	0.222	0.452
TG 50:1/16:1	1.00	3.72	2.92	0.18	0.84	1.06	0.029	0.162	0.615
TG 50:2/16:1	1.00	10.00	7.13	0.10	2.75	3.32	0.026	0.151	0.573
TG 50:3/16:1	1.00	16.05	10.68	0.15	4.91	5.45	0.034	0.164	0.537
TG 52:5/20:4	1.00	18.18	13.81	0.06	5.13	7.10	0.024	0.158	0.671
TG 54:5/20:4	1.00	8.52	6.67	0.05	2.47	2.51	0.035	0.089	0.655
TG 56:5/18:1	1.00	7.86	6.22	0.06	2.52	1.88	0.051	0.048	0.655
TG 56:5/20:4	1.00	4.29	4.01	0.12	1.13	0.95	0.042	0.030	0.870
TG 58:8/22:6	1.00	7.17	6.03	0.08	1.96	2.11	0.031	0.077	0.736
TG 60:7/22:6	1.00	2.34	2.10	0.24	0.13	0.61	0.005	0.182	0.739
TG 60:8/22:6	1.00	2.85	2.85	0.23	0.38	0.56	0.010	0.034	0.996
TG 60:9/22:6	1.00	2.98	2.48	0.16	0.48	0.44	0.013	0.030	0.519
Cer d18:1/16:1	1.00	0.73	1.14	0.11	0.04	0.09	0.082	0.397	0.010
MhCer d18:0/16:1	1.00	0.98	0.98	0.06	0.07	0.03	0.825	0.791	0.977
MhCer d18:0/18:1	1.00	0.85	1.14	0.04	0.06	0.05	0.112	0.106	0.015
MhCer d18:0/26:1	1.00	0.77	1.00	0.08	0.04	0.03	0.060	0.982	0.005
MhCer d18:1/18:1	1.00	0.73	1.03	0.08	0.03	0.04	0.034	0.751	0.002
LacCer d18:0/20:0	1.00	0.73	0.98	0.07	0.04	0.04	0.025	0.824	0.007
SM d18:1/16:1	1.00	0.73	0.99	0.07	0.02	0.04	0.019	0.888	0.001
LIPIDS	**CTRL Average**	**TESA Average**	**T+R Average**	**CTRL SE**	**TESA SE**	**T+R SE**	**CTRL vs**	**CTRL vs T+R**	**TESA vs T+R**

							TESA		
SM d18:1/18:1	1.00	0.72	1.05	0.06	0.05	0.05	0.020	0.614	0.005
SM d18:1/20:0	1.00	0.69	1.02	0.07	0.05	0.02	0.018	0.829	0.002
SM d18:1/20:1	1.00	1.70	1.18	0.08	0.13	0.12	0.008	0.315	0.045
SM d18:1/22:0	1.00	1.70	1.22	0.06	0.13	0.13	0.005	0.238	0.057
SM d18:1/22:1	1.00	1.82	1.94	0.12	0.31	0.31	0.065	0.043	0.812
SM d18:1/24:0	1.00	1.35	2.27	0.15	0.38	0.40	0.474	0.037	0.184
SM d18:1/24:1	1.00	0.99	0.58	0.06	0.33	0.14	0.977	0.045	0.351
dhSM d18:0/24:0	1.00	0.71	1.19	0.08	0.04	0.10	0.027	0.223	0.007
dhSM d18:0/24:1	1.00	0.69	0.55	0.10	0.06	0.02	0.050	0.007	0.105
Sulf d18:1/16:0	1.00	0.72	0.52	0.14	0.07	0.05	0.159	0.026	0.088
Sulf d18:1/16:1	1.00	0.33	0.67	0.23	0.07	0.21	0.047	0.385	0.220
Sulf d18:1/20:1	1.00	0.84	1.19	0.13	0.05	0.09	0.346	0.321	0.021
GM3 d18:0/16:0	1.00	3.26	2.63	0.25	1.09	0.78	0.120	0.125	0.685
GM3 d18:0/20:0	1.00	2.98	2.03	0.29	1.11	0.40	0.173	0.110	0.497
GM3 d18:0/22:0	1.00	3.03	2.79	0.29	1.04	0.68	0.144	0.075	0.870
GM3 d18:0/26:0	1.00	2.71	2.02	0.18	0.80	0.48	0.110	0.124	0.527
GM3 d18:1/16:0	1.00	2.78	2.06	0.39	1.01	0.42	0.191	0.148	0.577
GM3 d18:1/18:1	1.00	3.28	2.11	0.38	1.30	0.37	0.181	0.111	0.466
GM3 d18:1/22:0	1.00	2.59	2.25	0.36	0.84	0.44	0.170	0.094	0.756
GM3 d18:1/24:1	1.00	2.75	2.36	0.39	0.96	0.55	0.182	0.122	0.762
GB3 d18:1/16:0	1.00	1.86	0.98	0.06	0.21	0.21	0.013	0.939	0.040
PA 32:0	1.00	1.44	0.83	0.05	0.08	0.08	0.008	0.155	0.003
PA 34:0	1.00	1.04	0.69	0.07	0.03	0.03	0.679	0.011	0.000
PA 34:1	1.00	1.31	0.76	0.03	0.10	0.05	0.039	0.012	0.004
LIPIDS	**CTRL Average**	**TESA Average**	**T+R Average**	**CTRL SE**	**TESA SE**	**T+R SE**	**CTRL vs**	**CTRL vs T+R**	**TESA vs T+R**

							TESA		
PA 34:2	1.00	1.55	0.73	0.15	0.15	0.12	0.054	0.250	0.008
PA 36:1	1.00	1.14	0.72	0.08	0.09	0.05	0.325	0.028	0.009
PA 36:2	1.00	1.38	0.76	0.05	0.12	0.07	0.040	0.045	0.008
PA 36:3	1.00	1.40	0.79	0.03	0.10	0.05	0.014	0.016	0.003
PA 36:4	1.00	1.46	0.85	0.12	0.17	0.14	0.091	0.486	0.046
PA 38:0	1.00	1.19	0.86	0.04	0.08	0.08	0.119	0.236	0.049
PA 38:4	1.00	1.10	0.71	0.07	0.08	0.05	0.435	0.024	0.011
PA 38:5	1.00	1.38	0.74	0.09	0.17	0.11	0.122	0.154	0.030
PA 38:6	1.00	1.32	0.70	0.12	0.12	0.11	0.133	0.144	0.014
PC 32:0	1.00	0.78	1.00	0.04	0.04	0.11	0.013	0.975	0.137
PC 32:1	1.00	0.82	1.02	0.07	0.05	0.05	0.107	0.866	0.040
PC 34:0	1.00	0.67	1.18	0.07	0.02	0.07	0.006	0.132	0.001
PC 34:1	1.00	0.60	1.12	0.06	0.04	0.08	0.002	0.319	0.001
PC 34:2	1.00	0.60	1.00	0.11	0.07	0.11	0.031	0.990	0.039
PC 36:0	1.00	0.59	1.12	0.07	0.04	0.12	0.004	0.457	0.009
PC 36:1	1.00	0.64	1.14	0.07	0.03	0.12	0.004	0.406	0.012
PC 36:2	1.00	0.62	1.10	0.08	0.05	0.15	0.015	0.642	0.041
PC 36:3	1.00	0.61	1.09	0.09	0.06	0.11	0.019	0.585	0.013
PC 36:4	1.00	0.62	1.04	0.06	0.03	0.12	0.002	0.773	0.020
PC 38:0	1.00	0.72	1.10	0.08	0.03	0.03	0.022	0.327	0.000
PC 38:1	1.00	0.72	0.99	0.07	0.01	0.01	0.011	0.947	0.000
PC 38:2	1.00	0.53	0.97	0.14	0.04	0.15	0.025	0.905	0.041
PC 38:3	1.00	0.53	1.09	0.09	0.09	0.19	0.018	0.731	0.058
PC 38:4	1.00	0.53	1.16	0.11	0.08	0.20	0.023	0.563	0.040
PC 38:5	1.00	0.52	1.18	0.09	0.06	0.17	0.009	0.436	0.019
PC 38:6	1.00	0.46	1.10	0.11	0.08	0.19	0.013	0.691	0.032
PC 40:4	1.00	0.48	1.28	0.13	0.07	0.32	0.018	0.503	0.075

PC 40:5	1.00	0.52	1.18	0.11	0.07	0.19	0.018	0.496	0.027
PC 40:6	1.00	0.50	1.04	0.10	0.08	0.19	0.012	0.858	0.057
PC 40:7	1.00	0.65	1.08	0.09	0.04	0.10	0.018	0.602	0.013
PC 42:5	1.00	1.69	1.09	0.15	0.20	0.18	0.049	0.752	0.091
PC 42:6	1.00	0.67	0.97	0.08	0.07	0.16	0.033	0.869	0.175
PC 42:7	1.00	0.81	1.03	0.06	0.06	0.04	0.115	0.765	0.044
PCe 32:1	1.00	0.80	1.20	0.06	0.05	0.00	0.059	0.024	0.000
PCe 34:0	1.00	0.69	0.99	0.04	0.03	0.07	0.002	0.928	0.011
PCe 34:1	1.00	0.65	1.01	0.07	0.04	0.10	0.008	0.916	0.022
PCe 34:2	1.00	0.57	0.91	0.09	0.04	0.09	0.007	0.530	0.022
PCe 36:0	1.00	0.56	1.00	0.12	0.04	0.17	0.019	0.988	0.062
PCe 36:1	1.00	0.54	0.97	0.09	0.04	0.14	0.005	0.865	0.041
PCe 36:2	1.00	0.52	0.87	0.10	0.06	0.18	0.010	0.582	0.150
PCe 36:3	1.00	0.51	0.91	0.10	0.06	0.12	0.010	0.648	0.036
PCe 36:4	1.00	0.60	1.14	0.08	0.05	0.13	0.009	0.430	0.013
PCe 38:0	1.00	0.63	1.14	0.06	0.06	0.07	0.008	0.232	0.003
PCe 38:1	1.00	0.53	1.04	0.11	0.04	0.17	0.011	0.880	0.038
PCe 38:2	1.00	0.50	1.02	0.14	0.08	0.25	0.034	0.960	0.128
PCe 38:3	1.00	0.32	0.90	0.19	0.05	0.28	0.024	0.798	0.119
PCe 38:4	1.00	0.45	1.06	0.15	0.07	0.22	0.024	0.859	0.059
PCe 38:5	1.00	0.48	1.15	0.13	0.08	0.13	0.020	0.477	0.007
PCe 38:6	1.00	0.44	1.15	0.10	0.08	0.17	0.006	0.533	0.016
PCe 40:4	1.00	0.47	1.03	0.13	0.06	0.23	0.016	0.925	0.075
PCe 40:5	1.00	0.62	0.99	0.08	0.04	0.14	0.011	0.944	0.068
PCe 40:6	1.00	0.69	1.06	0.11	0.03	0.10	0.045	0.745	0.022
PCe 40:7	1.00	0.72	1.09	0.08	0.03	0.03	0.022	0.331	0.000
PCe 42:5	1.00	0.57	0.93	0.09	0.05	0.17	0.010	0.748	0.117
LIPIDS	**CTRL Average**	**TESA Average**	**T+R Average**	**CTRL SE**	**TESA SE**	**T+R SE**	**CTRL vs TESA**	**CTRL vs T+R**	**TESA vs T+R**

PCe 42:6	1.00	0.72	1.05	0.06	0.06	0.17	0.025	0.805	0.142
PCe 42:7	1.00	0.78	0.96	0.07	0.02	0.06	0.036	0.717	0.044
PE 34:2	1.00	1.27	0.84	0.12	0.14	0.06	0.236	0.324	0.046
PE 36:0	1.00	0.50	0.85	0.27	0.03	0.06	0.152	0.643	0.004
PE 36:1	1.00	1.18	1.29	0.07	0.11	0.07	0.264	0.040	0.454
PE 38:0	1.00	0.40	0.75	0.29	0.05	0.09	0.117	0.496	0.021
PE 38:1	1.00	0.36	0.85	0.30	0.01	0.06	0.103	0.671	0.001
PE 38:2	1.00	0.69	0.99	0.08	0.05	0.15	0.029	0.953	0.139
PE 38:4	1.00	0.70	1.03	0.15	0.06	0.09	0.140	0.901	0.038
PE 38:5	1.00	0.61	0.89	0.09	0.05	0.07	0.017	0.438	0.028
PE 40:4	1.00	0.36	0.67	0.20	0.09	0.24	0.038	0.387	0.319
PE 40:6	1.00	0.41	0.67	0.33	0.02	0.08	0.159	0.410	0.027
PE 42:6	1.00	0.37	0.66	0.17	0.05	0.17	0.020	0.256	0.178
PE 42:7	1.00	0.56	0.99	0.11	0.06	0.12	0.018	0.949	0.029
PEp 36:4	1.00	0.86	1.28	0.12	0.08	0.09	0.419	0.140	0.021
PEp 38:4	1.00	0.68	1.04	0.16	0.04	0.07	0.136	0.858	0.008
PEp 38:5	1.00	0.61	0.94	0.27	0.07	0.04	0.257	0.846	0.013
PEp 38:6	1.00	0.50	0.85	0.27	0.03	0.06	0.151	0.643	0.004
PEp 40:5	1.00	0.40	0.80	0.29	0.03	0.12	0.118	0.590	0.032
PEp 40:6	1.00	0.36	0.72	0.30	0.04	0.10	0.106	0.460	0.022
PEp 40:7	1.00	0.36	0.85	0.30	0.01	0.06	0.108	0.670	0.000
PEp 42:5	1.00	0.38	0.69	0.15	0.08	0.21	0.016	0.323	0.254
PEp 42:6	1.00	0.41	0.72	0.12	0.03	0.12	0.006	0.196	0.059
PS 38:0	1.00	0.68	0.88	0.13	0.04	0.06	0.088	0.482	0.045
PS 42:7	1.00	0.81	1.01	0.06	0.02	0.12	0.045	0.941	0.202
PI 38:3	1.00	1.99	1.94	0.22	0.82	0.30	0.337	0.065	0.964
PI 42:7	1.00	1.56	2.24	0.18	0.71	0.32	0.517	0.023	0.463
PG 30:0	1.00	1.15	0.73	0.11	0.08	0.07	0.364	0.116	0.013
LIPIDS	**CTRL Average**	**TESA Average**	**T+R Average**	**CTRL SE**	**TESA SE**	**T+R SE**	**CTRL vs TESA**	**CTRL vs T+R**	**TESA vs T+R**

PG 34:0	1.00	1.22	1.01	0.15	0.06	0.03	0.260	0.965	0.031
PG 36:4	1.00	4.56	2.33	0.40	0.86	0.54	0.015	0.128	0.098
PG 38:1	1.00	1.82	0.93	0.31	0.22	0.15	0.101	0.868	0.024
PG 38:2	1.00	1.74	0.91	0.32	0.22	0.16	0.139	0.837	0.033
BMP 30:0	1.00	0.41	0.88	0.13	0.15	0.22	0.037	0.692	0.164
BMP 32:0	1.00	0.41	0.79	0.15	0.05	0.21	0.017	0.494	0.159
BMP 38:5	1.00	1.02	0.81	0.14	0.04	0.06	0.908	0.313	0.038
AcylPG 16:0-34:1	1.00	1.11	0.84	0.08	0.08	0.04	0.434	0.170	0.036
AcylPG 16:0-38:4	1.00	0.68	0.88	0.10	0.02	0.08	0.027	0.412	0.081
LPCe 16:1	1.00	0.81	0.88	0.04	0.16	0.10	0.348	0.329	0.763
LPCe 20:1	1.00	0.72	0.83	0.09	0.05	0.11	0.046	0.305	0.459
LPCe 20:2	1.00	0.33	0.58	0.19	0.08	0.22	0.029	0.242	0.387
LPCe 20:3	1.00	0.81	0.63	0.10	0.06	0.06	0.199	0.029	0.091
LPE 20:1	1.00	0.67	0.51	0.13	0.04	0.11	0.066	0.041	0.272
LPE 20:2	1.00	0.88	0.63	0.09	0.13	0.05	0.519	0.015	0.170
NAPE 16:0/18:0/20:4	1.00	0.43	0.60	0.17	0.08	0.09	0.034	0.104	0.253
NAPE p18:0/18:1/20:4	1.00	1.08	0.83	0.09	0.05	0.02	0.505	0.140	0.007
NAPE p18:0/22:4/20:4	1.00	0.43	0.94	0.26	0.07	0.06	0.110	0.852	0.002
NAPE p18:0/22:6/20:4	1.00	0.52	0.81	0.15	0.03	0.07	0.033	0.351	0.013
NAPE p18:1/20:4/20:4	1.00	0.71	1.00	0.12	0.08	0.03	0.121	0.983	0.018
NAPS 16:0-36:1	1.00	3.79	1.69	0.48	0.67	0.54	0.023	0.431	0.071
NAPS 16:0-38:3	1.00	1.36	0.16	0.53	0.17	0.05	0.585	0.210	0.001
NSer 16:1	1.00	1.11	0.59	0.21	0.16	0.06	0.727	0.143	0.034
NSer 18:1	1.00	1.27	0.71	0.21	0.11	0.07	0.339	0.287	0.008

Table 10. Cardiac lipid species that were significantly different in mice treated with CHOW diet containing TESA or combination of TESA and RSV compared to control group. Statistical analysis was performed with unpaired 2-tailed Students test between groups.

5.3.12 Combined treatment of diabetic mice with tesaglitazar and resveratrol maintains the anti-hyperglycemic and anti-hyperlipidemic effect of tesaglitazar and alleviates cardiac dysfunction

We next examined whether the combined treatment with tesaglitazar and resveratrol would exert its beneficial effect in leptin receptor deficient mice (*db/db*), which is a model of Type 2 diabetes. Therefore, *db/db* mice were given either CHOW diet, or diets containing tesaglitazar or combination of tesaglitazar and resveratrol for 6 weeks. No significant effect was observed on weight gain rate between mice treated with tesaglitazar or tesaglitazar and resveratrol **(Figure 30)**. Treatment with combination of tesaglitazar and resveratrol corrected hyperlipidemia (**Figure 31A**) and hyperglycemia (**Figure 31B**) to a similar extent with tesaglitazar Thus, as in C57BL/6 WT mice, both tesaglitazar alone and combination of tesaglitazar and resveratrol maintained the beneficial metabolic effects of tesaglitazar in diabetic mice without indications of an additive effect. Despite the similar effect of tesaglitazar and combined tesaglitazar and resveratrol treatments in reducing plasma lipids and glucose levels, 2D-echocardiography that was performed 3 weeks (**Figure 31C, 31D**) and 6 weeks (**Figure 31E, 31F**) after beginning of the treatment showed that only treatment with tesaglitazar alone caused cardiac dysfunction. Combined treatment with tesaglitazar and resveratrol was protective **(Figure 31C-31F and Table 12)**.

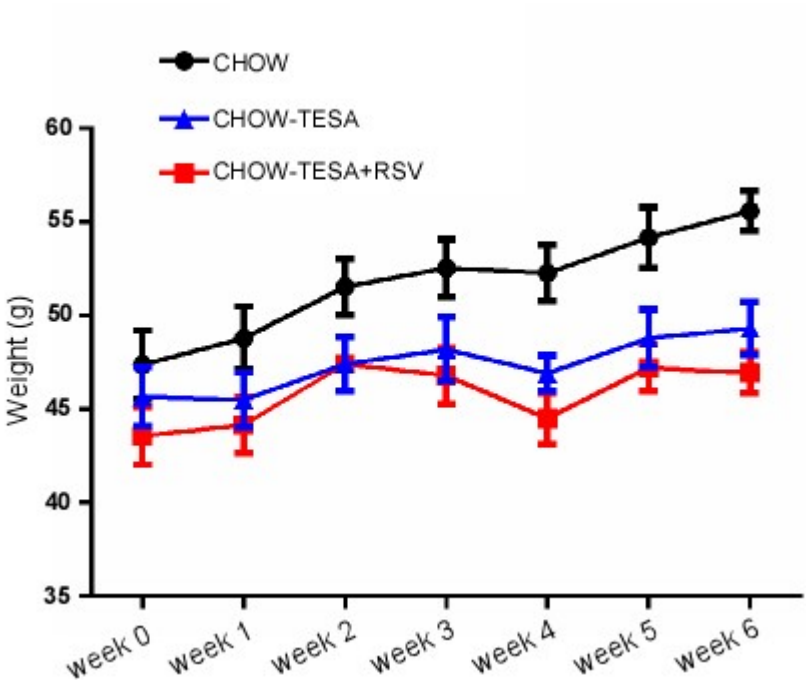

Figure 30. Weight gain rate curve of db/db mice treated with CHOW diet containing TESA (0.5 μmol/kg body weight) or containing TESA (0.5 μmol/kg body weight) and RSV (100 mg/kg/day) for 6 weeks.

As in C57BL/6 mice, *db/db* mice that were treated with CHOW diet containing a combination of tesaglitazar and resveratrol had significantly lower (68%) ac-PGC1α/total PGC1α ratio compared to *db/db* mice treated with tesaglitazar alone (**Figure 31G, 31H**). Increased cardiac ac-PGC1α levels in tesaglitazar-treated diabetic mice and restoration with tesaglitazar and resveratrol treatment was accompanied by according changes in cardiac SIRT1 protein levels. SIRT1 was decreased (50%) with tesaglitazar and restored to normal levels with tesaglitazar and resveratrol (**Figure 31G, 31H**). Accordingly, treatment of mice with tesaglitazar increased (20%) lysine acetylome of cardiac mitochondrial proteins isolated from *db/db* mice, which was restored to normal levels following combined tesaglitazar and resveratrol treatment (**Figure 31I, 31J**).

5.3.13 Tesaglitazar and resveratrol treatment abolished its cardioprotective effect in aMHC-SIRT1$^{-/-}$ mice

We sought to confirm involvement of SIRT1 in mediating the cardioprotective effect of resveratrol in mice treated with tesaglitazar. Therefore, we treated C57BL/6 and *αMHC-SIRT1-/-* mice with CHOW diet containing combination of tesaglitazar and resveratrol. Combined treatment did not rescue cardiac function in *αMHC-SIRT1*$^{-/-}$ mice, unlike the effects of this combination in WT mice (**Figure 31K, 31L**). Thus, cardiomyocyte SIRT1 is crucial in mediating the protective effect of resveratrol.

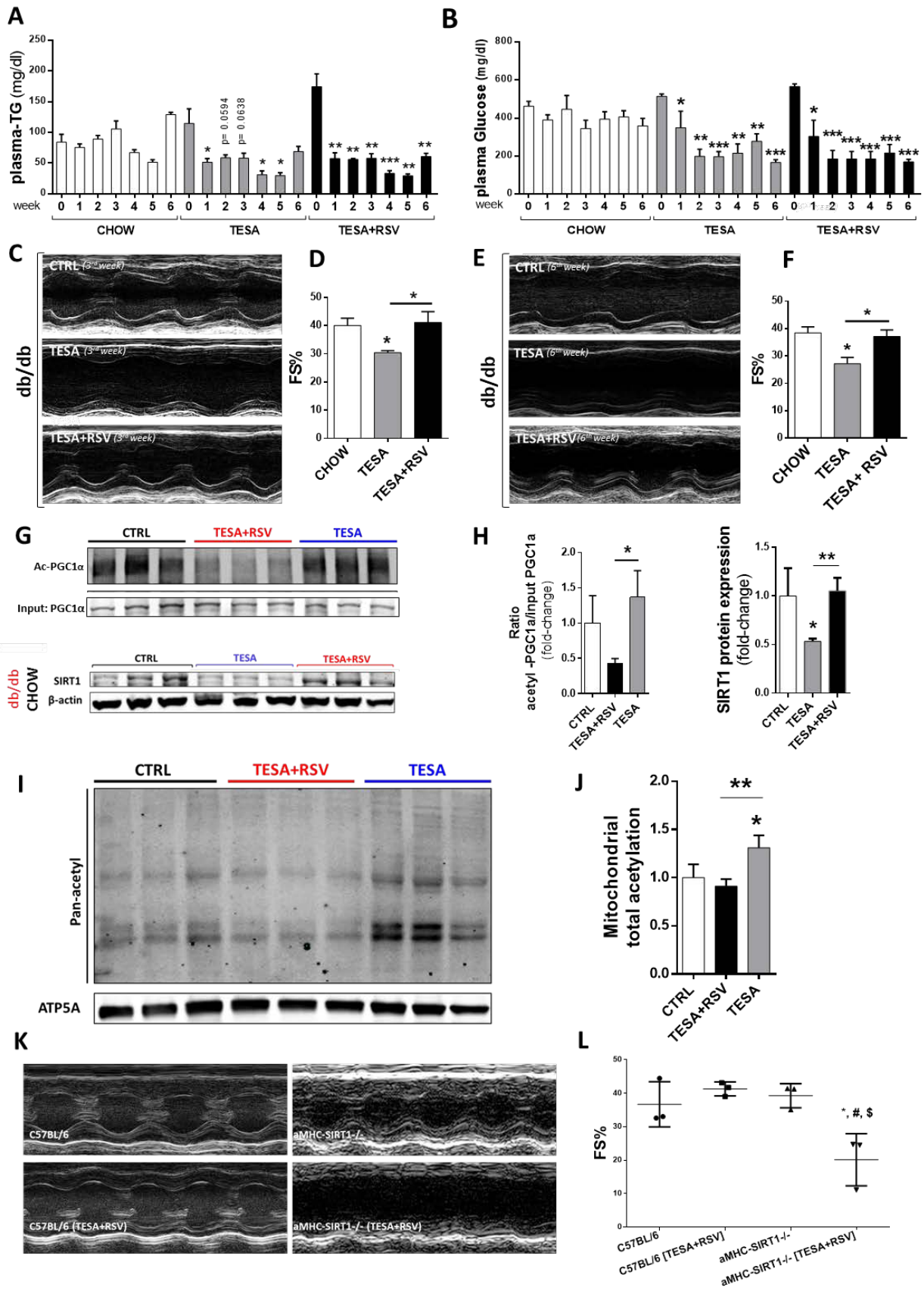
A
plasma-TG (mg/dl)
p= 0.0594
p= 0.0638
week
CHOW
TESA
TESA+RSV
B
plasma Glucose (mg/dl)
C
db/db
CTRL (3rd week)
TESA (3rd week)
TESA+RSV (3rd week)
D
FS%
CHOW
TESA
TESA+RSV
E
CTRL (6th week)
TESA (6th week)
TESA+RSV (6th week)
F
TESA+ RSV
G
CTRL
TESA+RSV
TESA
Ac-PGC1α
Input: PGC1α
db/db
CHOW
SIRT1
β-actin
H
Ratio acetyl -PGC1a/Input PGC1a (fold-change)
SIRT1 protein expression (fold-change)
I
Pan-acetyl
ATP5A
J
Mitochondrial total acetylation
K
C57BL/6
aMHC-SIRT1-/-
C57BL/6 (TESA+RSV)
aMHC-SIRT1-/- (TESA+RSV)
L
*, #, $
C57BL/6
C57BL/6 [TESA+RSV]
aMHC-SIRT1-/-
aMHC-SIRT1-/- [TESA+RSV]

Figure 31. A-H: Plasma TG (A), plasma glucose (B), representative short-axis M-mode images (C, E), fractional shortening (%) (D, F), cardiac Ac-PGC1α, total PGC1α, SIRT1, β-actin immunoblots (G) and densitometric analysis (H) of *db/db* mice treated with CHOW containing tesaglitazar or combination of tesaglitazar and resveratrol. Statistical analysis for plasma TG and glucose was performed with unpaired 2-tailed Student's t-test, *P<0.05, **P,0.01, ***P<0.001,(n=3-4). Statistical Analysis for echocardiography results was performed with 1-way ANOVA Error bars represent SEM. **I, J:** Immunoblot (I) and densitometric analysis (J) of total acetylome and ATP5A of cardiac mitochondrial lysates obtained from *db/db* mice fed with CHOW diet containing tesaglitazar (0.5 μmol/kg) or combination of tesaglitazar (0.5 μmol/kg) and resveratrol (100 mg/kg/day) for 6 weeks, (n=3). **K, L:** Representative short-axis M-mode images (K), fractional shortening (%) (L) of C57BL/6 mice and *αMHC-SIRT1*$^{-/-}$ mice fed with CHOW diet containing combination of tesaglitazar (0.5 μmol/kg) and resveratrol (100 mg/kg/day). Statistical analysis for FS% performed using 1-way ANOVA analysis *P<0.05 vs. aMHC-SIRT1$^{-/-}$, #P<0.01 vs C57BL/6 mice fed with CHOW diet containing tesaglitazar and resveratrol, $P<0.05 vs. C57BL/6*; (n=3*). Statistical analyses were performed with unpaired 2-tailed Student's t-test between groups, *p<0.05, **p<0.01, ***p<0.001. Error bars represent SEM.

Echocardiography parameters	CHOW	CHOW-TESA	CHOW-TESA+RSV
EF	68.9	52.8*,#	67.1#
FS	38.4	27.1*,#	37.1#
LV Mass	137.2	130.7	124.3
LV Mass (Cor)	109.7	104.6	99.4
LV Vol;d	79.8	91.0	83.1
LV Vol;s	24.4	42.84*,#	27.32#
IVS;d	0.9	0.8	0.7
IVS;s	1.4	1.1123**	1.2
LVID;d	4.2	4.5	4.3
LVID;s	2.6	3.25**,#	2.70#
LVPW;d	0.8	0.7	0.8
LVPW;s	1.3	0.94**,#	1.18#

Table 11 - Table of 2D-echocardiography parameters of *db/db* mice treated with CHOW or HFD containing TESA (0.5 μmol/kg body weight) or TESA (0.5 μmol/kg body weight) and RSV (100 mg/kg/day) for 6 weeks. Statistical analysis was performed with unpaired 2-tailed Student's t-test between groups, *p>0.05, **p<0.005, (# P<0.05, significant between TESA vs TESA+RSV) (n=7-8).

5.4 DISCUSSION

Agonists for PPARs are used to reduce hyperglycemia and hypertriglyceridemia in patients with Type 2 diabetes. Despite these benefits, some PPARγ agonists, such as rosiglitazone and pioglitazone, have been associated with increased heart failure due to direct cardiac effects or indirect effects, such as fluid retention (Home et al., 2009)'(Kernan et al., 2016). However, the mechanisms that mediate these adverse effects remain unclear.

Efforts to discover new PPAR agonists without adverse effects led to the development of dual agonists (glitazars) that activate both PPARα and PPARγ, thus combining the lipid-lowering effects of PPARα with the insulin sensitizing effects of PPARγ. Although glitazars lowered plasma glucose and triglycerides (Chatterjee et al., 2015), they were associated with ischemic events (Lincoff et al., 2014) and congestive heart failure (Discovery, 2013). A dual agonist, saroglitazar, has been approved for clinical use but there is a precautionary statement for patients with diabetes and congestive heart failure (Discovery, 2013). Other glitazars, such as tesaglitazar, aleglitazar, muraglitazar, and cevoglitazar, were abandoned after late stage clinical trials showed adverse side effects, including increased risk of heart failure and myocardial ischemia (Lincoff et al., 2014). Our study shows that the cardiotoxic effect of tesaglitazar is accounted for by inhibition of cardiac PGC1α expression and post-translational activation by SIRT1. PGC1α is the transcriptional co-activator of PPARs and controls FAO-related gene expression (Arany et al., 2005) and mitochondrial biogenesis (Lehman et al., 2000).

PPARs respond to various endogenous ligands such as steroids, retinoids, cholesterol metabolites, and dietary lipids (Pol et al., 2015). PPARs heterodimerize with retinoid X receptors (RXR) and bind to cis-acting DNA-elements (PPREs), to increase gene transcription. PPARs have broad tissue distribution and regulate lipid metabolism in several organs including the heart (Auboeuf et al., 1997). PPARα promotes FA uptake and FAO (Finck et al., 2002) and PPARγ increases lipid accumulation (Son et al., 2007). PPARγ can also induce cardiac FAO-related gene expression (Son et al., 2007), particularly when PPARα is inhibited (Drosatos et al., 2013; Son et al., 2010). FAO is the primary source of cardiac ATP and its' inhibition is associated with cardiac dysfunction (Drosatos and Schulze, 2013; Neubauer, 2007). Therefore, it seems paradoxical that combined activation of two positive regulators of FAO, PPARα and PPARγ, causes cardiac dysfunction. Cardiac toxicity may be attributed to lipo-gluco-toxicity due to combined increase in PPARγ-driven insulin sensitization and glucose uptake in the setting of higher PPARα-induced FA metabolism (Nolan et al., 2015). In the present study, we showed that combined PPARα/γ activation inhibits SIRT1 and PGC1α.

Our previous studies had indicated that combined PPARα and PPARγ activation may compromise cardiac function. In those studies, we investigated the cardiac effects of PPARγ activation (Drosatos et al., 2013; Son et al., 2007; Son et al., 2010) and, showed that cardiomyocyte-specific overexpression of PPARγ causes intramyocardial lipid accumulation and cardiac dysfunction (Son et al., 2007). We had shown that the observed excessive lipid accumulation may account for some components of cardiac dysfunction, such as β-adrenergic desensitization (Drosatos and Schulze, 2013) and arrhythmia (Morrow et al., 2011). However, constitutive PPARγ expression in

cardiomyocytes of *Pparα-/-* mice did not cause cardiac dysfunction, although myocardial lipids were still increased (Son et al., 2010). Triglyceride-derived FAs activate PPARα (Lahey et al., 2014). Thus, cardiac dysfunction in mice that overexpress cardiomyocyte PPARγ may be accounted for, at least partially, by PPARα activation, which does not occur in *Pparα-/-* mice (Son et al., 2010). Administration of dual PPARα/γ agonist, tesaglitazar, in the present study also caused cardiac dysfunction that was associated with accumulation of cardiac lipids including some toxic lipids, such as acyl-carnitines and diacylglycerols that have been linked with cardiac lipotoxicity (Drosatos et al., 2011; Son et al., 2010). These findings prompted us to explore why loss of PPARα mitigates the lipotoxic effects of PPARγ activation.

Our study shows that activation of PPARα in mice that were treated with PPARγ agonist, rosiglitazone, reduced PGC1α expression, decreased mitochondrial number and prevented rosiglitazone-mediated increased FAO-related gene expression. Accordingly, we show that although pharmacologic or genetic PPARγ activation induces PGC1α expression, this effect is lost with dual activators or combined administration of single agonists of PPARα and PPARγ. This is consistent with our previous findings showing that pharmacologic activation of PPARα in *αMHC-Pparγ* mice reduced cardiac expression of PGC1α and FA metabolism-related genes (Son et al., 2010). Similarly, PPARγ activation in *LDLr*$^{-/-}$ mice fed with HFD, which increases cardiac PPARα levels (Cole et al., 2016; Li et al., 2009), reduces PGC1α expression and causes cardiac hypertrophy (Verschuren et al., 2014). Conversely, we have shown that activation of cardiac PPARγ in mice with low levels of cardiac PPARα expression increases profoundly PGC1α expression (Drosatos et al., 2013). Thus, PPARα activation appears

to be a critical component of PPARγ-related cardiac toxicity, which involves altered expression of PGC1α.

Heart failure has been associated with insufficient energy production, which can be caused by deprivation from energetic fuels or mitochondrial dysfunction (Neubauer, 2007). Cardiac PGC1α expression is decreased in animals and humans with heart failure (Sihag et al., 2009). Accordingly, *PGC1α*$^{-/-}$ mice develop moderate cardiac dysfunction(Arany et al., 2005), which is aggravated with pressure overload (Arany et al., 2006b). The milder cardiac phenotype at baseline may be accounted for by compensatory function of PGC1β, which shares functional redundancy with PGC1α. Indeed, combined knock-out of both *Pgc1α* and *Pgc1β* inhibits perinatal cardiac mitochondrial biogenesis and causes cardiomyopathy and post-birth death (Lai et al., 2008). On the other hand, overexpression (Lehman et al., 2000) of cardiomyocyte PGC1α also causes cardiac dysfunction. This toxic effect may be caused by the profound and long-term increase of PGC1α expression that impaired mitochondrial biogenesis and function. Nevertheless, the same study (Lehman et al., 2000) reported that cardiac function is normal in transgenic lines with lower PGC1α constitutive expression. Accordingly, short-term PGC1α overexpression in cultured cardiomyocytes improved mitochondrial biogenesis and oxidative respiration, which has been associated with better cardiac function. Thus, the level of cardiomyocyte PGC1α activation seems to be critical for determining its' protective or aggravating role.

The role of PGC1α inhibition as a key event that mediates the cardiotoxic effect of dual PPARα/γ activation is new. Our data show that dual-PPARα/γ activation reduce both expression and activation of cardiac PGC1α by enhancing acetylation. It has been

suggested that lower acetylation of cardiac PGC1α may account for the shift from glycolysis to FAO that occurs during maturation (Fukushima et al., 2016).

PGC1α acetylation is controlled by SIRT1 (Rodgers et al., 2005). We observed that cardiac SIRT1 expression was reduced and PGC1α acetylation increased following treatment with dual PPARα/γ agonist. SIRT1 is a member of the sirtuin family. Various forms of cardiac stress, such as ischemia/reperfusion (I/R) and cardiac aging inhibit expression and activation of SIRT1 (Matsushima and Sadoshima, 2015). Cardiac-specific SIRT1$^{-/-}$ mice display exacerbated I/R-related injury. SIRT1 and PGC1α are activated by resveratrol, which is a polyphenolic compound of grapes and red wine with anti-oxidant and anti-inflammatory properties (Baur and Sinclair, 2006). The beneficial cardiac effects of resveratrol have been attributed, at least in part, to the activation of SIRT1(Lagouge et al., 2006). Resveratrol, as well as its molecular target, SIRT1, have been associated with mitochondrial biogenesis (Dolinsky and Dyck, 2014). Inhibition of SIRT1 has been correlated with diabetes-related cardiometabolic abnormalities, while protective role has been suggested for activated SIRT1 (Winnik et al., 2015). Mitochondrial dysfunction plays a key role in diabetes (Bugger and Abel, 2010) and it is prevented by administration of resveratrol in rats with type 2 diabetes (Beaudoin et al., 2014). A recent study, showed that resveratrol regulates lipid metabolism through the AMPKα-Sirt1-PGC1α in zebrafish (Ran et al., 2017). Also, resveratrol attenuates cardiac injury in type 1 diabetic rats through SIRT1-mediated regulation of mitochondrial function and PGC-1α deacetylation (Fang et al., 2017). In our study, tesaglitazar reduced mitochondria abundance and respiratory capacity in cardiomyocytes. Our findings from EM analysis of cardiomyocytes suggest that the dual PPARα/γ agonists may interfere with mitochondrial fission and fusion balance as we observed smaller and

spherical mitochondria. Thus, activation of the “metabolic network” that involves SIRT1 and PGC1α alleviates cardiac toxicity of glitazars via regulation of cardiac mitochondrial biology and energy homeostasis.

In summary, our previous (Drosatos and Schulze, 2013; Son et al., 2010) and present findings indicate that combined PPARα and PPARγ activation leads to inhibition of PGC1α expression and activation, via inhibition of SIRT1 expression (**Figure 32**). Our observations can explain the mechanism that underlies the cardiotoxic effects of dual PPARα/γ agonists. We show for the first time that the negative effects of these drugs can be effectively reversed upon combined administration with resveratrol. Combined administration of tesaglitazar and resveratrol maintained the beneficial anti-hyperlipidemic and anti-hyperglycemic effects of tesaglitazar, while resveratrol alone is not sufficient to reduce plasma TG levels (Dash et al., 2013). Thus, combination of dual PPARα/γ agonists and resveratrol holds promise for future therapeutic applications in type 2 diabetes. Moreover, our study provides a guide for design of future PPAR agonists that should not inhibit PGC1α activity and maintain mitochondrial biogenesis and FAO.

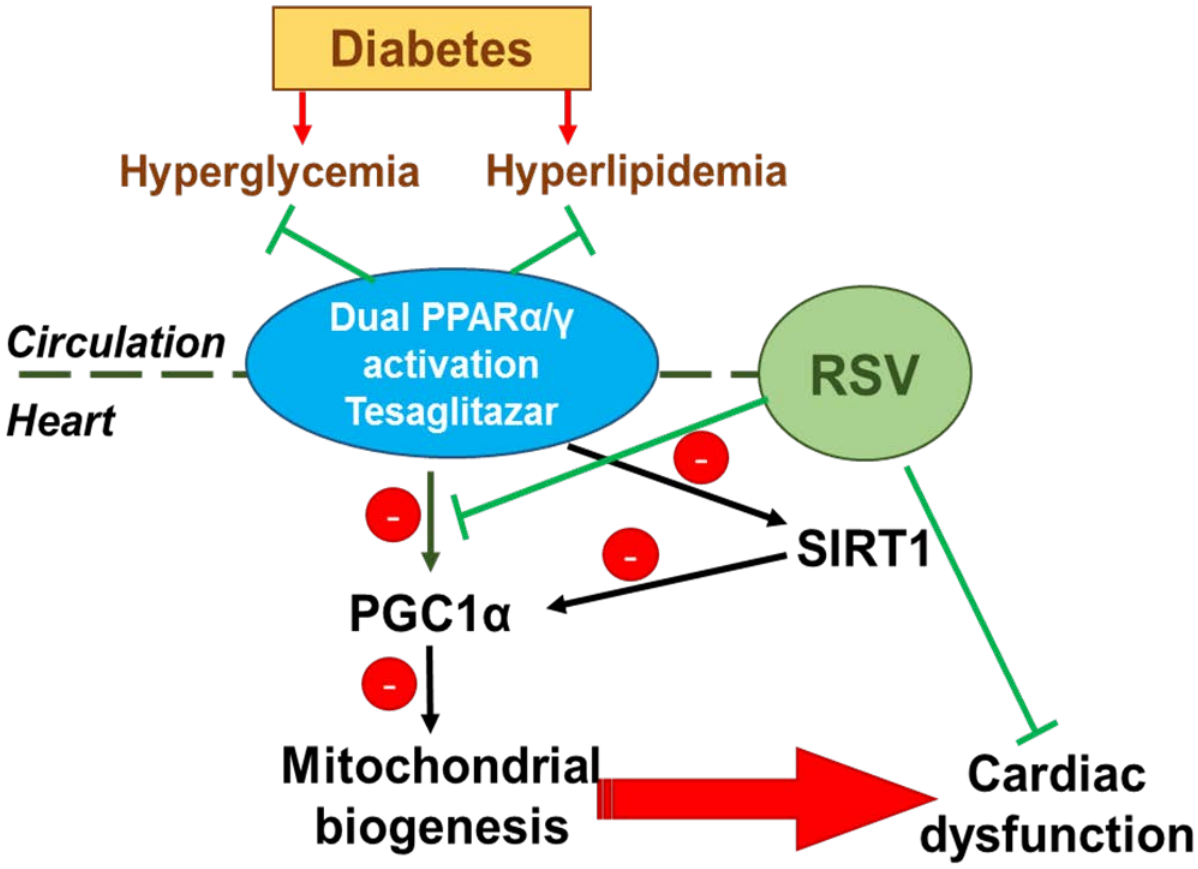

Figure 32: Schematic representation of the proposed model.

REFERENCES

(1998). Intensive blood-glucose control with sulphonylureas or insulin compared with conventional treatment and risk of complications in patients with type 2 diabetes (UKPDS 33). UK Prospective Diabetes Study (UKPDS) Group. Lancet *352*, 837-853.
2013, I.D.F.I.A.
(ADA), A.D.A.
(www.cdc.gov/diabetes), U.C.f.D.C.a.P.
Amano, Y., Yamaguchi, T., Ohno, K., Niimi, T., Orita, M., Sakashita, H., and Takeuchi, M. (2012). Structural basis for telmisartan-mediated partial activation of PPAR gamma. Hypertension research : official journal of the Japanese Society of Hypertension *35*, 715-719.
American Diabetes, A. (2010). Diagnosis and classification of diabetes mellitus. Diabetes Care *33 Suppl 1*, S62-69.
An, D., Pulinilkunnil, T., Qi, D., Ghosh, S., Abrahani, A., and Rodrigues, B. (2005). The metabolic "switch" AMPK regulates cardiac heparin-releasable lipoprotein lipase. American journal of physiology. Endocrinology and metabolism *288*, E246-253.
Anderson, R.M., Barger, J.L., Edwards, M.G., Braun, K.H., O'Connor, C.E., Prolla, T.A., and Weindruch, R. (2008). Dynamic regulation of PGC-1alpha localization and turnover implicates mitochondrial adaptation in calorie restriction and the stress response. Aging cell *7*, 101-111.
Arany, Z., He, H., Lin, J., Hoyer, K., Handschin, C., Toka, O., Ahmad, F., Matsui, T., Chin, S., Wu, P.H., et al. (2005). Transcriptional coactivator PGC-1 alpha controls the energy state and contractile function of cardiac muscle. Cell Metab *1*, 259-271.
Arany, Z., Novikov, M., Chin, S., Ma, Y., Rosenzweig, A., and Spiegelman, B.M. (2006a). Transverse aortic constriction leads to accelerated heart failure in mice lacking PPAR-gamma coactivator 1alpha. Proc Natl Acad Sci U S A *103*, 10086-10091.
Arany, Z., Novikov, M., Chin, S., Ma, Y., Rosenzweig, A., and Spiegelman, B.M. (2006b). Transverse aortic constriction leads to accelerated heart failure in mice lacking PPAR-gamma coactivator 1alpha. Proceedings of the National Academy of Sciences of the United States of America *103*, 10086-10091.
Atkinson, L.L., Kozak, R., Kelly, S.E., Onay Besikci, A., Russell, J.C., and Lopaschuk, G.D. (2003). Potential mechanisms and consequences of cardiac triacylglycerol accumulation in insulin-resistant rats. American journal of physiology. Endocrinology and metabolism *284*, E923-930.
Auboeuf, D., Rieusset, J., Fajas, L., Vallier, P., Frering, V., Riou, J.P., Staels, B., Auwerx, J., Laville, M., and Vidal, H. (1997). Tissue distribution and quantification of the expression of mRNAs of peroxisome proliferator-activated receptors and liver X receptor-alpha in humans: no alteration in adipose tissue of obese and NIDDM patients. Diabetes *46*, 1319-1327.
Baartscheer, A., Schumacher, C.A., van Borren, M.M., Belterman, C.N., Coronel, R., Opthof, T., and Fiolet, J.W. (2005). Chronic inhibition of Na+/H+-exchanger attenuates cardiac hypertrophy and prevents cellular remodeling in heart failure. Cardiovascular research *65*, 83-92.
Barger, P.M., Brandt, J.M., Leone, T.C., Weinheimer, C.J., and Kelly, D.P. (2000). Deactivation of peroxisome proliferator-activated receptor-alpha during cardiac hypertrophic growth. The Journal of clinical investigation *105*, 1723-1730.
Baur, J.A., and Sinclair, D.A. (2006). Therapeutic potential of resveratrol: the in vivo evidence. Nat Rev Drug Discov *5*, 493-506.
Beaudoin, M.S., Perry, C.G., Arkell, A.M., Chabowski, A., Simpson, J.A., Wright, D.C., and Holloway, G.P. (2014). Impairments in mitochondrial palmitoyl-CoA respiratory kinetics that precede development of diabetic cardiomyopathy are prevented by resveratrol in ZDF rats. The Journal of physiology *592*, 2519-2533.
Berger, J., and Moller, D.E. (2002). The mechanisms of action of PPARs. Annu Rev Med *53*, 409-435.

Bosma, M., Dapito, D.H., Drosatos-Tampakaki, Z., Huiping-Son, N., Huang, L.S., Kersten, S., Drosatos, K., and Goldberg, I.J. (2014). Sequestration of fatty acids in triglycerides prevents endoplasmic reticulum stress in an in vitro model of cardiomyocyte lipotoxicity. Biochimica et biophysica acta *1841*, 1648-1655.
Bugger, H., and Abel, E.D. (2010). Mitochondria in the diabetic heart. Cardiovasc Res *88*, 229-240.
Bulynko, Y.A., and O'Malley, B.W. (2011). Nuclear receptor coactivators: structural and functional biochemistry. Biochemistry *50*, 313-328.
Campbell, F.M., Kozak, R., Wagner, A., Altarejos, J.Y., Dyck, J.R., Belke, D.D., Severson, D.L., Kelly, D.P., and Lopaschuk, G.D. (2002). A role for peroxisome proliferator-activated receptor alpha (PPARalpha) in the control of cardiac malonyl-CoA levels: reduced fatty acid oxidation rates and increased glucose oxidation rates in the hearts of mice lacking PPARalpha are associated with higher concentrations of malonyl-CoA and reduced expression of malonyl-CoA decarboxylase. The Journal of biological chemistry *277*, 4098-4103.
Canto, C., and Auwerx, J. (2009). PGC-1alpha, SIRT1 and AMPK, an energy sensing network that controls energy expenditure. Curr Opin Lipidol *20*, 98-105.
Canto, C., Gerhart-Hines, Z., Feige, J.N., Lagouge, M., Noriega, L., Milne, J.C., Elliott, P.J., Puigserver, P., and Auwerx, J. (2009). AMPK regulates energy expenditure by modulating NAD+ metabolism and SIRT1 activity. Nature *458*, 1056-1060.
Carley AN, A.L., Bonen A, Harper ME, Kunnathu S, Lopaschuk GD, Severson DL. (2007). Mechanisms responsible for enhanced fatty acid utilization by perfused hearts from type 2 diabetic db/db mice. Arch Physiol Biochem *113*, 65–75.
Carroll, J.S., Meyer, C.A., Song, J., Li, W., Geistlinger, T.R., Eeckhoute, J., Brodsky, A.S., Keeton, E.K., Fertuck, K.C., Hall, G.F., et al. (2006). Genome-wide analysis of estrogen receptor binding sites. Nat Genet *38*, 1289-1297.
Chan, R.B., Oliveira, T.G., Cortes, E.P., Honig, L.S., Duff, K.E., Small, S.A., Wenk, M.R., Shui, G., and Di Paolo, G. (2012). Comparative lipidomic analysis of mouse and human brain with Alzheimer disease. J Biol Chem *287*, 2678-2688.
Chandra, V., Huang, P., Hamuro, Y., Raghuram, S., Wang, Y., Burris, T.P., and Rastinejad, F. (2008). Structure of the intact PPAR-gamma-RXR- nuclear receptor complex on DNA. Nature *456*, 350-356.
Chatterjee, S., Majumder, A., and Ray, S. (2015). Observational study of effects of Saroglitazar on glycaemic and lipid parameters on Indian patients with type 2 diabetes. Sci Rep *5*, 7706.
Christ, E.A., Meals, E., and English, B.K. (1997). Streptococcal pyrogenic exotoxins A (SpeA) and C (SpeC) stimulate the production of inducible nitric oxide synthase (iNOS) protein in RAW 264.7 macrophages. Shock *8*, 450-453.
Cole, M.A., Abd Jamil, A.H., Heather, L.C., Murray, A.J., Sutton, E.R., Slingo, M., Sebag-Montefiore, L., Tan, S.C., Aksentijevic, D., Gildea, O.S., et al. (2016). On the pivotal role of PPARalpha in adaptation of the heart to hypoxia and why fat in the diet increases hypoxic injury. FASEB J *30*, 2684-2697.
Cooke, D.W., and Plotnick, L. (2008). Type 1 diabetes mellitus in pediatrics. Pediatrics in review *29*, 374-384; quiz 385.
Dash, S., Xiao, C., Morgantini, C., Szeto, L., and Lewis, G.F. (2013). High-dose resveratrol treatment for 2 weeks inhibits intestinal and hepatic lipoprotein production in overweight/obese men. Arterioscler Thromb Vasc Biol *33*, 2895-2901.
de Duve, C. (1969). The peroxisome: a new cytoplasmic organelle. Proceedings of the Royal Society of London. Series B, Biological sciences *173*, 71-83.
Defronzo, R.A. (2009). Banting Lecture. From the triumvirate to the ominous octet: a new paradigm for the treatment of type 2 diabetes mellitus. Diabetes *58*, 773-795.
DeFronzo, R.A., Bonadonna, R.C., and Ferrannini, E. (1992). Pathogenesis of NIDDM. A balanced overview. Diabetes Care *15*, 318-368.

Delea, T.E., Edelsberg, J.S., Hagiwara, M., Oster, G., and Phillips, L.S. (2003). Use of thiazolidinediones and risk of heart failure in people with type 2 diabetes: a retrospective cohort study. Diabetes Care *26*, 2983-2989.
Desvergne, B., Michalik, L., and Wahli, W. (2006). Transcriptional regulation of metabolism. Physiol Rev *86*, 465-514.
Dictionary, O.E. (2011).
Discovery, Z. (2013). Lipaglyn Product Information.
Discovery Z. Lipaglyn—Product Information.
Doenst, T., Nguyen, T.D., and Abel, E.D. (2013). Cardiac metabolism in heart failure: implications beyond ATP production. Circulation research *113*, 709-724.
Dolinsky, V.W., and Dyck, J.R. (2014). Experimental studies of the molecular pathways regulated by exercise and resveratrol in heart, skeletal muscle and the vasculature. Molecules *19*, 14919-14947.
Dreyer, C., Krey, G., Keller, H., Givel, F., Helftenbein, G., and Wahli, W. (1992). Control of the peroxisomal beta-oxidation pathway by a novel family of nuclear hormone receptors. Cell *68*, 879-887.
Drosatos, K., Bharadwaj, K.G., Lymperopoulos, A., Ikeda, S., Khan, R., Hu, Y., Agarwal, R., Yu, S., Jiang, H., Steinberg, S.F., et al. (2011). Cardiomyocyte lipids impair beta-adrenergic receptor function via PKC activation. Am J Physiol Endocrinol Metab *300*, E489-499.
Drosatos, K., Khan, R.S., Trent, C.M., Jiang, H., Son, N.H., Blaner, W.S., Homma, S., Schulze, P.C., and Goldberg, I.J. (2013). Peroxisome proliferator-activated receptor-gamma activation prevents sepsis-related cardiac dysfunction and mortality in mice. Circ Heart Fail *6*, 550-562.
Drosatos, K., Pollak, N.M., Pol, C.J., Ntziachristos, P., Willecke, F., Valenti, M.C., Trent, C.M., Hu, Y., Guo, S., Aifantis, I., et al. (2016). Cardiac Myocyte KLF5 Regulates Ppara Expression and Cardiac Function. Circulation research *118*, 241-253.
Drosatos, K., and Schulze, P.C. (2013). Cardiac lipotoxicity: molecular pathways and therapeutic implications. Curr Heart Fail Rep *10*, 109-121.
Dyck JR, K.N., Barr AJ, Davies SP, Hardie DG, Lopaschuk GD (1999.). Phosphorylation control of cardiac acetyl-CoA carboxylase by cAMP-dependent protein kinase and 5 -AMP activated protein kinase. Eur J Biochem .*262*, 184–190.
Dyck, J.R., and Lopaschuk, G.D. (2006). AMPK alterations in cardiac physiology and pathology: enemy or ally? The Journal of physiology *574*, 95-112.
Echeverria, P.C., and Picard, D. (2010). Molecular chaperones, essential partners of steroid hormone receptors for activity and mobility. Biochim Biophys Acta *1803*, 641-649.
Erdmann, E., Charbonnel, B., Wilcox, R.G., Skene, A.M., Massi-Benedetti, M., Yates, J., Tan, M., Spanheimer, R., Standl, E., Dormandy, J.A., et al. (2007). Pioglitazone use and heart failure in patients with type 2 diabetes and preexisting cardiovascular disease: data from the PROactive study (PROactive 08). Diabetes Care *30*, 2773-2778.
Fang, W.J., Wang, C.J., He, Y., Zhou, Y.L., Peng, X.D., and Liu, S.K. (2017). Resveratrol alleviates diabetic cardiomyopathy in rats by improving mitochondrial function through PGC-1alpha deacetylation. Acta Pharmacol Sin.
Fernandez-Marcos, P.J., and Auwerx, J. (2011). Regulation of PGC-1alpha, a nodal regulator of mitochondrial biogenesis. The American journal of clinical nutrition *93*, 884S-890.
Finck, B.N., Han, X., Courtois, M., Aimond, F., Nerbonne, J.M., Kovacs, A., Gross, R.W., and Kelly, D.P. (2003). A critical role for PPARalpha-mediated lipotoxicity in the pathogenesis of diabetic cardiomyopathy: modulation by dietary fat content. Proc Natl Acad Sci U S A *100*, 1226-1231.
Finck, B.N., and Kelly, D.P. (2002). Peroxisome proliferator-activated receptor alpha (PPARalpha) signaling in the gene regulatory control of energy metabolism in the normal and diseased heart. Journal of molecular and cellular cardiology *34*, 1249-1257.
Finck, B.N., and Kelly, D.P. (2006). PGC-1 coactivators: inducible regulators of energy metabolism in health and disease. J Clin Invest *116*, 615-622.

Finck, B.N., and Kelly, D.P. (2007). Peroxisome proliferator-activated receptor gamma coactivator-1 (PGC-1) regulatory cascade in cardiac physiology and disease. Circulation *115*, 2540-2548.
Finck, B.N., Lehman, J.J., Leone, T.C., Welch, M.J., Bennett, M.J., Kovacs, A., Han, X., Gross, R.W., Kozak, R., Lopaschuk, G.D., et al. (2002). The cardiac phenotype induced by PPARalpha overexpression mimics that caused by diabetes mellitus. J Clin Invest *109*, 121-130.
Fruchart, J.C. (2009). Peroxisome proliferator-activated receptor-alpha (PPARalpha): at the crossroads of obesity, diabetes and cardiovascular disease. Atherosclerosis *205*, 1-8.
Fukushima, A., Alrob, O.A., Zhang, L., Wagg, C.S., Altamimi, T., Rawat, S., Rebeyka, I.M., Kantor, P.F., and Lopaschuk, G.D. (2016). Acetylation and succinylation contribute to maturational alterations in energy metabolism in the newborn heart. Am J Physiol Heart Circ Physiol *311*, H347-363.
Gabaldon, T. (2010). Peroxisome diversity and evolution. Philosophical transactions of the Royal Society of London. Series B, Biological sciences *365*, 765-773.
Garnier, A., Fortin, D., Delomenie, C., Momken, I., Veksler, V., and Ventura-Clapier, R. (2003). Depressed mitochondrial transcription factors and oxidative capacity in rat failing cardiac and skeletal muscles. The Journal of physiology *551*, 491-501.
Gerhart-Hines, Z., Rodgers, J.T., Bare, O., Lerin, C., Kim, S.H., Mostoslavsky, R., Alt, F.W., Wu, Z., and Puigserver, P. (2007). Metabolic control of muscle mitochondrial function and fatty acid oxidation through SIRT1/PGC-1alpha. EMBO J *26*, 1913-1923.
Gertz, E.W., Wisneski, J.A., Stanley, W.C., and Neese, R.A. (1988). Myocardial substrate utilization during exercise in humans. Dual carbon-labeled carbohydrate isotope experiments. The Journal of clinical investigation *82*, 2017-2025.
Glass, C.K., and Rosenfeld, M.G. (2000). The coregulator exchange in transcriptional functions of nuclear receptors. Genes Dev *14*, 121-141.
Gleyzer, N., Vercauteren, K., and Scarpulla, R.C. (2005). Control of mitochondrial transcription specificity factors (TFB1M and TFB2M) by nuclear respiratory factors (NRF-1 and NRF-2) and PGC-1 family coactivators. Mol Cell Biol *25*, 1354-1366.
Goldberg, I.J., Eckel, R.H., and Abumrad, N.A. (2009). Regulation of fatty acid uptake into tissues: lipoprotein lipase- and CD36-mediated pathways. Journal of lipid research *50 Suppl*, S86-90.
Gollamudi, R., Gupta, D., Goel, S., and Mani, S. (2008). Novel orphan nuclear receptors-coregulator interactions controlling anti-cancer drug metabolism. Current drug metabolism *9*, 611-613.
Graham, D.J., Ouellet-Hellstrom, R., MaCurdy, T.E., Ali, F., Sholley, C., Worrall, C., and Kelman, J.A. (2010). Risk of acute myocardial infarction, stroke, heart failure, and death in elderly Medicare patients treated with rosiglitazone or pioglitazone. Jama *304*, 411-418.
Grant, R.W., Moore, A.F., and Florez, J.C. (2009). Genetic architecture of type 2 diabetes: recent progress and clinical implications. Diabetes Care *32*, 1107-1114.
Gross, B., and Staels, B. (2007). PPAR agonists: multimodal drugs for the treatment of type-2 diabetes. Best practice & research. Clinical endocrinology & metabolism *21*, 687-710.
Group, A.S., Ginsberg, H.N., Elam, M.B., Lovato, L.C., Crouse, J.R., 3rd, Leiter, L.A., Linz, P., Friedewald, W.T., Buse, J.B., Gerstein, H.C., et al. (2010). Effects of combination lipid therapy in type 2 diabetes mellitus. N Engl J Med *362*, 1563-1574.
Guan, Y., Hao, C., Cha, D.R., Rao, R., Lu, W., Kohan, D.E., Magnuson, M.A., Redha, R., Zhang, Y., and Breyer, M.D. (2005). Thiazolidinediones expand body fluid volume through PPARgamma stimulation of ENaC-mediated renal salt absorption. Nat Med *11*, 861-866.
H, S. (2007). Oxidation of Fatty Acids in Eukaryotes. Amsterdam: Elsevier, 131–154.
Harrity, T., Farrelly, D., Tieman, A., Chu, C., Kunselman, L., Gu, L., Ponticiello, R., Cap, M., Qu, F., Shao, C., et al. (2006). Muraglitazar, a novel dual (alpha/gamma) peroxisome proliferator-activated receptor activator, improves diabetes and other metabolic abnormalities and preserves beta-cell function in db/db mice. Diabetes *55*, 240-248.

Hauner, H. (2002). The mode of action of thiazolidinediones. Diabetes Metab Res Rev *18 Suppl 2*, S10-15.
Hauton, D., Bennett, M.J., and Evans, R.D. (2001). Utilisation of triacylglycerol and non-esterified fatty acid by the working rat heart: myocardial lipid substrate preference. Biochim Biophys Acta *1533*, 99-109.
Heusch, G., Libby, P., Gersh, B., Yellon, D., Bohm, M., Lopaschuk, G., and Opie, L. (2014). Cardiovascular remodelling in coronary artery disease and heart failure. Lancet *383*, 1933-1943.
Hill, B.G., and Schulze, P.C. (2014). Insights into metabolic remodeling of the hypertrophic and failing myocardium. Circulation. Heart failure *7*, 874-876.
Hodanova, Z. (1976). [Methodological aid for the department of health education of the district Institute of National Health]. Zdravotnicka pracovnice *26*, 585-587.
Home, P.D., Pocock, S.J., Beck-Nielsen, H., Curtis, P.S., Gomis, R., Hanefeld, M., Jones, N.P., Komajda, M., McMurray, J.J., and Team, R.S. (2009). Rosiglitazone evaluated for cardiovascular outcomes in oral agent combination therapy for type 2 diabetes (RECORD): a multicentre, randomised, open-label trial. Lancet *373*, 2125-2135.
Houtkooper, R.H., Canto, C., Wanders, R.J., and Auwerx, J. (2010). The secret life of NAD+: an old metabolite controlling new metabolic signaling pathways. Endocrine reviews *31*, 194-223.
How, O.J., Aasum, E., Kunnathu, S., Severson, D.L., Myhre, E.S., and Larsen, T.S. (2005). Influence of substrate supply on cardiac efficiency, as measured by pressure-volume analysis in ex vivo mouse hearts. Am J Physiol Heart Circ Physiol *288*, H2979-2985.
How, O.J., Aasum, E., Severson, D.L., Chan, W.Y., Essop, M.F., and Larsen, T.S. (2006). Increased myocardial oxygen consumption reduces cardiac efficiency in diabetic mice. Diabetes *55*, 466-473.
Hsu, C.P., Zhai, P., Yamamoto, T., Maejima, Y., Matsushima, S., Hariharan, N., Shao, D., Takagi, H., Oka, S., and Sadoshima, J. (2010). Silent information regulator 1 protects the heart from ischemia/reperfusion. Circulation *122*, 2170-2182.
Hu, F.B. (2011). Globalization of diabetes: the role of diet, lifestyle, and genes. Diabetes Care *34*, 1249-1257.
Huss, J.M., and Kelly, D.P. (2004). Nuclear receptor signaling and cardiac energetics. Circulation research *95*, 568-578.
Issemann, I., and Green, S. (1990). Activation of a member of the steroid hormone receptor superfamily by peroxisome proliferators. Nature *347*, 645-650.
Jager, S., Handschin, C., St-Pierre, J., and Spiegelman, B.M. (2007). AMP-activated protein kinase (AMPK) action in skeletal muscle via direct phosphorylation of PGC-1alpha. Proc Natl Acad Sci U S A *104*, 12017-12022.
Joseph, L.C., Kokkinaki, D., Valenti, M.C., Kim, G.J., Barca, E., Tomar, D., Hoffman, N.E., Subramanyam, P., Colecraft, H.M., Hirano, M., et al. (2017). Inhibition of NADPH oxidase 2 (NOX2) prevents sepsis-induced cardiomyopathy by improving calcium handling and mitochondrial function. JCI Insight *2*.
Jun, M., Foote, C., Lv, J., Neal, B., Patel, A., Nicholls, S.J., Grobbee, D.E., Cass, A., Chalmers, J., and Perkovic, V. (2010). Effects of fibrates on cardiovascular outcomes: a systematic review and meta-analysis. Lancet *375*, 1875-1884.
Kahn, S.E. (2001). Clinical review 135: The importance of beta-cell failure in the development and progression of type 2 diabetes. The Journal of clinical endocrinology and metabolism *86*, 4047-4058.
Kahn, S.E., Prigeon, R.L., McCulloch, D.K., Boyko, E.J., Bergman, R.N., Schwartz, M.W., Neifing, J.L., Ward, W.K., Beard, J.C., Palmer, J.P., et al. (1993). Quantification of the relationship between insulin sensitivity and beta-cell function in human subjects. Evidence for a hyperbolic function. Diabetes *42*, 1663-1672.
Kamei, Y., Ohizumi, H., Fujitani, Y., Nemoto, T., Tanaka, T., Takahashi, N., Kawada, T., Miyoshi, M., Ezaki, O., and Kakizuka, A. (2003). PPARgamma coactivator 1beta/ERR ligand 1 is an ERR protein ligand, whose expression induces a high-energy expenditure and antagonizes obesity. Proc Natl Acad Sci U S A *100*, 12378-12383.

Kaul, S., Bolger, A.F., Herrington, D., Giugliano, R.P., and Eckel, R.H. (2010). Thiazolidinedione drugs and cardiovascular risks: a science advisory from the American Heart Association and American College of Cardiology Foundation. Circulation *121*, 1868-1877.
Kelly, D.P., and Scarpulla, R.C. (2004). Transcriptional regulatory circuits controlling mitochondrial biogenesis and function. Genes Dev *18*, 357-368.
Kelly, T.J., Lerin, C., Haas, W., Gygi, S.P., and Puigserver, P. (2009). GCN5-mediated transcriptional control of the metabolic coactivator PGC-1beta through lysine acetylation. The Journal of biological chemistry *284*, 19945-19952.
Kenchaiah, S., Evans, J.C., Levy, D., Wilson, P.W., Benjamin, E.J., Larson, M.G., Kannel, W.B., and Vasan, R.S. (2002). Obesity and the risk of heart failure. N Engl J Med *347*, 305-313.
Kernan, W.N., Viscoli, C.M., Furie, K.L., Young, L.H., Inzucchi, S.E., Gorman, M., Guarino, P.D., Lovejoy, A.M., Peduzzi, P.N., Conwit, R., et al. (2016). Pioglitazone after Ischemic Stroke or Transient Ischemic Attack. N Engl J Med *374*, 1321-1331.
Kitabchi, A.E., Umpierrez, G.E., Miles, J.M., and Fisher, J.N. (2009). Hyperglycemic crises in adult patients with diabetes. Diabetes Care *32*, 1335-1343.
Knowler, W.C., Barrett-Connor, E., Fowler, S.E., Hamman, R.F., Lachin, J.M., Walker, E.A., Nathan, D.M., and Diabetes Prevention Program Research, G. (2002). Reduction in the incidence of type 2 diabetes with lifestyle intervention or metformin. N Engl J Med *346*, 393-403.
Kolwicz, S.C., Jr., Purohit, S., and Tian, R. (2013). Cardiac metabolism and its interactions with contraction, growth, and survival of cardiomyocytes. Circulation research *113*, 603-616.
Koonen, D.P., Glatz, J.F., Bonen, A., and Luiken, J.J. (2005). Long-chain fatty acid uptake and FAT/CD36 translocation in heart and skeletal muscle. Biochim Biophys Acta *1736*, 163-180.
Kressler, D., Schreiber, S.N., Knutti, D., and Kralli, A. (2002). The PGC-1-related protein PERC is a selective coactivator of estrogen receptor alpha. The Journal of biological chemistry *277*, 13918-13925.
Kudo, N., Gillespie, J.G., Kung, L., Witters, L.A., Schulz, R., Clanachan, A.S., and Lopaschuk, G.D. (1996). Characterization of 5'AMP-activated protein kinase activity in the heart and its role in inhibiting acetyl-CoA carboxylase during reperfusion following ischemia. Biochim Biophys Acta *1301*, 67-75.
Lagouge, M., Argmann, C., Gerhart-Hines, Z., Meziane, H., Lerin, C., Daussin, F., Messadeq, N., Milne, J., Lambert, P., Elliott, P., et al. (2006). Resveratrol improves mitochondrial function and protects against metabolic disease by activating SIRT1 and PGC-1alpha. Cell *127*, 1109-1122.
Lahey, R., Wang, X., Carley, A.N., and Lewandowski, E.D. (2014). Dietary fat supply to failing hearts determines dynamic lipid signaling for nuclear receptor activation and oxidation of stored triglyceride. Circulation *130*, 1790-1799.
Lai, L., Leone, T.C., Zechner, C., Schaeffer, P.J., Kelly, S.M., Flanagan, D.P., Medeiros, D.M., Kovacs, A., and Kelly, D.P. (2008). Transcriptional coactivators PGC-1alpha and PGC-lbeta control overlapping programs required for perinatal maturation of the heart. Genes Dev *22*, 1948-1961.
Lehman, J.J., Barger, P.M., Kovacs, A., Saffitz, J.E., Medeiros, D.M., and Kelly, D.P. (2000). Peroxisome proliferator-activated receptor gamma coactivator-1 promotes cardiac mitochondrial biogenesis. J Clin Invest *106*, 847-856.
Leone, T.C., Lehman, J.J., Finck, B.N., Schaeffer, P.J., Wende, A.R., Boudina, S., Courtois, M., Wozniak, D.F., Sambandam, N., Bernal-Mizrachi, C., et al. (2005). PGC-1alpha deficiency causes multi-system energy metabolic derangements: muscle dysfunction, abnormal weight control and hepatic steatosis. PLoS biology *3*, e101.
Lerin, C., Rodgers, J.T., Kalume, D.E., Kim, S.H., Pandey, A., and Puigserver, P. (2006). GCN5 acetyltransferase complex controls glucose metabolism through transcriptional repression of PGC-1alpha. Cell Metab *3*, 429-438.
Lewis, J.D., Habel, L.A., Quesenberry, C.P., Strom, B.L., Peng, T., Hedderson, M.M., Ehrlich, S.F., Mamtani, R., Bilker, W., Vaughn, D.J., et al. (2015). Pioglitazone Use and Risk of Bladder Cancer and Other Common Cancers in Persons With Diabetes. Jama *314*, 265-277.

Li, X., Monks, B., Ge, Q., and Birnbaum, M.J. (2007). Akt/PKB regulates hepatic metabolism by directly inhibiting PGC-1alpha transcription coactivator. Nature *447*, 1012-1016.
Li, Y., Cheng, L., Qin, Q., Liu, J., Lo, W.K., Brako, L.A., and Yang, Q. (2009). High-fat feeding in cardiomyocyte-restricted PPARdelta knockout mice leads to cardiac overexpression of lipid metabolic genes but fails to rescue cardiac phenotypes. J Mol Cell Cardiol *47*, 536-543.
Lin, J., Puigserver, P., Donovan, J., Tarr, P., and Spiegelman, B.M. (2002). Peroxisome proliferator-activated receptor gamma coactivator 1beta (PGC-1beta), a novel PGC-1-related transcription coactivator associated with host cell factor. The Journal of biological chemistry *277*, 1645-1648.
Lincoff, A.M., Tardif, J.C., Schwartz, G.G., Nicholls, S.J., Ryden, L., Neal, B., Malmberg, K., Wedel, H., Buse, J.B., Henry, R.R., et al. (2014). Effect of aleglitazar on cardiovascular outcomes after acute coronary syndrome in patients with type 2 diabetes mellitus: the AleCardio randomized clinical trial. JAMA *311*, 1515-1525.
Lincoff, A.M., Wolski, K., Nicholls, S.J., and Nissen, S.E. (2007). Pioglitazone and risk of cardiovascular events in patients with type 2 diabetes mellitus: a meta-analysis of randomized trials. Jama *298*, 1180-1188.
Lopaschuk, G.D., Belke, D.D., Gamble, J., Itoi, T., and Schonekess, B.O. (1994). Regulation of fatty acid oxidation in the mammalian heart in health and disease. Biochim Biophys Acta *1213*, 263-276.
Lopaschuk, G.D., Ussher, J.R., Folmes, C.D., Jaswal, J.S., and Stanley, W.C. (2010). Myocardial fatty acid metabolism in health and disease. Physiol Rev *90*, 207-258.
Lopaschuk GD, W.L., Itoi T, Barr R, Barr A. (1994.). Acetyl-CoA carboxylase involvement in the rapid maturation of fatty acid oxidation in the newborn rabbit heart. J Biol Chem *269:*, 25871–25878.
Luiken, J.J., Arumugam, Y., Dyck, D.J., Bell, R.C., Pelsers, M.M., Turcotte, L.P., Tandon, N.N., Glatz, J.F., and Bonen, A. (2001). Increased rates of fatty acid uptake and plasmalemmal fatty acid transporters in obese Zucker rats. The Journal of biological chemistry *276*, 40567-40573.
Luiken, J.J., Coort, S.L., Koonen, D.P., van der Horst, D.J., Bonen, A., Zorzano, A., and Glatz, J.F. (2004). Regulation of cardiac long-chain fatty acid and glucose uptake by translocation of substrate transporters. Pflugers Archiv : European journal of physiology *448*, 1-15.
Madrazo, J.A., and Kelly, D.P. (2008). The PPAR trio: regulators of myocardial energy metabolism in health and disease. J Mol Cell Cardiol *44*, 968-975.
Mahaffey, K.W., Hafley, G., Dickerson, S., Burns, S., Tourt-Uhlig, S., White, J., Newby, L.K., Komajda, M., McMurray, J., Bigelow, R., et al. (2013). Results of a reevaluation of cardiovascular outcomes in the RECORD trial. Am Heart J *166*, 240-249 e241.
Matsushima, S., and Sadoshima, J. (2015). The role of sirtuins in cardiac disease. Am J Physiol Heart Circ Physiol *309*, H1375-1389.
Matthews, D.R., Cull, C.A., Stratton, I.M., Holman, R.R., and Turner, R.C. (1998). UKPDS 26: Sulphonylurea failure in non-insulin-dependent diabetic patients over six years. UK Prospective Diabetes Study (UKPDS) Group. Diabetic medicine : a journal of the British Diabetic Association *15*, 297-303.
McGarry, J.D., and Brown, N.F. (1997). The mitochondrial carnitine palmitoyltransferase system. From concept to molecular analysis. European journal of biochemistry *244*, 1-14.
Medicine, N.L.o.
Mills, G.W., Avery, P.J., McCarthy, M.I., Hattersley, A.T., Levy, J.C., Hitman, G.A., Sampson, M., and Walker, M. (2004). Heritability estimates for beta cell function and features of the insulin resistance syndrome in UK families with an increased susceptibility to type 2 diabetes. Diabetologia *47*, 732-738.
Morrow, J.P., Katchman, A., Son, N.H., Trent, C.M., Khan, R., Shiomi, T., Huang, H., Amin, V., Lader, J.M., Vasquez, C., et al. (2011). Mice with cardiac overexpression of peroxisome proliferator-activated receptor gamma have impaired repolarization and spontaneous fatal ventricular arrhythmias. Circulation *124*, 2812-2821.

Mozaffarian, D., Benjamin, E.J., Go, A.S., Arnett, D.K., Blaha, M.J., Cushman, M., de Ferranti, S., Despres, J.P., Fullerton, H.J., Howard, V.J., et al. (2015). Heart disease and stroke statistics--2015 update: a report from the American Heart Association. Circulation *131*, e29-322.
Murthy, V.K., and Shipp, J.C. (1977). Accumulation of myocardial triglycerides ketotic diabetes; evidence for increased biosynthesis. Diabetes *26*, 222-229.
Myrmel, T., Forsdahl, K., and Larsen, T.S. (1992). Triacylglycerol metabolism in hypoxic, glucose-deprived rat cardiomyocytes. Journal of molecular and cellular cardiology *24*, 855-868.
Nathan, D.M., Buse, J.B., Davidson, M.B., Ferrannini, E., Holman, R.R., Sherwin, R., Zinman, B., American Diabetes, A., and European Association for Study of, D. (2009). Medical management of hyperglycemia in type 2 diabetes: a consensus algorithm for the initiation and adjustment of therapy: a consensus statement of the American Diabetes Association and the European Association for the Study of Diabetes. Diabetes Care *32*, 193-203.
Neely, J.R., and Morgan, H.E. (1974). Relationship between carbohydrate and lipid metabolism and the energy balance of heart muscle. Annual review of physiology *36*, 413-459.
Nesto, R.W., Bell, D., Bonow, R.O., Fonseca, V., Grundy, S.M., Horton, E.S., Le Winter, M., Porte, D., Semenkovich, C.F., Smith, S., et al. (2003). Thiazolidinedione use, fluid retention, and congestive heart failure: a consensus statement from the American Heart Association and American Diabetes Association. October 7, 2003. Circulation *108*, 2941-2948.
Neubauer, S. (2007). The failing heart--an engine out of fuel. N Engl J Med *356*, 1140-1151.
Nissen, S.E., and Wolski, K. (2007). Effect of rosiglitazone on the risk of myocardial infarction and death from cardiovascular causes. N Engl J Med *356*, 2457-2471.
Nolan, C.J., Ruderman, N.B., Kahn, S.E., Pedersen, O., and Prentki, M. (2015). Insulin resistance as a physiological defense against metabolic stress: implications for the management of subsets of type 2 diabetes. Diabetes *64*, 673-686.
Nuclear Receptors Nomenclature, C. (1999). A unified nomenclature system for the nuclear receptor superfamily. Cell *97*, 161-163.
Olefsky, J., Farquhar, J.W., and Reaven, G. (1973). Relationship between fasting plasma insulin level and resistance to insulin-mediated glucose uptake in normal and diabetic subjects. Diabetes *22*, 507-513.
Opie, L.H. (1969). Metabolism of the heart in health and disease. 3. Am Heart J *77*, 383-410.
Organization, W.H.
Page, R.L., 2nd, Gozansky, W.S., and Ruscin, J.M. (2003). Possible heart failure exacerbation associated with rosiglitazone: case report and literature review. Pharmacotherapy *23*, 945-954.
Patel, M.S., and Korotchkina, L.G. (2006). Regulation of the pyruvate dehydrogenase complex. Biochem Soc Trans *34*, 217-222.
Pol, C.J., Lieu, M., and Drosatos, K. (2015). PPARs: Protectors or Opponents of Myocardial Function? PPAR Res *2015*, 835985.
Poulsen, L., Siersbaek, M., and Mandrup, S. (2012). PPARs: fatty acid sensors controlling metabolism. Seminars in cell & developmental biology *23*, 631-639.
Puigserver, P., Adelmant, G., Wu, Z., Fan, M., Xu, J., O'Malley, B., and Spiegelman, B.M. (1999). Activation of PPARgamma coactivator-1 through transcription factor docking. Science *286*, 1368-1371.
Puigserver, P., Rhee, J., Lin, J., Wu, Z., Yoon, J.C., Zhang, C.Y., Krauss, S., Mootha, V.K., Lowell, B.B., and Spiegelman, B.M. (2001). Cytokine stimulation of energy expenditure through p38 MAP kinase activation of PPARgamma coactivator-1. Mol Cell *8*, 971-982.
Puigserver, P., Wu, Z., Park, C.W., Graves, R., Wright, M., and Spiegelman, B.M. (1998). A cold-inducible coactivator of nuclear receptors linked to adaptive thermogenesis. Cell *92*, 829-839.
Ran, G., Ying, L., Li, L., Yan, Q., Yi, W., Ying, C., Wu, H., and Ye, X. (2017). Resveratrol ameliorates diet-induced dysregulation of lipid metabolism in zebrafish (Danio rerio). PLoS One *12*, e0180865.
Reibel, D.K., Wyse, B.W., Berkich, D.A., and Neely, J.R. (1981). Regulation of coenzyme A synthesis in heart muscle: effects of diabetes and fasting. The American journal of physiology *240*, H606-611.

Roberts, J.S.s. ((2015).). Distillations *1 (4)*, 12–15.
Rodgers, J.T., Lerin, C., Haas, W., Gygi, S.P., Spiegelman, B.M., and Puigserver, P. (2005). Nutrient control of glucose homeostasis through a complex of PGC-1alpha and SIRT1. Nature *434*, 113-118.
Rousset, S., Alves-Guerra, M.C., Mozo, J., Miroux, B., Cassard-Doulcier, A.M., Bouillaud, F., and Ricquier, D. (2004). The biology of mitochondrial uncoupling proteins. Diabetes *53 Suppl 1*, S130-135.
Rubins, H.B., Robins, S.J., Collins, D., Fye, C.L., Anderson, J.W., Elam, M.B., Faas, F.H., Linares, E., Schaefer, E.J., Schectman, G., et al. (1999). Gemfibrozil for the secondary prevention of coronary heart disease in men with low levels of high-density lipoprotein cholesterol. Veterans Affairs High-Density Lipoprotein Cholesterol Intervention Trial Study Group. N Engl J Med *341*, 410-418.
Sakamoto J, B.R., Kavanagh KM, Lopaschuk GD (2000.). Contribution of malonyl-CoA decarboxylase to the high fatty acid oxidation rates seen in the diabetic heart. Am J Physiol Heart Circ Physiol *278:*, H1196–H1204.
Sano, M., Izumi, Y., Helenius, K., Asakura, M., Rossi, D.J., Xie, M., Taffet, G., Hu, L., Pautler, R.G., Wilson, C.R., et al. (2007). Menage-a-trois 1 is critical for the transcriptional function of PPARgamma coactivator 1. Cell Metab *5*, 129-142.
Sano M, W.S., Shirai M, Scaglia F, Xie M, Sakai S, Tanaka T,, Kulkarni PA, B.P., Youker KA, Taffet GE, Hamamori Y, Michael, and LH, C.W., Schneider MD. (2004). Activation of cardiac Cdk9 represses

PGC-1 and confers a predisposition to heart failure. . EMBO J *23*, 3559–3569.
Scarpulla, R.C. (2002). Nuclear activators and coactivators in mammalian mitochondrial biogenesis. Biochim Biophys Acta *1576*, 1-14.
Schaffer, J.E. (2003). Lipotoxicity: when tissues overeat. Curr Opin Lipidol *14*, 281-287.
Schwenk, R.W., Luiken, J.J., Bonen, A., and Glatz, J.F. (2008). Regulation of sarcolemmal glucose and fatty acid transporters in cardiac disease. Cardiovascular research *79*, 249-258.
Sharma A, S.A., Kushwah DS and S R.. (2014). Saroglitazar, a novel cardiometabolic agent for diabetic dyslipidemia - A Review. Journal of Young Pharmacists. *7*, 2-6.
Sharma, S., Adrogue, J.V., Golfman, L., Uray, I., Lemm, J., Youker, K., Noon, G.P., Frazier, O.H., and Taegtmeyer, H. (2004). Intramyocardial lipid accumulation in the failing human heart resembles the lipotoxic rat heart. FASEB journal : official publication of the Federation of American Societies for Experimental Biology *18*, 1692-1700.
Shore, D., Squire, M., and Nasmyth, K.A. (1984). Characterization of two genes required for the position-effect control of yeast mating-type genes. EMBO J *3*, 2817-2823.
Sihag, S., Cresci, S., Li, A.Y., Sucharov, C.C., and Lehman, J.J. (2009). PGC-1alpha and ERRalpha target gene downregulation is a signature of the failing human heart. Journal of molecular and cellular cardiology *46*, 201-212.
Son, N.H., Park, T.S., Yamashita, H., Yokoyama, M., Huggins, L.A., Okajima, K., Homma, S., Szabolcs, M.J., Huang, L.S., and Goldberg, I.J. (2007). Cardiomyocyte expression of PPARgamma leads to cardiac dysfunction in mice. J Clin Invest *117*, 2791-2801.
Son, N.H., Yu, S., Tuinei, J., Arai, K., Hamai, H., Homma, S., Shulman, G.I., Abel, E.D., and Goldberg, I.J. (2010). PPARgamma-induced cardiolipotoxicity in mice is ameliorated by PPARalpha deficiency despite increases in fatty acid oxidation. J Clin Invest *120*, 3443-3454.
Southgate, R.J., Bruce, C.R., Carey, A.L., Steinberg, G.R., Walder, K., Monks, R., Watt, M.J., Hawley, J.A., Birnbaum, M.J., and Febbraio, M.A. (2005). PGC-1alpha gene expression is down-regulated by Akt-mediated phosphorylation and nuclear exclusion of FoxO1 in insulin-stimulated skeletal muscle. FASEB journal : official publication of the Federation of American Societies for Experimental Biology *19*, 2072-2074.
St-Pierre, J., Lin, J., Krauss, S., Tarr, P.T., Yang, R., Newgard, C.B., and Spiegelman, B.M. (2003). Bioenergetic analysis of peroxisome proliferator-activated receptor gamma coactivators 1alpha and 1beta (PGC-1alpha and PGC-1beta) in muscle cells. The Journal of biological chemistry *278*, 26597-26603.

Staels, B., Dallongeville, J., Auwerx, J., Schoonjans, K., Leitersdorf, E., and Fruchart, J.C. (1998). Mechanism of action of fibrates on lipid and lipoprotein metabolism. Circulation *98*, 2088-2093.
Staels, B., and Fruchart, J.C. (2005). Therapeutic roles of peroxisome proliferator-activated receptor agonists. Diabetes *54*, 2460-2470.
Stanley, W.C., Lopaschuk, G.D., Hall, J.L., and McCormack, J.G. (1997). Regulation of myocardial carbohydrate metabolism under normal and ischaemic conditions. Potential for pharmacological interventions. Cardiovascular research *33*, 243-257.
Stirban, A.O., Andjelkovic, M., Heise, T., Nosek, L., Fischer, A., Gastaldelli, A., and Herz, M. (2016). Aleglitazar, a dual peroxisome proliferator-activated receptor-alpha/gamma agonist, improves insulin sensitivity, glucose control and lipid levels in people with type 2 diabetes: findings from a randomized, double-blind trial. Diabetes, obesity & metabolism *18*, 711-715.
Tonelli, J., Li, W., Kishore, P., Pajvani, U.B., Kwon, E., Weaver, C., Scherer, P.E., and Hawkins, M. (2004). Mechanisms of early insulin-sensitizing effects of thiazolidinediones in type 2 diabetes. Diabetes *53*, 1621-1629.
Turner, R.C., Cull, C.A., Frighi, V., and Holman, R.R. (1999). Glycemic control with diet, sulfonylurea, metformin, or insulin in patients with type 2 diabetes mellitus: progressive requirement for multiple therapies (UKPDS 49). UK Prospective Diabetes Study (UKPDS) Group. Jama *281*, 2005-2012.
Tyagi, S., Gupta, P., Saini, A.S., Kaushal, C., and Sharma, S. (2011). The peroxisome proliferator-activated receptor: A family of nuclear receptors role in various diseases. Journal of advanced pharmaceutical technology & research *2*, 236-240.
Unger, R.H., and Zhou, Y.T. (2001). Lipotoxicity of beta-cells in obesity and in other causes of fatty acid spillover. Diabetes *50 Suppl 1*, S118-121.
van den Bosch, B.J., van den Burg, C.M., Schoonderwoerd, K., Lindsey, P.J., Scholte, H.R., de Coo, R.F., van Rooij, E., Rockman, H.A., Doevendans, P.A., and Smeets, H.J. (2005). Regional absence of mitochondria causing energy depletion in the myocardium of muscle LIM protein knockout mice. Cardiovascular research *65*, 411-418.
van der Vusse, G.J., van Bilsen, M., and Glatz, J.F. (2000). Cardiac fatty acid uptake and transport in health and disease. Cardiovascular research *45*, 279-293.
Vega, R.B., Huss, J.M., and Kelly, D.P. (2000). The coactivator PGC-1 cooperates with peroxisome proliferator-activated receptor alpha in transcriptional control of nuclear genes encoding mitochondrial fatty acid oxidation enzymes. Mol Cell Biol *20*, 1868-1876.
Verschuren, L., Wielinga, P.Y., Kelder, T., Radonjic, M., Salic, K., Kleemann, R., van Ommen, B., and Kooistra, T. (2014). A systems biology approach to understand the pathophysiological mechanisms of cardiac pathological hypertrophy associated with rosiglitazone. BMC Med Genomics *7*, 35.
Wallberg, A.E., Yamamura, S., Malik, S., Spiegelman, B.M., and Roeder, R.G. (2003). Coordination of p300-mediated chromatin remodeling and TRAP/mediator function through coactivator PGC-1alpha. Mol Cell *12*, 1137-1149.
Wallenius, K., Kjellstedt, A., Thalen, P., Lofgren, L., and Oakes, N.D. (2013). The PPAR alpha / gamma Agonist, Tesaglitazar, Improves Insulin Mediated Switching of Tissue Glucose and Free Fatty Acid Utilization In Vivo in the Obese Zucker Rat. PPAR Res *2013*, 305347.
Watanabe, K., Fujii, H., Takahashi, T., Kodama, M., Aizawa, Y., Ohta, Y., Ono, T., Hasegawa, G., Naito, M., Nakajima, T., et al. (2000). Constitutive regulation of cardiac fatty acid metabolism through peroxisome proliferator-activated receptor alpha associated with age-dependent cardiac toxicity. The Journal of biological chemistry *275*, 22293-22299.
Weis, B.C., Cowan, A.T., Brown, N., Foster, D.W., and McGarry, J.D. (1994). Use of a selective inhibitor of liver carnitine palmitoyltransferase I (CPT I) allows quantification of its contribution to total CPT I activity in rat heart. Evidence that the dominant cardiac CPT I isoform is identical to the skeletal muscle enzyme. The Journal of biological chemistry *269*, 26443-26448.

Winnik, S., Auwerx, J., Sinclair, D.A., and Matter, C.M. (2015). Protective effects of sirtuins in cardiovascular diseases: from bench to bedside. Eur Heart J *36*, 3404-3412.
Wisneski, J.A., Gertz, E.W., Neese, R.A., Gruenke, L.D., Morris, D.L., and Craig, J.C. (1985). Metabolic fate of extracted glucose in normal human myocardium. The Journal of clinical investigation *76*, 1819-1827.
Wu, Z., Puigserver, P., Andersson, U., Zhang, C., Adelmant, G., Mootha, V., Troy, A., Cinti, S., Lowell, B., Scarpulla, R.C., et al. (1999). Mechanisms controlling mitochondrial biogenesis and respiration through the thermogenic coactivator PGC-1. Cell *98*, 115-124.
www.cdc.gov/diabetes.
Yagyu, H., Chen, G., Yokoyama, M., Hirata, K., Augustus, A., Kako, Y., Seo, T., Hu, Y., Lutz, E.P., Merkel, M., et al. (2003). Lipoprotein lipase (LpL) on the surface of cardiomyocytes increases lipid uptake and produces a cardiomyopathy. The Journal of clinical investigation *111*, 419-426.
Yang, Q., and Li, Y. (2007). Roles of PPARs on regulating myocardial energy and lipid homeostasis. Journal of molecular medicine *85*, 697-706.
Young, M.E., Guthrie, P.H., Razeghi, P., Leighton, B., Abbasi, S., Patil, S., Youker, K.A., and Taegtmeyer, H. (2002). Impaired long-chain fatty acid oxidation and contractile dysfunction in the obese Zucker rat heart. Diabetes *51*, 2587-2595.
Yu, J.G., Javorschi, S., Hevener, A.L., Kruszynska, Y.T., Norman, R.A., Sinha, M., and Olefsky, J.M. (2002). The effect of thiazolidinediones on plasma adiponectin levels in normal, obese, and type 2 diabetic subjects. Diabetes *51*, 2968-2974.
Zhou, Y.T., Grayburn, P., Karim, A., Shimabukuro, M., Higa, M., Baetens, D., Orci, L., and Unger, R.H. (2000). Lipotoxic heart disease in obese rats: implications for human obesity. Proc Natl Acad Sci U S A *97*, 1784-1789.
Zierz, S., and Engel, A.G. (1987). Different sites of inhibition of carnitine palmitoyltransferase by malonyl-CoA, and by acetyl-CoA and CoA, in human skeletal muscle. The Biochemical journal *245*, 205-209.